

Competitive Adsorption and Optimization of
Bimolecular Fluidized Bed Reactor

by

Ankur R. Patel

Submitted in Partial Fulfillment of the Requirements

for the Degree of

Master of Science in Engineering

in the

Chemical and Environmental Engineering

Program

YOUNGSTOWN STATE UNIVERSITY

August, 2004

Competitive Adsorption and Optimization of
Bimolecular Fluidized Bed Reactor

Ankur R. Patel

I hereby release this thesis to public. I understand that this thesis will be made available from the OhioLINK ETD Center and the Maag Library Circulation Desk for public access. I also authorize the University or other individuals to make copies of this thesis as needed for scholarly research.

Signature: Ankur R. Patel 07/30/2004
Ankur R. Patel, Student Date

Approvals: Douglas M. Price 8/2/04
Dr. Douglas M. Price, Thesis Advisor Date

Scott C. Martin 7/30/04
Dr. Scott C. Martin, Committee Member Date

S. Lim 7/30/04
Dr. Soon Sik Lim, Committee Member Date

Peter J. Kasvinsky 8/4/04
Peter J. Kasvinsky, Dean of Graduate Studies and Research Date

ABSTRACT

A numerical study has been performed in order to evaluate the performance of a fluidized bed reactor under the competitive effects of adsorption rate. For this purpose, a steady state model is coupled with a detailed dynamic model. The model is employed to investigate the effect of various operating conditions and rate constants on the efficiency of a fluidized bed reactor. Two reactants are fed to the reactor along with an inert gas to maintain fluidization in the bed. The reactants adsorb reversibly to the catalyst surface and react to form the product which desorbs irreversibly. The reaction kinetics consist of the reaction rate, adsorption and desorption rate constants, and reactant and inert flow rates. Each kinetic variable has a specific range of operation at which studies can be performed at steady state for all combinations of these variables. For each combination of the kinetic variables there exists an optimum product output. For the system studied, conditions were specified which optimize the conversion to the reaction product when the reactor is operated under steady state conditions. Further, it is shown that improvements can be made to this conversion by employing a sinusoidal feed rate of one or both reactants to the reactor.

DEDICATION

This thesis is dedicated with love and affection to

My parents

Dr. Ram V. Patel and Bhanu R. Patel

and

My family

ACKNOWLEDGEMENTS

First of all, I wish to express my appreciation and gratitude to those who have helped during the development of this thesis. I sincerely want to thank Dr. Douglas M. Price, my research advisor, for his guidance and advice throughout this work. Working with him was always interesting and rewarding. Without his help and suggestion, this thesis would not have been possible.

I particularly want to thank Dr. Scott C. Martin, Chairperson, Department of Civil/Environmental and Chemical Engineering at Youngstown State University (YSU), Youngstown for his guidance and support during my study at YSU. My special gratitude is to the faculty and staff of Civil/Environmental and Chemical Engineering department for providing very enjoyable learning experience and their support. I wish to thank Dr. Lim and Dr. Scott Martin for accepting to serve on my defense committee. I also want to thank International office of Studies and Programs for their help throughout my stay. I am also very thankful to School of Graduate studies and my department for the opportunity to pursue my graduate study and giving me financial support.

I am gratified by the friendship and love of all my friends here and in India. Finally, I am very grateful to my parents and my family for their unconditional love, support and believing in me.

TABLE OF CONTENTS

| | PAGE |
|---|-------------|
| ABSTRACT | iii |
| ACKNOWLEDGEMENT | v |
| TABLE OF CONTENTS | vi |
| LIST OF FIGURES | viii |
| LIST OF TABLES | xi |
| CHAPTER | |
| 1. INTRODUCTION | 1 |
| 1.1 MODEL DESCRIPTION | 4 |
| 1.2 THEORY | 7 |
| 2. LITERATURE SURVEY | 14 |
| 2.1 INDUSTRIAL APPLICATION | 14 |
| 2.2 ADVANTAGES AND DISADVANTAGES OF FLUIDIZED BED | 15 |
| 2.3 UNIT OPERATION OF ADSORPTION | 16 |
| 2.4 SUMMARIES | 20 |
| 3. METHOD AND PROCEDURES | 22 |
| 4. RESULTS, DISCUSSION AND RECOMMENDATIONS | 25 |
| 4.1 OPTIMIZATION WITH SLOW AND FAST REACTION RATE FOR STEADY STATE MODEL | 25 |
| 4.2 STEADY STATE MODEL AND TRANSIENT CONDITION | 41 |
| 4.3 EFFECT OF INERT GAS | 43 |

| | |
|---|-----------|
| 4.4 DYNAMIC MODEL AND TRANSIENT CONDITION | 60 |
| 4.5 COMPARISON OF TRANSIENT INPUT AND FIXED INPUT RESPONSE FOR DYNAMIC MODEL STUDY | 70 |
| 5. SUMMARY AND RECOMMEDATIONS | 79 |
| 5.1 SUMMARY | 79 |
| 5.2 RECOMMENDATIONS | 80 |
| NOMENCLATURE | 81 |
| REFERENCES | 83 |
| APPENDIX | 86 |
| A.I.1. STEADY STATE MODEL CODE | 86 |
| A.II.1 DYNAMIC MODEL CODE | 94 |

LIST OF FIGURES

| Figure | | Page |
|--------|---|------|
| 1.1 | Schematic of a Fluidized Bed Reactor | 6 |
| 1.2 | Schematic of a Catalyst Surface Reaction | 6 |
| 3.1 | Sinusoidal variance of flow rate | 24 |
| 4.1.1 | Mole fraction of C, X_C with Adsorption rate k_{Aa} and k_{Ba} , $k_r = 1250$ | 26 |
| 4.1.2 | Mole fraction of C, X_C with Adsorption rate k_{Aa} and k_{Ba} , $k_r = 2500$ | 27 |
| 4.1.3 | X_{ain} with Adsorption rate k_{Aa} and k_{Ba} , $k_r = 1250$ | 28 |
| 4.1.4 | X_{ain} with Adsorption rate k_{Aa} and k_{Ba} , $k_r = 2500$ | 29 |
| 4.1.5 | X_{bin} with Adsorption rate k_{Aa} and k_{Ba} , $k_r = 1250$ | 30 |
| 4.1.6 | X_{bin} with Adsorption rate k_{Aa} and k_{Ba} , $k_r = 2500$ | 31 |
| 4.1.7 | X_{aout} with Adsorption rate k_{Aa} and k_{Ba} , $k_r = 1250$ | 32 |
| 4.1.8 | X_{aout} with Adsorption rate k_{Aa} and k_{Ba} , $k_r = 2500$ | 33 |
| 4.1.9 | X_{bout} with Adsorption rate k_{Aa} and k_{Ba} , $k_r = 1250$ | 34 |
| 4.1.10 | X_{bout} with Adsorption rate k_{Aa} and k_{Ba} , $k_r = 2500$ | 35 |
| 4.1.11 | Y_a with Adsorption rate k_{Aa} and k_{Ba} , $k_r = 1250$ | 36 |
| 4.1.12 | Y_a with Adsorption rate k_{Aa} and k_{Ba} , $k_r = 2500$ | 37 |
| 4.1.13 | Y_b with Adsorption rate k_{Aa} and k_{Ba} , $k_r = 1250$ | 38 |
| 4.1.14 | Y_b with Adsorption rate k_{Aa} and k_{Ba} , $k_r = 2500$ | 39 |
| 4.1.15 | Flow rate Q with Adsorption rate k_{Aa} and k_{Ba} , $k_r = 1250$ | 40 |
| 4.1.16 | Flow rate Q with Adsorption rate k_{Aa} and k_{Ba} , $k_r = 2500$ | 41 |

| Figure | | Page |
|---------------|--|-------------|
| 4.2.1 | Mole fraction of C, X_C with Adsorption rate k_{Aa} and k_{Ba} , fixed and transient input condition | 42 |
| 4.3.1 | Mole fraction of C, X_C with t and Q_a , $k_{Aa} = 1$, $k_{Ba} = 3$, $Q_b = 50\%$, $Q_i = 50\%$ | 44 |
| 4.3.2 | Mole fraction of C, X_C with t and Q_a , $k_{Aa} = 3$, $k_{Ba} = 1$, $Q_b = 50\%$, $Q_i = 50\%$ | 45 |
| 4.3.3 | Mole fraction of C, X_C with t and Q_a , $k_{Aa} = 3$, $k_{Ba} = 3$, $Q_b = 50\%$, $Q_i = 50\%$ | 46 |
| 4.3.4 | Mole fraction of C, X_C with t and Q_a , $k_{Aa} = 3$, $k_{Ba} = 5$, $Q_b = 50\%$, $Q_i = 50\%$ | 47 |
| 4.3.5 | Mole fraction of C, X_C with t and Q_a , $k_{Aa} = 5$, $k_{Ba} = 3$, $Q_b = 50\%$, $Q_i = 50\%$ | 48 |
| 4.3.6 | Mole fraction of C, X_C with t and Q_a , $k_{Aa} = 1$, $k_{Ba} = 3$, $Q_b = 67\%$, $Q_i = 33\%$ | 49 |
| 4.3.7 | Mole fraction of C, X_C with t and Q_a , $k_{Aa} = 3$, $k_{Ba} = 1$, $Q_b = 67\%$, $Q_i = 33\%$ | 50 |
| 4.3.8 | Mole fraction of C, X_C with t and Q_a , $k_{Aa} = 3$, $k_{Ba} = 3$, $Q_b = 67\%$, $Q_i = 33\%$ | 51 |
| 4.3.9 | Mole fraction of C, X_C with t and Q_a , $k_{Aa} = 3$, $k_{Ba} = 5$, $Q_b = 67\%$, $Q_i = 33\%$ | 52 |
| 4.3.10 | Mole fraction of C, X_C with t and Q_a , $k_{Aa} = 5$, $k_{Ba} = 3$, $Q_b = 67\%$, $Q_i = 33\%$ | 53 |
| 4.3.11 | Mole fraction of C, X_C with t and Q_a , $k_{Aa} = 1$, $k_{Ba} = 3$, $Q_b = 33\%$, $Q_i = 67\%$ | 54 |
| 4.3.12 | Mole fraction of C, X_C with t and Q_a , $k_{Aa} = 3$, $k_{Ba} = 1$, $Q_b = 33\%$, $Q_i = 67\%$ | 55 |
| 4.3.13 | Mole fraction of C, X_C with t and Q_a , $k_{Aa} = 3$, $k_{Ba} = 3$, $Q_b = 33\%$, $Q_i = 67\%$ | 56 |
| 4.3.14 | Mole fraction of C, X_C with t and Q_a , $k_{Aa} = 3$, $k_{Ba} = 5$, $Q_b = 33\%$, $Q_i = 67\%$ | 57 |
| 4.3.15 | Mole fraction of C, X_C with t and Q_a , $k_{Aa} = 5$, $k_{Ba} = 3$, $Q_b = 33\%$, $Q_i = 67\%$ | 58 |
| 4.4.1 | Mole fraction of C, X_C with t and Q_a , $k_{Aa} = 1$, $k_{Ba} = 3$, $Q_a = Q_b + Q_i$ | 61 |
| 4.4.2 | Mole fraction of C, X_C with t and Q_a , $k_{Aa} = 3$, $k_{Ba} = 3$, $Q_a = Q_b + Q_i$ | 62 |
| 4.4.3 | Mole fraction of C, X_C with t and Q_a , $k_{Aa} = 5$, $k_{Ba} = 3$, $Q_a = Q_b + Q_i$ | 63 |
| 4.4.4 | Mole fraction of C, X_C with t and Q_a , $k_{Aa} = 1$, $k_{Ba} = 3$, $Q_b = 3 \times Q_i$ | 64 |
| 4.4.5 | Mole fraction of C, X_C with t and Q_a , $k_{Aa} = 3$, $k_{Ba} = 3$, $Q_b = 3 \times Q_i$ | 65 |
| 4.4.6 | Mole fraction of C, X_C with t and Q_a , $k_{Aa} = 5$, $k_{Ba} = 3$, $Q_b = 3 \times Q_i$ | 66 |

| Figure | Page |
|--|-------------|
| 4.4.7 Mole fraction of C, X_C with t and Q_a , $k_{Aa} = 1$, $k_{Ba} = 3$, $Q_i = 2 \times Q_b$ | 67 |
| 4.4.8 Mole fraction of C, X_C with t and Q_a , $k_{Aa} = 3$, $k_{Ba} = 3$, $Q_i = 2 \times Q_b$ | 68 |
| 4.4.9 Mole fraction of C, X_C with t and Q_a , $k_{Aa} = 5$, $k_{Ba} = 3$, $Q_i = 2 \times Q_b$ | 69 |
| 4.5.1 X_C with Q_a , Fixed and Transient input condition, $k_{Aa} = 1$, $k_{Ba} = 3$, $Q_b = Q_i$ | 70 |
| 4.5.2 X_C with Q_a , Fixed and Transient input condition, $k_{Aa} = 3$, $k_{Ba} = 3$, $Q_b = Q_i$ | 71 |
| 4.5.3 X_C with Q_a , Fixed and Transient input condition, $k_{Aa} = 5$, $k_{Ba} = 3$, $Q_b = Q_i$ | 72 |
| 4.5.4 X_C with Q_a , Fixed and Transient input condition, $k_{Aa} = 1$, $k_{Ba} = 3$, $Q_b = 3 \times Q_i$ | 73 |
| 4.5.5 X_C with Q_a , Fixed and Transient input condition, $k_{Aa} = 3$, $k_{Ba} = 3$, $Q_b = 3 \times Q_i$ | 74 |
| 4.5.6 X_C with Q_a , Fixed and Transient input condition, $k_{Aa} = 5$, $k_{Ba} = 3$, $Q_b = 3 \times Q_i$ | 75 |
| 4.5.7 X_C with Q_a , Fixed and Transient input condition, $k_{Aa} = 1$, $k_{Ba} = 3$, $Q_i = 2 \times Q_b$ | 76 |
| 4.5.8 X_C with Q_a , Fixed and Transient input condition, $k_{Aa} = 3$, $k_{Ba} = 3$, $Q_i = 2 \times Q_b$ | 77 |
| 4.5.9 X_C with Q_a , Fixed and Transient input condition, $k_{Aa} = 5$, $k_{Ba} = 3$, $Q_i = 2 \times Q_b$ | 78 |

LIST OF TABLES

| Table | | Page |
|-------|--|------|
| 4.5.1 | Mole fraction of C, X_C , Fixed and Transient input condition, $k_{Aa}=1$, $k_{Ba}=3$, $Q_b=Q_i$ | 70 |
| 4.5.2 | Mole fraction of C, X_C , Fixed and Transient input condition, $k_{Aa}=3$, $k_{Ba}=3$, $Q_b=Q_i$ | 71 |
| 4.5.3 | Mole fraction of C, X_C , Fixed and Transient input condition, $k_{Aa}=5$, $k_{Ba}=3$, $Q_b=Q_i$ | 72 |
| 4.5.4 | Mole fraction of C, X_C , Fixed and Transient input condition, $k_{Aa}=1$, $k_{Ba}=3$, $Q_b=3 \times Q_i$ | 73 |
| 4.5.5 | Mole fraction of C, X_C , Fixed and Transient input condition, $k_{Aa}=3$, $k_{Ba}=3$, $Q_b=3 \times Q_i$ | 74 |
| 4.5.6 | Mole fraction of C, X_C , Fixed and Transient input condition, $k_{Aa}=5$, $k_{Ba}=3$, $Q_b=3 \times Q_i$ | 75 |
| 4.5.7 | Mole fraction of C, X_C , Fixed and Transient input condition, $k_{Aa}=1$, $k_{Ba}=3$, $Q_i=2 \times Q_b$ | 76 |
| 4.5.8 | Mole fraction of C, X_C , Fixed and Transient input condition, $k_{Aa}=3$, $k_{Ba}=3$, $Q_i=2 \times Q_b$ | 77 |
| 4.5.9 | Mole fraction of C, X_C , Fixed and Transient input condition, $k_{Aa}=5$, $k_{Ba}=3$, $Q_i=2 \times Q_b$ | 78 |

CHAPTER 1

INTRODUCTION

During the past few decades fluidization technology and fluidized-bed reactor operations have seen a tremendous amount of applications in a wide range of process industries. In spite of the extensive application of the fluidization technique, the understanding of the fluidization phenomena is still far from adequate. The engineering design of a fluidized bed is based primarily on past experience along with a trial-and-error approach. An extensive research effort in the area of fluidization during the past decade is indicated by the thousands of published papers and the large numbers of patents issued in the related areas. The understanding of fluidization and design criteria for fluidized bed reactors can be attributed to the complex hydrodynamics of solids and fluids, physical phenomena on chemical rate processes in fluidized bed reactors, and to complicated geometrical factors associated with fluidized-bed units. Unfortunately, little research has been done on the understanding and analysis of adsorption as a significant factor in the overall reaction rate in fixed and fluidized bed reactors. Another problem associated with fluidized-bed operation is the question of unsteady-state phenomena existing between the solid particles and the gas in the bed. Since solid particles are subjected to rapid exposure to a gas phase of varying concentration, there could be different activity associated with the fluidized solids, compared to the steady-state activity of the particles in the bed, like unsteady state condition exists between the solid surface of catalyst and fluid flow. (9, 10)

In the last two decades, extensive research has been performed to study the dynamics of the fluidized bed reactors. Despite all these efforts, it has generally been agreed that the understanding is still incomplete. In particular, the complexity inside the bed has been identified as one of the major technical constraint that needs to be resolved for the optimization of the product. While designing a fluidized-bed reactor, it is essential to know effect of the reaction rate constant, adsorption rate of reactants, desorption rate of reactants and products, and the flow rate on the reacting system.

A variety of chemical reactors are being used in industrial practice, and it should be noted that most industrial chemical reactors present severe challenges to model these systems mathematically. A reaction engineer needs to be familiar with the basic concepts of the mathematical modeling of physical processes. The relative importance and roles of governing equations, constitutive equations, boundary conditions and input data need to be clearly understood while interpreting results and drawing engineering conclusions based on simulation results. Adequate mathematical representation of any complex physical process may require many different mathematical models, perhaps a continuum of models, each having different capabilities, appropriate to its specific objectives. Reaction engineers must recognize the possibility of employing a chain of models to develop the necessary understanding and to obtain the required information to achieve complex reactor engineering objectives. Sometimes it might be easier if there is a hierarchy of mathematical models, each having some unique features and corresponding range of application, which may be used to construct as complete a picture of the physical process as possible. Computational modeling is a very powerful tool and in principle, a

self-consistent, comprehensive mathematical model can be constructed to simulate the behavior of the reactor within the framework. It is often difficult to develop such a mathematical model which addresses the practical engineering problems directly. Instead, it is necessary to use different models to develop the required understanding and information, and combining this with engineering judgment to propose an appropriate reactor engineering design or simulation. Computation modeling certainly enhances the capability of a reaction engineer to make deeper journeys into the underlying physics for a better understanding. It should be used along with other models with different capabilities to construct an overall picture. The necessity of using models and establishing a clear relationship between the reactor engineering objectives and computational flow modeling is described here with the help of a few examples. (30)

The first step in any reaction engineering analysis is formulating a mathematical framework to describe the mechanism by which one chemical species is converted into another. The rate which is described as mass, in moles of a species, transformed per unit time, while the mechanism is the sequence of individual chemical events whose overall result produces the observed transformation. Though knowledge of the mechanism is not necessary for reaction engineering, it is of great value in generalizing and systematizing the reaction kinetics. Knowledge of the rate of transformation, however, is essential for any reaction engineering activity. The rate of transforming one chemical species into another cannot be predicted with accuracy. It is a system-specific quantity which must be determined from experimental measurements. Recent advancements in computational chemistry and molecular modeling have led to some successes in making *a priori*

predictions of reaction kinetics. However, in spite of such progress, most of the practical reaction engineering analysis will have to rely on experimental measurements of reaction kinetics (at least in the immediate or intermediate future).

The development of mathematical models for the simulation of a fluidized bed reactor is presented in this work, which analyzes

1. The competitive adsorption under steady and unsteady state conditions, of reactants in a simple bimolecular reaction on the overall conversion to a product.
2. The effect of inert gas on the total convergence of product.
3. The improvement of reactor performance by applying an oscillating feed rate to one or more components based on the overall conversion to the product.

1.1 MODEL DESCRIPTION

Every industrial chemical process is designed to economically produce a desired product from a variety of treatment steps. Here, we are concerned with a fluidized bed chemical reactor where the fluidized material is the catalyst for the reaction. The design of the reactor is no routine matter and many alternatives can be proposed for a process. In searching for the optimum, it is not just the cost of the reactor that must be minimized. One design may have lower reactor cost, but it must also give the optimum value of material leaving the reactor as a product. Hence, the overall process in the reactor must be considered. The kinetics of reaction in fluidized bed reactor depends on many factors such as reaction rate, adsorption rate, desorption rate, initial concentration of each components in the reactor, maximum surface sites available on the catalyst, concentration

of components per total concentration in the gas phase, volumetric flow rate of components, temperature, pressure, etc.,

In the following presentation, we will discuss the understanding of various aspects of adsorption on the fluidized bed reactor. It is hoped that research in this area will provide more systematic ways of analyzing, designing, and scaling-up fluidized beds.

A fluidized bed reactor is studied under steady state and transient conditions to determine the operating conditions that produce the maximum output for the given reaction kinetics. For purposes of developing a model for fluidized bed reactor, the irreversible bimolecular elementary reaction is proposed in Equation 1.



Reactants A and B can adsorb reversibly to the catalyst surface where the reaction takes place. The product C is formed only on the catalyst surface and immediately desorbs into the fluid. An inert component, I, may be used to promote acceptable fluidization of the solid catalyst, but does not participate in the reaction itself. Figure 1.1 displays the isothermal well-mixed fluidized bed reactor. The catalyst is assumed to be non-porous and mass transfer through the individual catalyst pellet is neglected. Figure 1.2 illustrates the conditions on the catalyst surface.

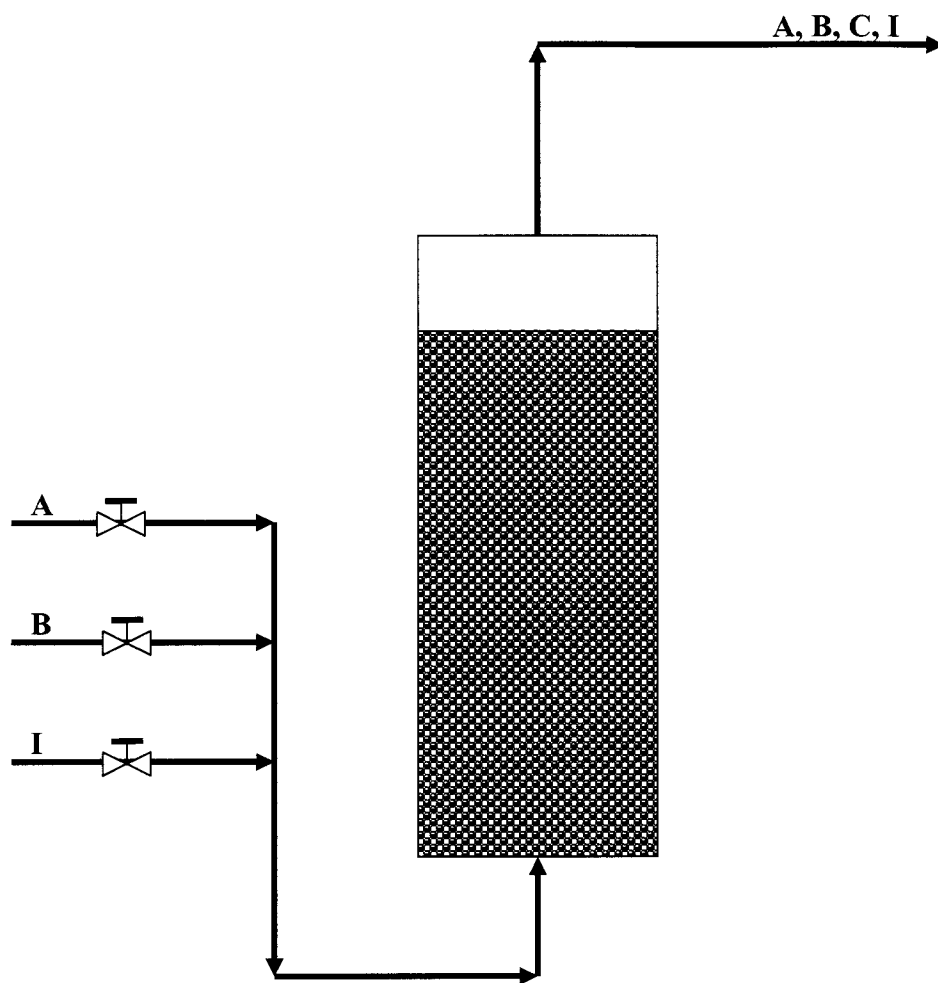


Figure 1.1 Schematic of a Fluidized Bed Reactor

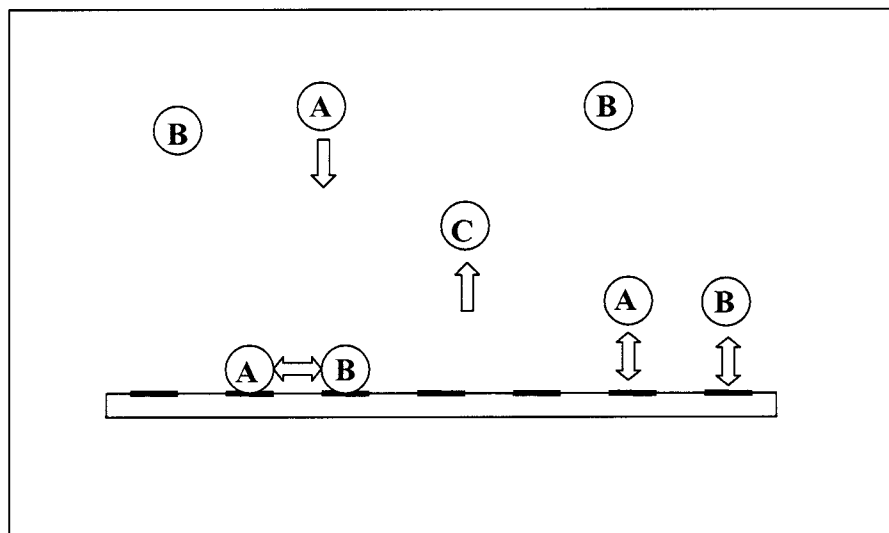


Figure 1.2 Schematic of a Catalyst Surface Reaction

1.2 THEORY

The fluidized bed reactor is studied and simulated numerically by developing the mass balance equations for the surface and fluid concentrations of each component. The kinetic model is based on the assumption that the gas and solid catalyst are well mixed, no catalyst leaves the reactor, desorption of the product C is instantaneous, there is negligible heat generated during the reaction, and the temperature is constant throughout the reactor. The concentration of the reactants A and B, and product C in the fluid are expressed by Equations 1.2.1, 1.2.2, and 1.2.3.

$$V \frac{dC_A}{dt} = Q_0 C_{A,feed} - QC_A - G[k_{Aa} C_A (n_S - n_A - n_B) - k_{Ad} n_A] \quad (1.2.1)$$

$$V \frac{dC_B}{dt} = Q_0 C_{B,feed} - QC_B - G[k_{Ba} C_B (n_S - n_A - n_B) - k_{Bd} n_B] \quad (1.2.2)$$

$$V \frac{dC_C}{dt} = Q_0 C_{C,feed} - QC_C + Gk_r n_A n_B \quad (1.2.3)$$

Where,

V = Volume of the reactor void, m³

G = Mass of catalyst in the reactor, kg

t = Time, sec

C_{A, feed}, C_{B, feed}, and C_{C, feed} = Feed concentrations of each component in the fluid, kg-mole m⁻³

C_A, C_B and C_C = Concentration in the reactor fluid, kg-mole m⁻³

k_{Aa}, k_{Ba} = Adsorption rate constants for components A and B, m³ kgmole⁻¹ sec⁻¹

k_{Ad}, k_{Bd} = Desorption rate constants for components A and B, sec⁻¹

k_r = Reaction rate constant, kg kgmole⁻¹ sec⁻¹

n_s = Maximum number of surface sites on catalyst, kg-mole kg^{-1}

n_A, n_B = Surface concentration of components A and B, kg-mole kg^{-1}

Q_0 = Inlet gas volumetric flow rate, $\text{m}^3 \text{sec}^{-1}$

Q = Volumetric flow rate leaving the reactor, $\text{m}^3 \text{sec}^{-1}$

Since one mole of product is produced for every two moles of reactant consumed, the volumetric flow rate leaving the reactor will be less than what is fed. Equation 1.2.4 relates the outlet flow as a function of the overall reaction rate.

$$Q = Q_0 - \frac{G}{C_f} [(k_{Aa}C_A + k_{Ba}C_B)(n_s - n_A - n_B) - k_{Ad}n_A - k_{Bd}n_B - k_r n_A n_B] \quad (1.2.4)$$

Where

C_f = Total molar concentration in the gas, kg-mole m^{-3}

Activity on the catalyst surface is described in Equations 1.2.5 and 1.2.6 which describe the change of surface concentration of the reactants with time.

$$\frac{dn_A}{dt} = k_{Aa}C_A(n_s - n_A - n_B) - k_{Ad}n_A - k_r n_A n_B \quad (1.2.5)$$

$$\frac{dn_B}{dt} = k_{Ba}C_B(n_s - n_A - n_B) - k_{Bd}n_B - k_r n_A n_B \quad (1.2.6)$$

The concentrations in the gas phase and on the surface are made dimensionless to allow for definite limits on these variables. By this operation, the variables will vary between 0.0 and 1.0. The gas phase and surface concentrations are redefined in Equations 1.2.7-1.2.11.

Redefining the variables:

$$y_A = \frac{n_A}{n_s}, y_B = \frac{n_B}{n_s}, x_A = \frac{C_A}{C_f}, x_B = \frac{C_B}{C_f}, x_C = \frac{C_C}{C_f} \quad (1.2.7-1.2.11)$$

Where:

y_A and y_B = Dimensionless concentration of reactants A and B on the catalyst surface

x_A, x_B and x_C = Dimensionless concentrations of A, B and C in the gas phase

Equations 1.2.1 – 1.2.6 can then be rewritten using redefined variables. The dimensionless surface concentration of each species is given by:

$$\frac{dy_A}{dt} = k_{Aa} C_f x_A (1 - y_A - y_B) - k_{Ad} y_A - k_r n_s y_A y_B \quad (1.2.12)$$

$$\frac{dy_B}{dt} = k_{Ba} C_f x_B (1 - y_A - y_B) - k_{Bd} y_B - k_r n_s y_A y_B \quad (1.2.13)$$

The dimensionless concentration of each species in the gas phase is given by:

$$\frac{dx_A}{dt} = \frac{1}{V} \left[Q_0 x_{A,feed} - Q x_A - G n_s \left[k_{Aa} x_A (1 - y_A - y_B) - \frac{k_{Ad} y_A}{C_f} \right] \right] \quad (1.2.14)$$

$$\frac{dx_B}{dt} = \frac{1}{V} \left[Q_0 x_{B,feed} - Q x_B - G n_s \left[k_{Ba} x_B (1 - y_A - y_B) - \frac{k_{Bd} y_B}{C_f} \right] \right] \quad (1.2.15)$$

$$\frac{dx_C}{dt} = \frac{1}{V} \left[Q_0 x_{C,feed} - Q x_C + G n_s^2 k_r y_A y_B \right] \quad (1.2.16)$$

The volumetric flow rate leaving the reactor with redefined variables:

$$Q = Q_0 - \frac{G n_s}{C_f} \left[(k_{Aa} C_f x_A + k_{Ba} C_f x_B) (1 - y_A - y_B) - k_{Ad} y_A - k_{Bd} y_B - k_r n_s y_A y_B \right] \quad (1.2.17)$$

At steady state, Equations 1.2.12 – 1.2.17 reduce to:

$$0 = k_{Ad} C_f x_A (1 - y_A - y_B) - k_{Ad} y_A - k_r n_s y_A y_B \quad (1.2.18)$$

$$0 = k_{Bd} C_f x_B (1 - y_A - y_B) - k_{Bd} y_B - k_r n_s y_A y_B \quad (1.2.19)$$

$$0 = \left[Q_0 x_{A,feed} - Q x_A - G n_s \left[k_{Aa} x_A (1 - y_A - y_B) - \frac{k_{Ad} y_A}{C_f} \right] \right] \quad (1.2.20)$$

$$0 = \left[Q_0 x_{B,feed} - Q x_B - G n_s \left[k_{Ba} x_B (1 - y_A - y_B) - \frac{k_{Bd} y_B}{C_f} \right] \right] \quad (1.2.21)$$

$$0 = \frac{1}{V} \left[Q_0 x_{C,feed} - Q x_A - G n_s^2 k_r y_A y_B \right] \quad (1.2.22)$$

In order to have the fluid and solid catalyst to be well mixed, the bed must be properly fluidized. To achieve this criterion, the gas feeding the reactor must have sufficient velocity. Fluidization is observed when a bed of solid particles comes in contact with a vertical upward fluid flow, in an intermediate range of flow rates. At low flow rates or velocities, the solid particles rest on one another and on the porous bottom of the column; they are said to be in fixed state. At high flow rates or velocities, the solid particles are conveyed out of the column, and this is known as hydraulic or pneumatic transport. For intermediate values, in a range large enough for practical purposes, each particle becomes individually suspended in the fluid flow, while on the whole the bed remains motionless relative to the column walls; the bed is said to be fluidized.

One of the main practical advantages of fluidization is connected with the liquid-like flowing properties of fluidized beds. Indeed it appears particularly simple and economical

to transport solid particles through pipes, to control the bed height by overflow or to circulate from one bed to another by gravity, thus avoiding the use of standard solid handling equipment, which is often mechanically complex and expensive to operate.

The necessary equipment for fluidizing solid particles with a liquid/gas is schematically shown in Figure 1.1. The vertical columns are often circular in cross-section, sometimes square or rectangular. The inlet section has to produce a uniform fluid velocity distribution throughout the entire cross-section of the column, otherwise fluidized beds exhibit deviations from their ideal behavior, such as channeling or gulf-streaming. This inlet section is often called the homogenizing section.

The minimum fluidization velocity occurs at the moment when the gas velocity allows a packed bed reactor to become a fluidized bed reactor. The bed is fluidized to increase the amount of time and space the gas has with the surface of the catalyst. Fluidization is used to allow all of the surface area of the catalyst to be utilized by the gas to adsorb and react. A generalized model for calculating the minimum fluidization velocity was developed by Wen and Yu *et al.* (31).

$$U_{mf} = \frac{\mu}{\rho_g d_p} \left[[33.7^2 + 0.0408 Ar]^{1/2} - 33.7 \right] \quad (1.2.23)$$

Where,

U_{mf} = Minimum fluidization velocity, $m s^{-1}$

μ = Viscosity of gas, $kg m^{-1} s^{-1}$

ρ_g = Density of gas, $kg m^{-3}$

d_p = Diameter of a particle, m

Ar = Archimedes number, as given in Equation 1.2.24

$$Ar = \frac{d_p^3 \rho_s g (\rho_s - \rho_g)}{\mu^2} \quad (1.2.24)$$

Where,

ρ_s = Density of solid, kg m⁻³

g = Gravitational acceleration, 9.8 m s⁻².

Using the reference conditions of air at 20 °C and 1 atmosphere of pressure, the viscosity is 1.6 x 10⁻⁵ kg m⁻¹ s⁻¹ and the density is 1.29 kg m⁻³. For the reactor in Figure 1.1 the particles have diameter of 2 x 10⁻³ m and density of 2500 kg m⁻³, King *et al.* (20). The Archimedes number is calculated to be 1.0 x 10⁶. Using the calculated Archimedes number the minimum fluidization velocity, U_{mf} (m s⁻¹), can be calculated.

The minimum fluidization velocity is calculated to be 1.0 m s⁻¹ under the above conditions. A relationship between the excess velocity, U_{xs} , and the actual velocity U (m s⁻¹) is shown in Equation 1.2.25.

$$U_{xs} = U - U_{mf} \quad (1.2.25)$$

The excess velocity is predetermined by the Archimedes number to be between 1.8 and 8.0 m s⁻¹. The velocity is then determined by Equation 1.2.25 to be 3.0 m s⁻¹. Using the diameter of the fluidized bed in this experiment of 0.064 m, the volumetric flow rate of

the gas, Q_0 , is calculated to be $9.6 \times 10^{-3} \text{ m}^3 \text{ s}^{-1}$. The volume of the gas in the reactor is determined by the void fraction and the weight of the catalyst, G , in the bed. With a void fraction of 0.77 and 10.0 kg of catalyst, the volume of the gas in the bed, V , is calculated to be $13.5 \times 10^{-3} \text{ m}^3$ King *et al.* (20). The total concentration of the gas, C_f , is set constant at $0.04 \text{ kg-mole m}^{-3}$. For any temperature and pressure the maximum surface concentration on the catalyst used in this fluidized bed was adapted from experiments carried out by Price *et al.* (26). The maximum surface concentration, n_s , is a function of the specific surface area of the catalyst, the affinity of the gas to the solid, and the size of the individual gas molecule. Literature values have given an average value of $0.001 \text{ kg-mole kg}^{-1}$, which will be used in this study.

CHAPTER 2

LITERATURE SURVEY

2.1 INDUSTRIAL APPLICATION

Since the early stages of their introduction in industrial practices, fluid beds have been used as chemical reactors. The old applications in the Winkler coal gasifiers (ca. 1920) and coal combustions are being revived and fluid bed reactors can be found today in the chemical, petroleum, environmental, metallurgical, and energy industries. Fluidized bed reactors played a key role in the widespread acceptance of catalytic cracking units in oil refineries, and the success of this operation paved the way for many other reactor applications in catalytic processes in the petrochemical and chemical industries such as fluid catalytic cracking, phthalic anhydride production, oxychlorination of ethylene, acrylonitrile production, chlorine production from HCl, alkylchloride production, etc.

The reason why a fluid bed reactor is selected for a certain process is often its favorable heat transport properties or its convenience for solids handling. The main objective of the operation is usually to bring gas in contact with a solid to achieve chemical conversion of the gas, the solid being catalyst or an inert heat carrier. Sometimes the objective is also to convert the solid and in that case, as in the catalyzed gas reaction, the solids flow and its behavior in the fluid bed have to be described. (16, 17)

2.2 ADVANTAGES AND DISADVANTAGES OF FLUIDIZED BED

The fluidized bed has desirable and undesirable characteristics. The advantages are:

1. The smooth, liquid-like flow of particles allows continuous automatically controlled operations with easy handling.
2. The rapid mixing of solids leads to isothermal conditions throughout the reactor; hence the operation can be controlled simply and reliably.
3. The whole vessel of well-mixed solids represents a large thermal flywheel that resists rapid temperature changes, responds slowly to abrupt changes in operating conditions, and gives a large margin of safety in avoiding temperature runaways for highly exothermic reactions.
4. The circulation of solids between two fluidized beds makes it possible to remove (or add) the vast quantities of heat produced (or needed) in large reactors.
5. It is suitable for large-scale operations.
6. Heat and mass transfer rates between gas and particulates are high when compared with other modes of contacting.
7. The rate of heat transfer between a fluidized bed and immersed object is high; hence heat exchangers within fluidized bed require relatively small surface areas.

Its disadvantages are:

1. For bubbling beds of particles, the difficult-to-describe flow of gas, with its large deviations from plug flow, represents inefficient contacting. This becomes especially serious when high conversion of gaseous reactant or high selectivity of a reaction intermediate is required.
2. The rapid mixing of solids in the bed leads to non-uniform residence times of solids in the reactor. For continuous treatment of solids, this gives a non-uniform product

and poorer performance, especially at high conversion levels. For catalytic reactions, the movements of porous catalyst particles, which continually capture and release reactant gas molecules, contribute to the backmixing of gaseous reactant, thereby reducing yield and performance.

3. Friable solids are pulverized and entrained by the gas and must be replaced.
4. Erosion of pipes and vessels from abrasion by particles can be serious.
5. For noncatalytic operations at high temperature, the agglomeration and sintering of fine particles can require a lowering in temperature of operations, thereby reducing the reaction rate considerably.

The compelling advantages of overall economy of fluidized contacting have been responsible for its successful use in industrial operations. But such success depends on the understanding and overcoming its disadvantages. (4)

2.4 THE UNIT OPERATION OF ADSORPTION

Adsorption concerns itself with the concentration, as the result of surface forces existing on a solid, of gases, liquids or solutes (i.e., solids dissolved in a solvent), dispersed materials or colloids. The nature of these surface forces is incompletely understood. The solids, termed “adsorbents” may effect concentration, localization, fixation, or separation of gases from gases, vapors from gases, liquids from liquids, solutes and dispersed materials from solutions. The extent of adsorption is large or small, depending on the nature and character of adsorbent and the adsorbate, that is, the material concentrated, localized, fixed or separated. The adsorbent may be employed only once, as in the case of carbon or chars, which remove odors or taste from water to make it potable, and then be

discarded; or it may be used once and then be removed and treated to eliminate the adsorbate and be rendered fit for re-use, a process termed “reactivation”; or it may be worked in such a manner as to be used, reactivated in place, and re-used in cyclic procedures. Adsorbents are specific in their nature and properties. From the application viewpoint, adsorption processes are often subdivided into:

1. Separation of gases from gases, as deodorizing of air, elimination of toxic gases.
2. Separation of vapors from gases, as recovery of solvents, drying of gases, dehumidification.
3. Separation of solutes and colloids from solutions, as decolorizing and clarifying of liquids.
4. Separation of ions from solutions, as concentrations of metals on adsorbents, recovery from wastes.
5. Removal of ions from solution, either partly as in water softening, or wholly as in demineralization.
6. Separation of dissolved gases or suspended solids from liquids, as in water treatment, removal of odors and tastes.
7. Concentration of dissolved materials, often toxic in nature, to eliminate them from liquids, as in the case of medicinal carbons, which take up poisonous chemical compounds.
8. Fractionation by selective adsorption of gases from gases, vapors from gases, vapors from vapors, liquids from liquids, dissolved materials from other solutes, and then concentrations of these.

9. Continuous fractionation by differential adsorption and desorption, with the adsorbent in motion rather than fixed in place, with continuous production of separated products as in hypersorption.

Adsorption may be defined in terms of unit operation in the chemical engineering sense as that operation which deals primarily with the utilization of surface forces and the concentration of materials on the surface of solids bodies referred to as adsorbents. The major chemical engineering use of this “unit operation” is in a manner supplementary or complementary to other unit operations. Adsorption should be sharply differentiated from absorption in that adsorption is commonly without chemical reactions between the adsorbent and the adsorbate, while absorption refers to more or less permanent chemical reaction or phase change as a function of the operation. A gas or vapor brought into contact with a solid substance has a tendency to collect on the surface of the solid. This phenomenon is known as adsorption. The term absorption, on the other hand, is used to describe the phenomenon that occurs when a gas or vapor penetrates the solid structure, producing a solid solution. Adsorption may occur alone but also may be accompanied by chemical reaction or the solution of the gas in the mass of solid. The general term “sorption” has been suggested to apply when a gas or vapor is taken up by a solid. The adsorbing solid, or adsorbent, is generally an externally porous “solid foam” with large internal surfaces, its external surface comprising only a small part of the total surfaces. Diffusion of the gas adsorbate into these ultramicroscopic pores and capillaries is easily confused with the absorptive process of solution in the interior of the solid. However, as long as the gas does not penetrate into the field of force that exists between the atoms, ions, or molecules inside the solid, it is considered adsorbed on the surface of the solid

even if this surface is an internal one. The adsorbed atoms or molecules may be bound to the surface of the solid in different ways: there may be a weak interaction between solid and gas, similar to condensation, or a strong interaction, similar to chemical reaction. The former is called physical or van der Waals adsorption since the forces involved are the same as the van der Waals forces that produce condensation in liquids; the latter, termed “chemisorption,” is also known as “activated adsorption,” which implies that this type of adsorption requires activation energies much the same as do chemical reactions. The commercially important solid adsorbents are, Fuller’s earth, bauxite, acid-treated clays, bone char or bone black, decolorizing carbons and water carbons, gas-adsorbent carbon, alumina, silica gel, ion-exchange materials, base-exchange silicates, synthetic-resin exchangers, medicinal carbons, metal-adsorbent chars, bentonites and acid-treated clays, magnesia, etc. (3)

Molecules of adsorbate distribute themselves between the gas phase and the adsorbed phase practically instantaneously in some cases, in others at a measurable rate, until a state of equilibrium is reached. Although the study of adsorption deals with both rate processes and equilibria, by far the most work has been done on equilibria, as true adsorption processes are very rapid. On the other hand, equilibria are seldom of importance in practice, rate being a factor of major consideration, as in the adsorption of war gases where speed of action, as well as adsorptive capacity, is of the utmost importance (4).

Adsorption phenomena are operative in most natural physical, biological, and chemical systems, and adsorption operations employing solids such as activated carbon and synthetic resins are used widely in industrial applications and for purification of waters and wastewaters. The process of adsorption involves separation of a substance from one phase accompanied by its accumulation or concentration at the surface of another. Adsorption accompanied by a single step or multiple reactions is encountered in many industrial processes. A number of specific complex reaction schemes such as two-step, consecutive, etc. have been analyzed in the literature.

2.5 SUMMARIES

Reshetnikov *et al.* (28) studied the performance enhancement by unsteady state reactor operation: theoretical analysis for a two-site kinetic model. The experiment focused on two types of kinetic models. Model I assumed that one of the active sites is blocked by a reactant. Model II suggested that a transformation of active sites takes place by forced oscillations of temperature and feed concentration and by catalyst circulation between two reactors in a dual reactor system. It was found overall that by using kinetic model I that the mean reaction rates were two times higher than steady state and kinetic model II showed a 20% increase in product selectivity. This concluded that unsteady state operation increased reactor performance. Increasing of carbon monoxide methanation rate by forced feed composition cycling was the experimental study conducted by Klusacek *et al.* (21). The feed concentration was changed in two ways. Step changes were used to observe elementary system dynamics and forced feed composition cycling to observe the effect on the time-averaged reaction rate. It was found that forced feed

composition cycling increased the reaction rate. This held true for any composition of the feed including the composition that led to the steady state maximum. It had been found that steady state activity of a catalyst could be significantly improved through operating at unsteady state conditions. Hoebink *et al.* (13) found that operating under transient conditions increased reactor performance due to non-linear reactor kinetics during CO oxidation in fixed bed reactor with high frequency cycling of the feed. Kim *et al.* (19) studied the CCO oxidation in hydrogen rich mixtures on Pt/aluminum catalyst, and established a link between adsorption of CO and temperature. More studies can be found in Quah *et al.* (27) and Klusacek *et al.* (21, 22). Competitive diffusion-adsorption of polymers of differing chain lengths on solid surfaces was observed in the experiment by Devotta *et al.* (7). Their experiment focused on polymer competitive adsorption with different polymer molecular weights. It was shown that higher molecular weight components adsorb better than lower molecular weight components. The results showed that the higher molecular weight polymer is thermodynamically favored over the lower molecular weight polymer. It was also found that desorption for the short chain polymer is faster than the longer chain polymer, and that at short times the short chain polymer adsorbed faster than the long chain polymer. However, at long times, since the long chain polymer was thermodynamically favored over the short chain polymer, the short chain polymer desorbed much quicker. Studies conducted by Das *et al.* (6), focused on the non-uniform adsorption of NO, O₂, and SO₂ on the surface of a Na- γ -Al₂O₃ sorbent.

CHAPTER 3

METHOD AND PROCEDURES

The steady state and non-steady state model equations governing the process are quite complex, non-linear and coupled and have no analytical solution. The Newton-Raphson technique was employed for solving the steady state equations and a fourth-order Runge-Kutta algorithm was used to solve the dynamic equations. The Golden Search method was used for optimizing the steady state equations. Details of the programming codes for both models are shown in the Appendix A.I.1 and A.II.1. By supplying the feed flow rates of each species and the physical parameters of the reactor and the various rate constants, the reactor outlet concentration of all species was determined. The objective was to maximize the production of the product C under applied initial conditions.

To understand the effect of adsorption phenomena on the reaction kinetics of fluidized bed reactor, two different computational models were developed: 1) steady-state model and 2) dynamic model, with and without feed oscillation.

The first order desorption rate constants (k_{Ad} and k_{Bd}) were held constant at 0.1 sec^{-1} throughout the entire study. The volume of the void (V) and the mass of the catalyst (G) were also held constant at 13.3 liters and 10,000 g, respectively. The surface saturation constant, n_s , was maintained at $0.001 \text{ kg-moles kg}^{-1}$, and the molar concentration of the fluid in the reactor void, $C_{f,s}$, was set to $0.04 \text{ kg-moles m}^{-3}$. In the dynamic model, the reaction rate, k_r was held at $2500 \text{ kg kg-mole}^{-1} \text{ sec}^{-1}$, irrespective to steady state model

where two values of reaction rate constant, 1250 and 2500 kg kg-mole⁻¹ sec⁻¹, King *et al.* (20). Adsorption rate constants of the feed components were varied to determine their contribution to the overall conversion of reactants into the product. The dynamic model equations were solved using a fourth-order Runge-Kutta algorithm and the Visual Basic code developed to solve these equations can be found in Appendix A.II.1.

Experimental and theoretical studies on catalysts during the last decades have given evidence that reactor performance under the unsteady state conditions can lead to improve process efficiency compared to steady state condition. Under the transient conditions it is possible to maintain the catalyst surface in an optimal state, increasing the mean reaction rate and selectivity towards a specific product, resulting in an enhanced reactor performance. There have been a number of theoretical attempts to model reaction schemes and to distinguish classes of chemical reaction, for which the increased efficiency under unsteady state conditions can be predicted (2, 10-13). The present study was aimed at the comparative study of the reaction efficiency under the unsteady state conditions created via sinusoidal input in reactor system. Both models were used for this study. Sinusoidal variation in flow rates of the feed components was introduced in the dynamic model, as shown in Equation 3.1 and depicted in Figure 3.1:

$$Q_{i,feed} = Q_{i,base} + \text{Amp} \times \text{SIN}(\tau \times t) \quad (3.1)$$

Where,

$Q_{i, feed}$ = Volumetric feed flow rate of component i at time t, liters sec⁻¹

$Q_{i, base}$ = Time-averaged feed flow rate of component i, liters sec⁻¹

Amp = Amplitude, set at 0.8 throughout model runs, liters sec⁻¹

t = time, sec

$T = 0.1$, sec

Frequency of the wave = $2\pi / T$, sec^{-1} (3.2)

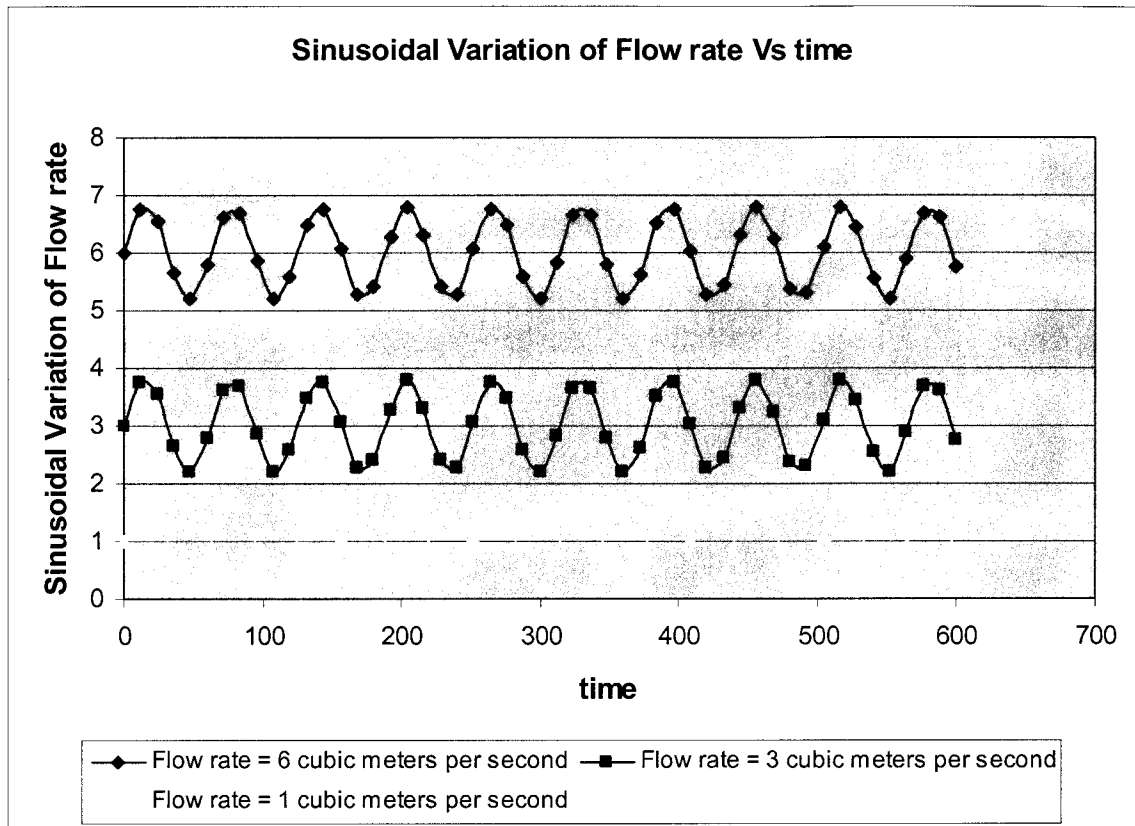


Figure 3.1 Sinusoidal Variation of Flow rate

CHAPTER 4

RESULTS AND DISCUSSION

4.1 OPTIMIZATION WITH SLOW AND FAST REACTION RATE FOR STEADY STATE MODEL

The reactor output of the product was maximized for various combinations of the adsorption rate constants of the reactants at two different values of the reaction rate constant, k_r : $2500 \text{ kg kg-mole}^{-1} \text{ sec}^{-1}$ and $1250 \text{ kg kg-mole}^{-1} \text{ sec}^{-1}$. The total flow of feed in the reactor was held at $9.6 \times 10^{-3} \text{ m}^3 \text{ sec}^{-1}$ for the steady state tests. Volume was held constant at 13.3 liters along with the catalyst mass of 10,000 grams. The mole fraction of C was maximized by varying the mole fractions of A and B in the feed. This optimization was achieved by employing the Golden Search method for optimization and Newton-Raphson for solving the set of nonlinear equations.

Figure 4.1.1 shows the results obtained from the model run where the reaction rate was set at $1250 \text{ kg kg-mole}^{-1} \text{ sec}^{-1}$ which is referred here as slow reaction. The maximum value of the mole fraction of the product, X_c is plotted against the two adsorption rate constants, k_{Aa} and k_{Ba} ($\text{m}^3 \text{ kgmole}^{-1} \text{ sec}^{-1}$). It is observed from this figure that the maximum value of X_c increases as both k_{Aa} and k_{Ba} increase which indicates that the adsorption rate of both reactants limits the overall reaction conversion.

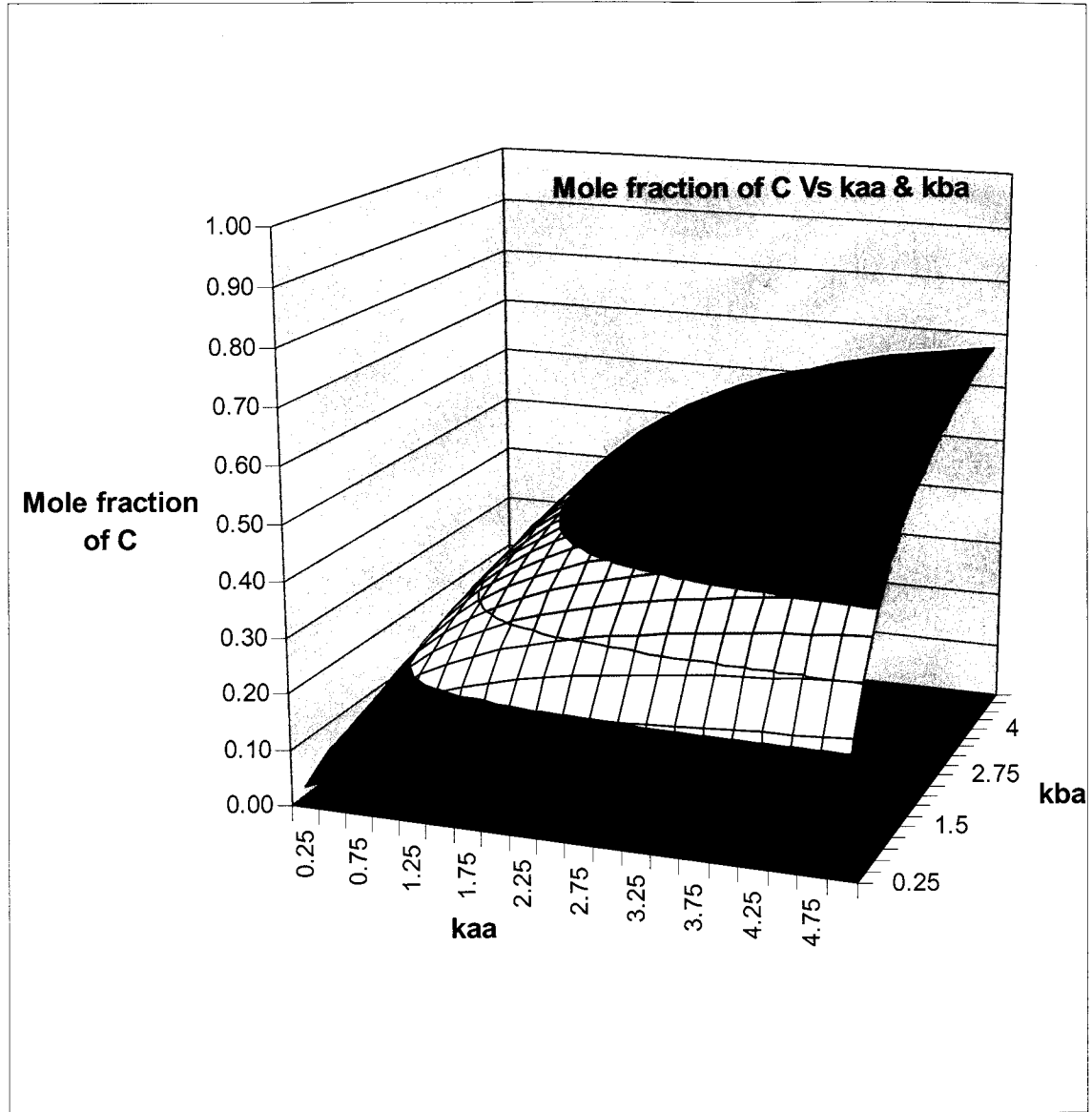


Figure 4.1.1 Mole fraction of C (X_c) with Adsorption rate k_{Aa} and k_{Ba} ($m^3 \text{ kgmole}^{-1} \text{ sec}^{-1}$), Reaction rate $k_r = 1250 \text{ kg kg-mole}^{-1} \text{ sec}^{-1}$

Figure 4.1.2 shows the results where the reaction rate constant is doubled to $2500 \text{ kg kg-mole}^{-1} \text{ sec}^{-1}$. Even at this high value of the reaction rate constant, little increase is observed in the output of the product. In all runs it was determined that the product is maximized when no inert is present in the feed.

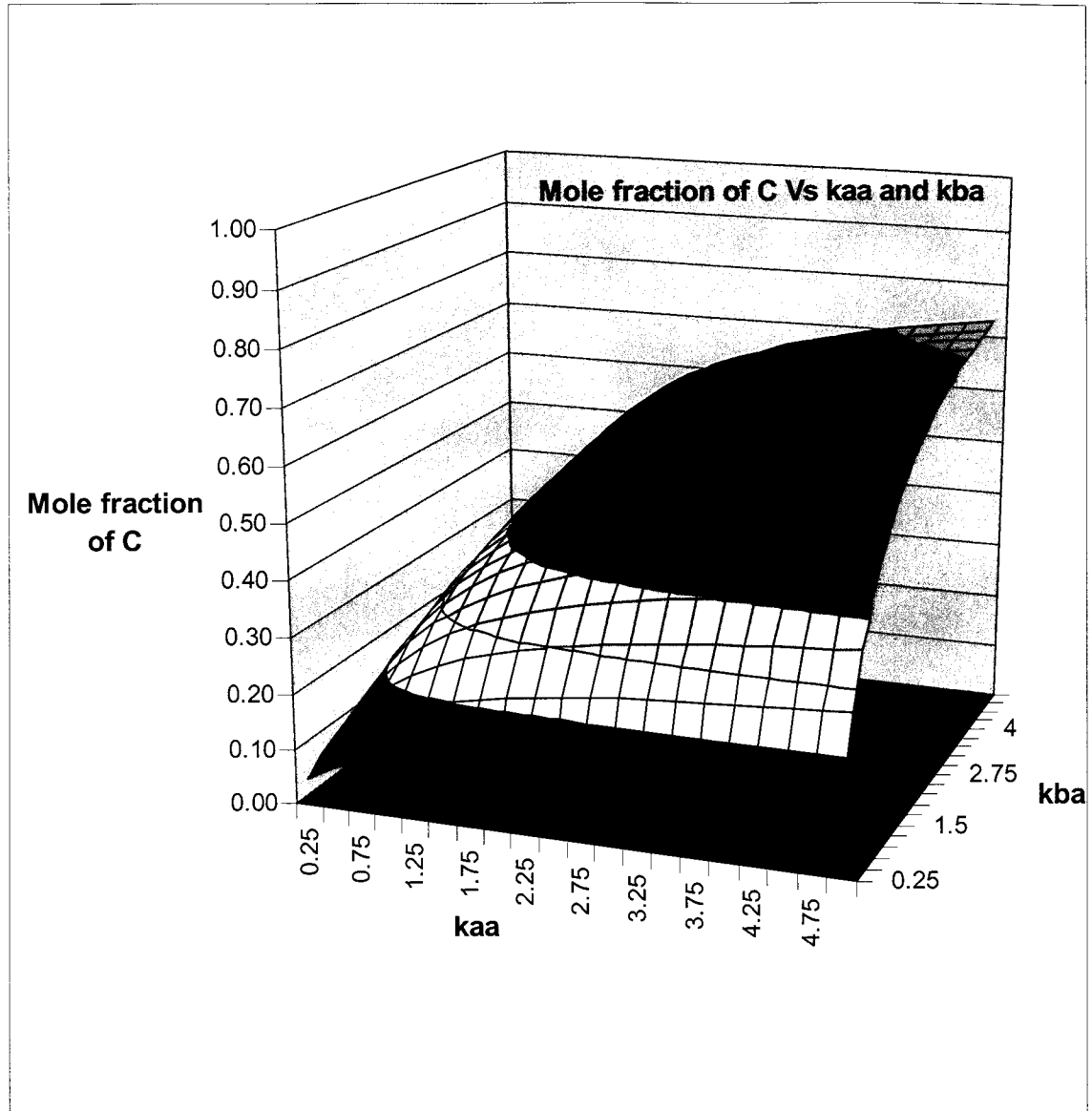


Figure 4.1.2 Mole fraction of C (X_c) with Adsorption rate k_{Aa} and k_{Ba} ($m^3 \text{ kgmole}^{-1} \text{ sec}^{-1}$), Reaction rate $k_r = 2500 \text{ kg kg-mole}^{-1} \text{ sec}^{-1}$

Figures 4.1.3 and 4.1.4 show the mole fraction of components A in the feed which corresponds to the maximum production of the product. Here it can be seen that at a fixed value of k_{Ba} , the optimum mole fraction of A in the feed decreases as k_{Aa} increases. This is due to the competition of the two reactants for adsorption sites. When the adsorption rate constants for A and B are equal, the feed should contain an equimolar

concentration for both reactants. Figures 4.1.5 and 4.1.6 show the optimum feed concentration of B in the feed as a function of the two adsorption rate constants. It can also be seen that at a fixed value of k_{Ba} , the optimum mole fraction of B in the feed increases as k_{Aa} increases.

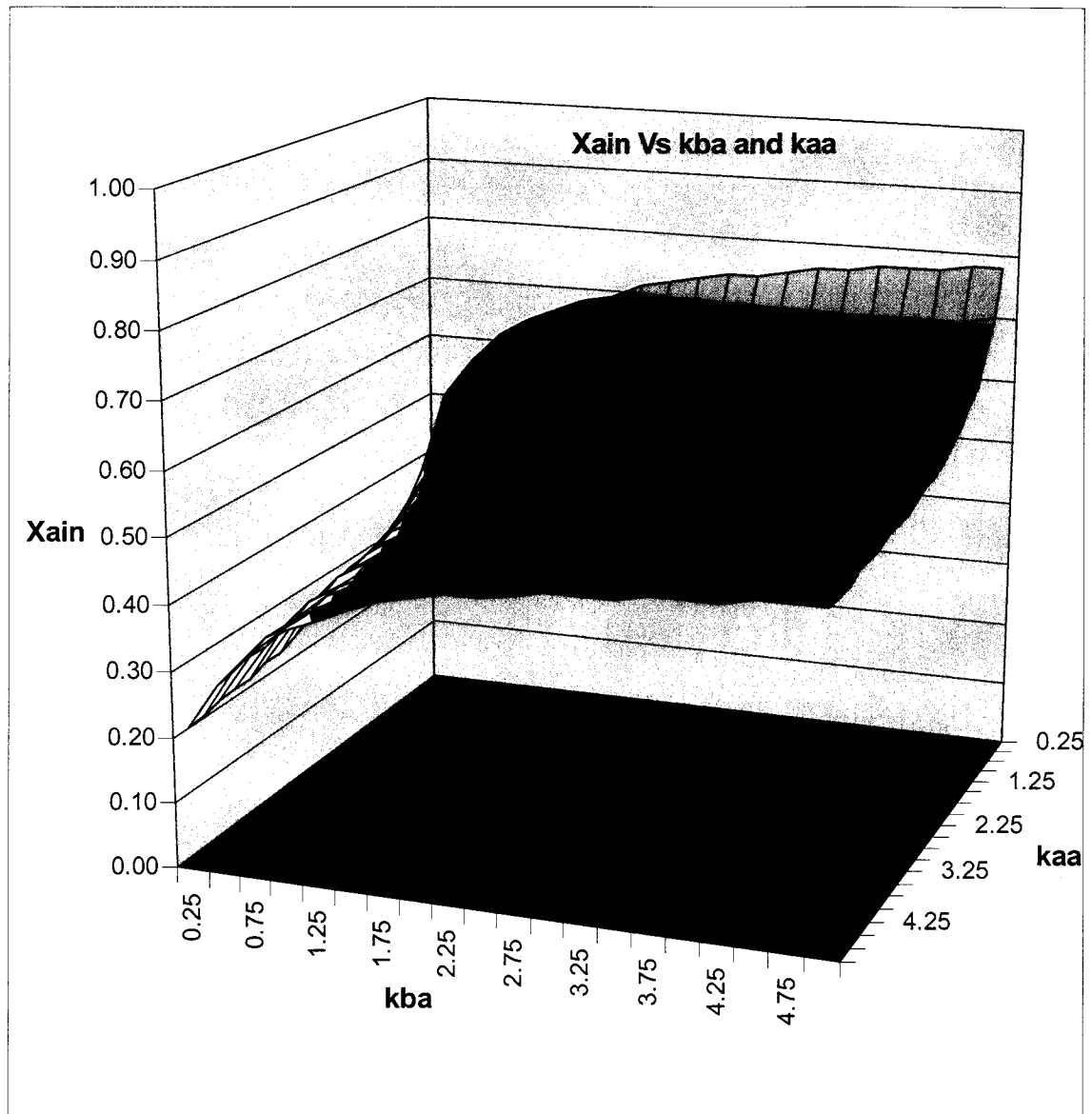


Figure 4.1.3 X_{ain} with Adsorption rate k_{Aa} and k_{Ba} ($m^3 \text{ kgmole}^{-1} \text{ sec}^{-1}$),
Reaction rate $k_r = 1250 \text{ kg kg-mole}^{-1} \text{ sec}^{-1}$

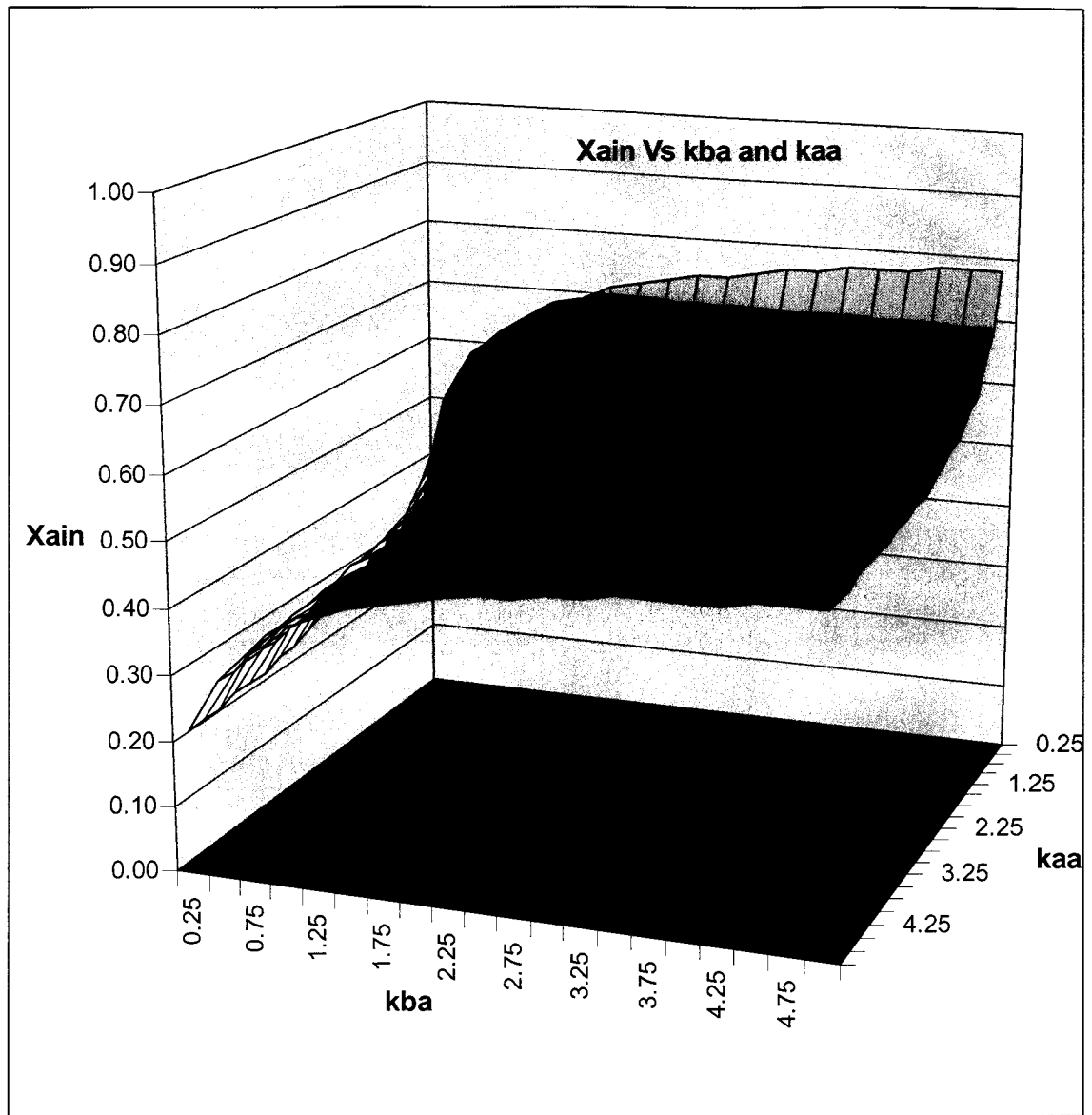


Figure 4.1.4 X_{ain} with Adsorption rate k_{Aa} and k_{Ba} ($m^3 \text{ kgmole}^{-1} \text{ sec}^{-1}$),
 Reaction rate $k_r = 2500 \text{ kg kg-mole}^{-1} \text{ sec}^{-1}$

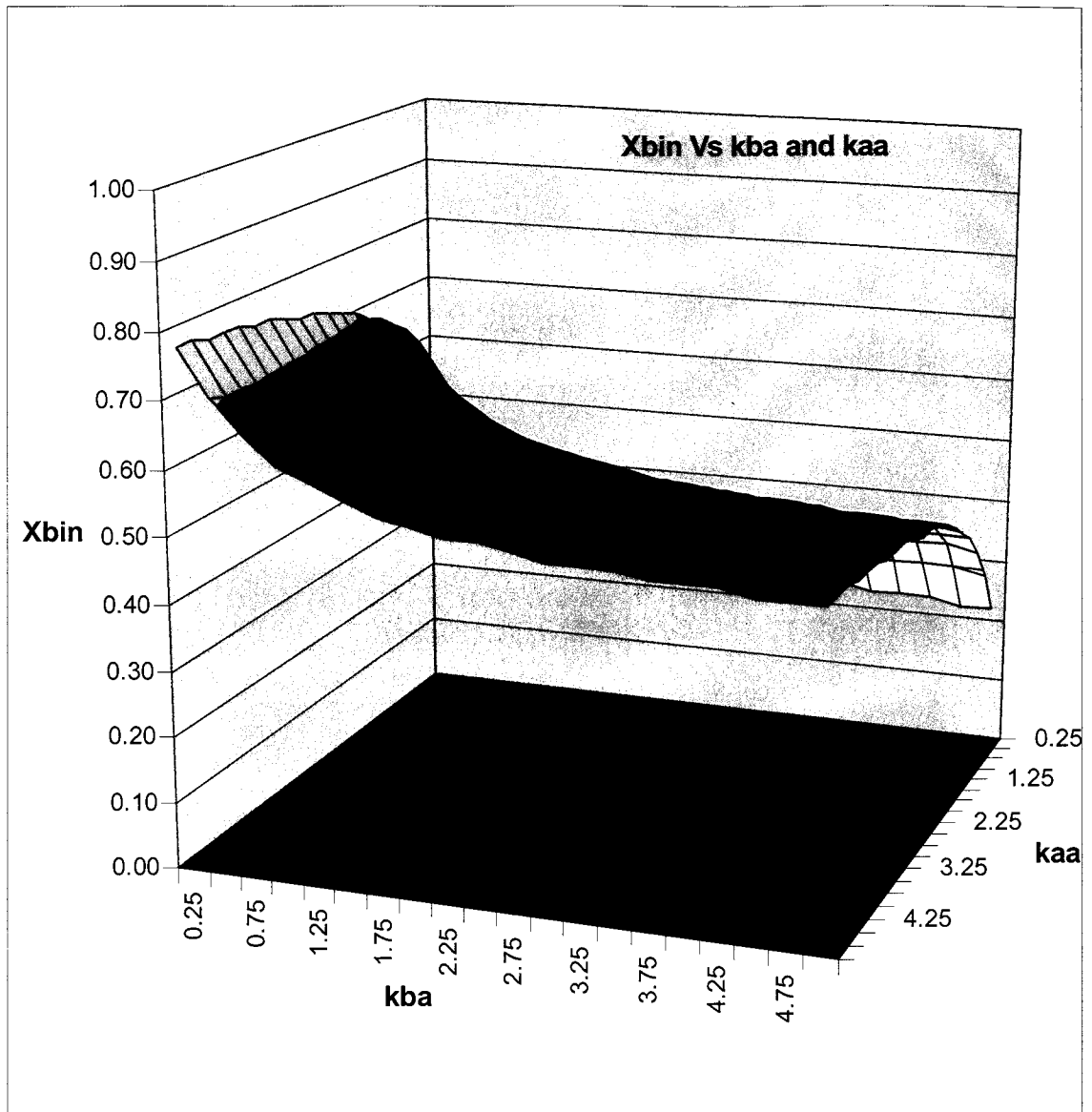


Figure 4.1.5 X_{bin} with Adsorption rate k_{Aa} and k_{Ba} ($m^3 \text{ kgmole}^{-1} \text{ sec}^{-1}$),
 Reaction rate = $1250 \text{ kg kg-mole}^{-1} \text{ sec}^{-1}$

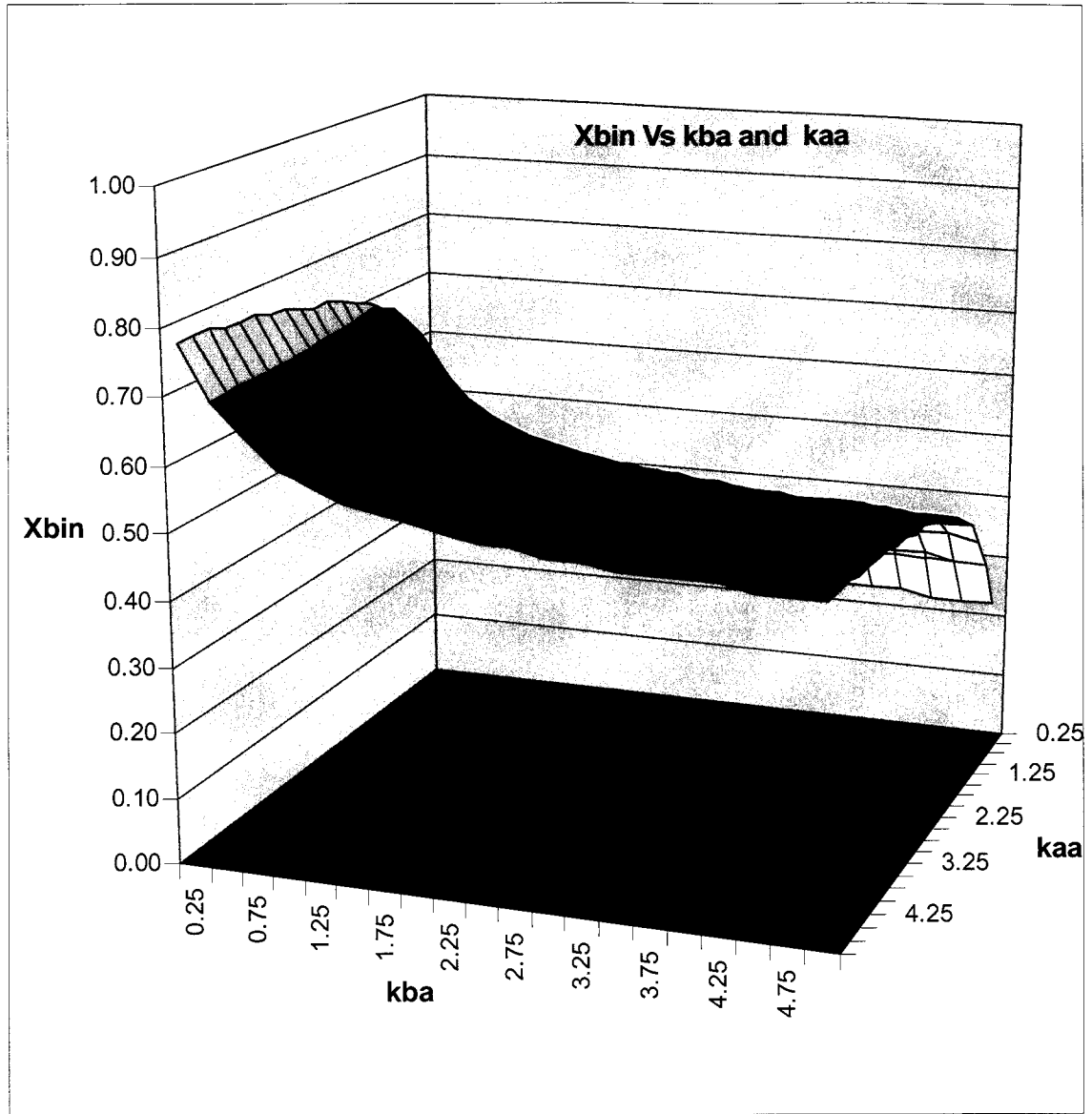


Figure 4.1.6 X_{bin} with Adsorption rate k_{Aa} and k_{Ba} ($m^3 \text{ kgmole}^{-1} \text{ sec}^{-1}$),
 Reaction rate $k_r = 2500 \text{ kg kg-mole}^{-1} \text{ sec}^{-1}$

The outlet concentrations of components A and B are shown in Figures 4.1.7 through 4.1.10.

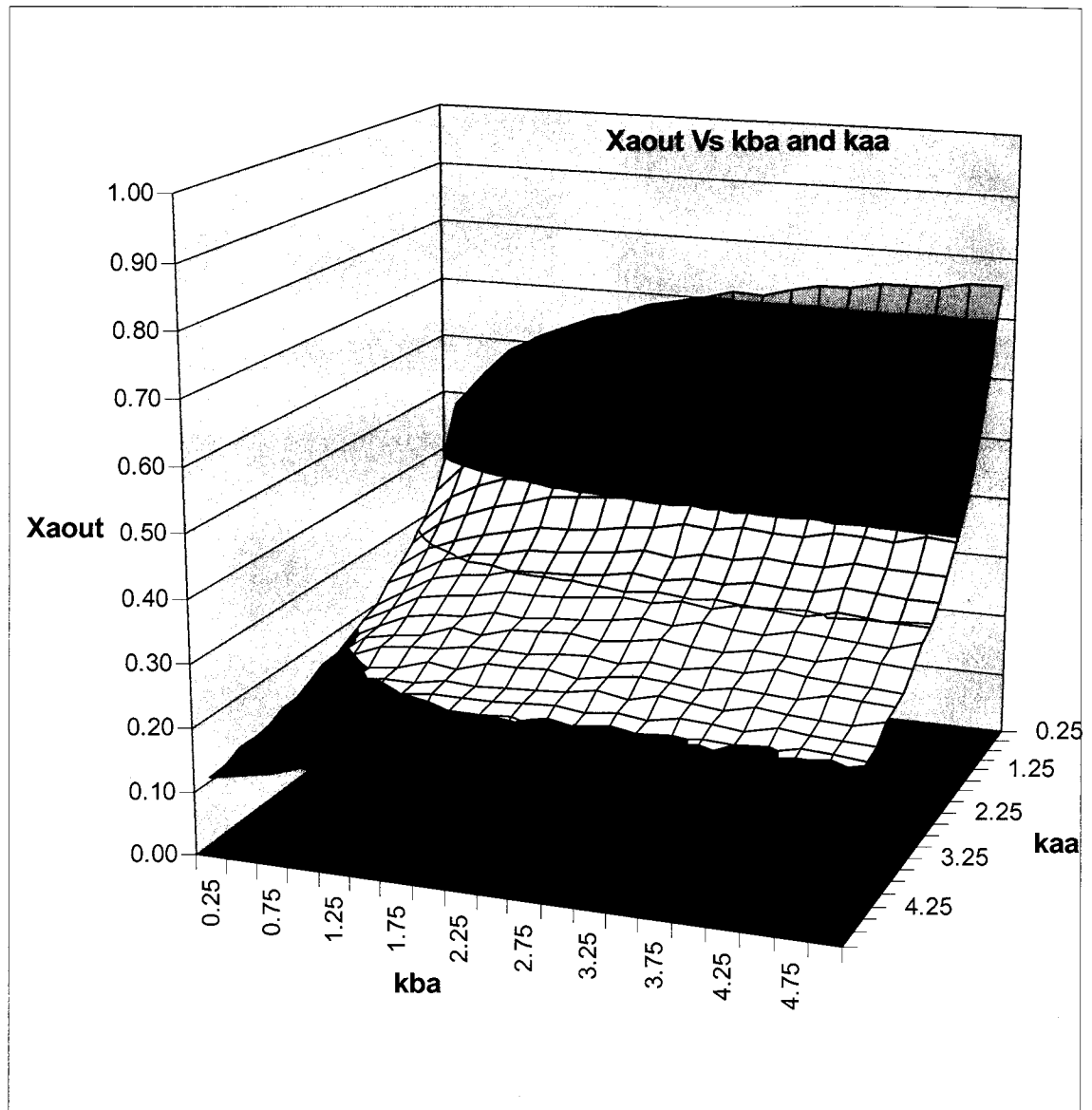


Figure 4.1.7 X_{aout} with Adsorption rate k_{Aa} and k_{Ba} ($m^3 \text{ kgmole}^{-1} \text{ sec}^{-1}$),
Reaction rate $k_r = 1250 \text{ kg kg-mole}^{-1} \text{ sec}^{-1}$

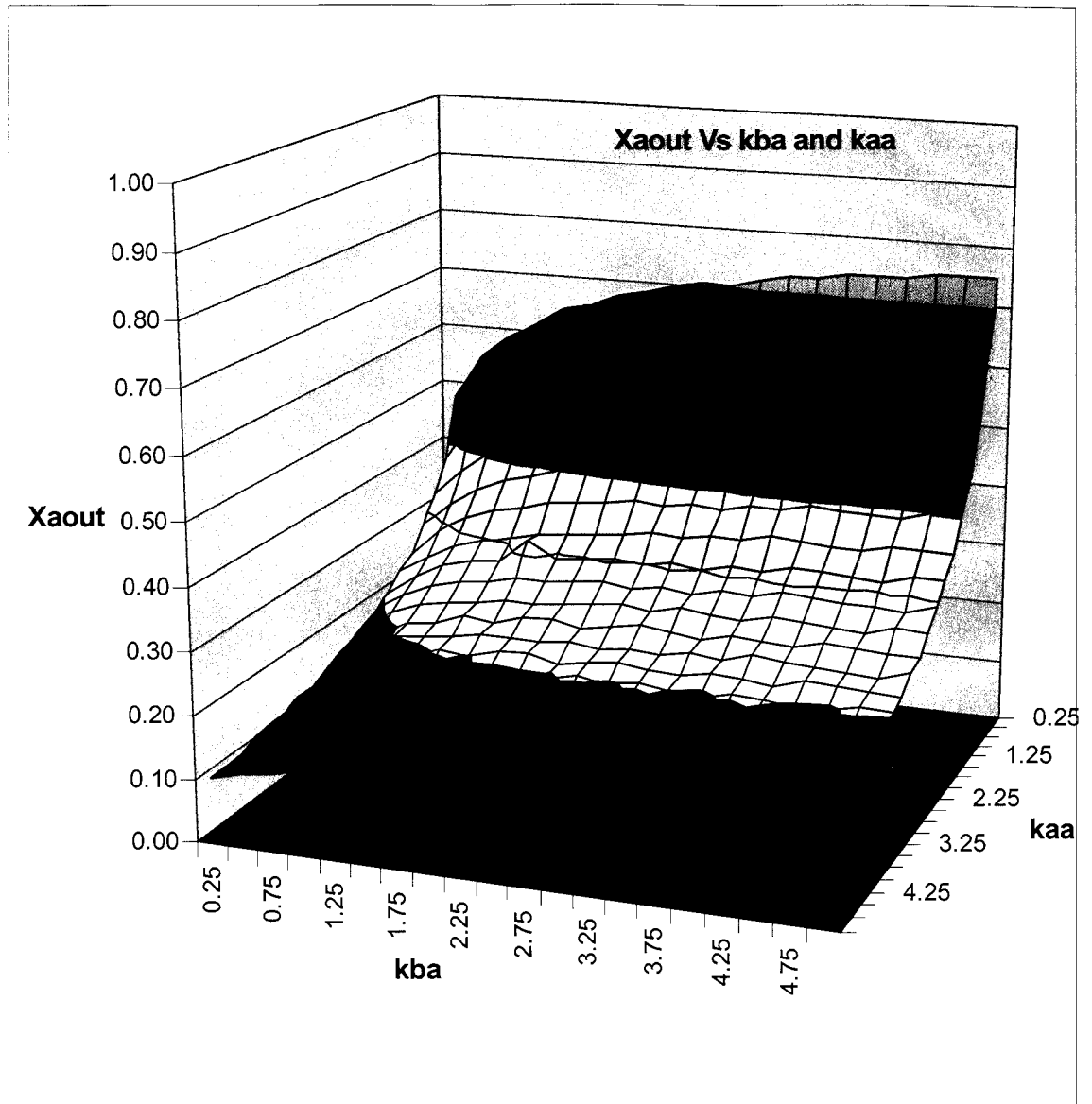


Figure 4.1.8 X_{aout} with Adsorption rate k_{Aa} and k_{Ba} ($m^3 \text{ kgmole}^{-1} \text{ sec}^{-1}$),
 Reaction rate $k_r = 2500 \text{ kg kg-mole}^{-1} \text{ sec}^{-1}$

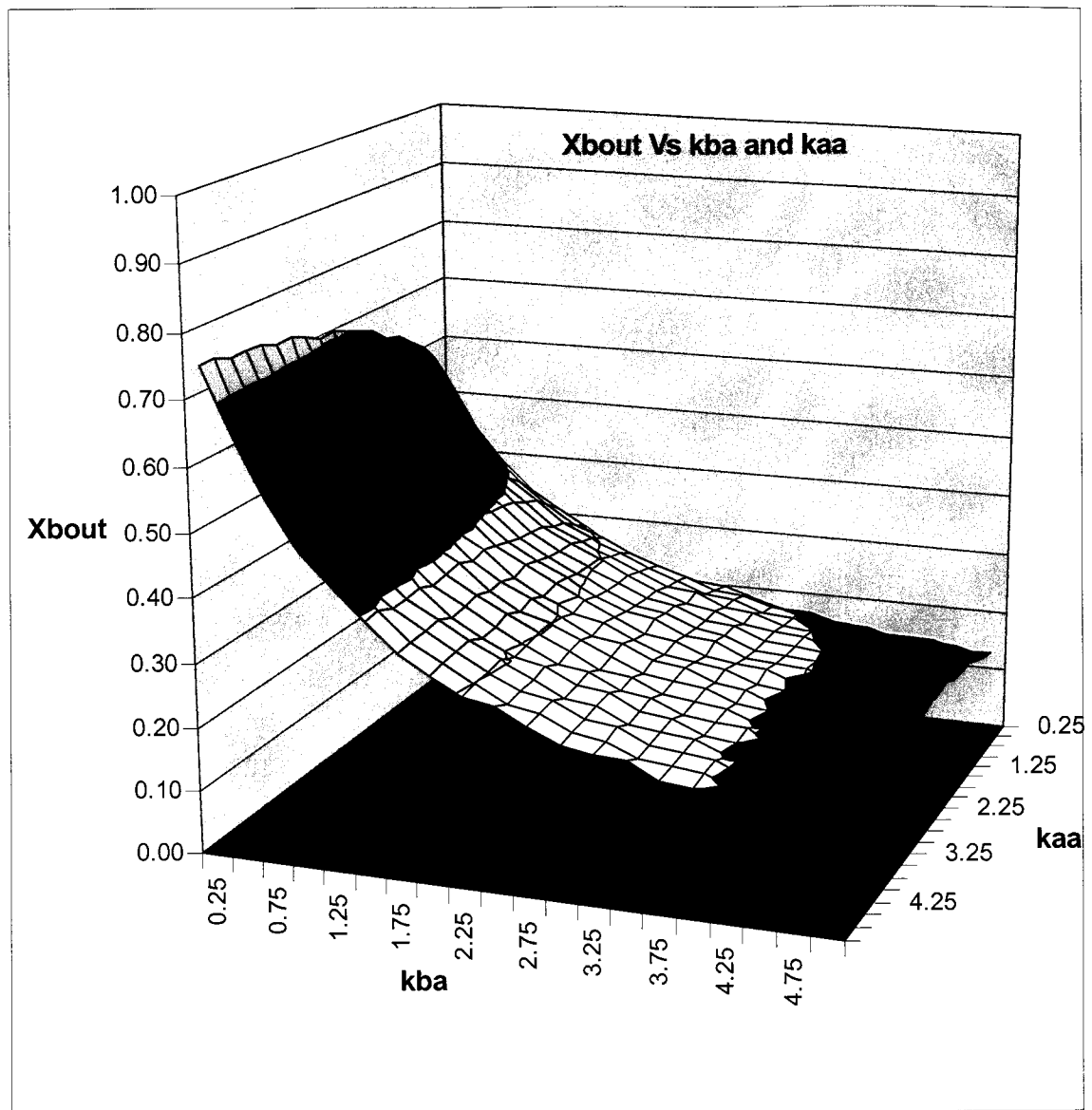


Figure 4.1.9 X_{bout} with Adsorption rate k_{Aa} and k_{Ba} ($\text{m}^3 \text{kgmole}^{-1} \text{sec}^{-1}$),
 Reaction rate $k_r = 1250 \text{ kg kg-mole}^{-1} \text{sec}^{-1}$

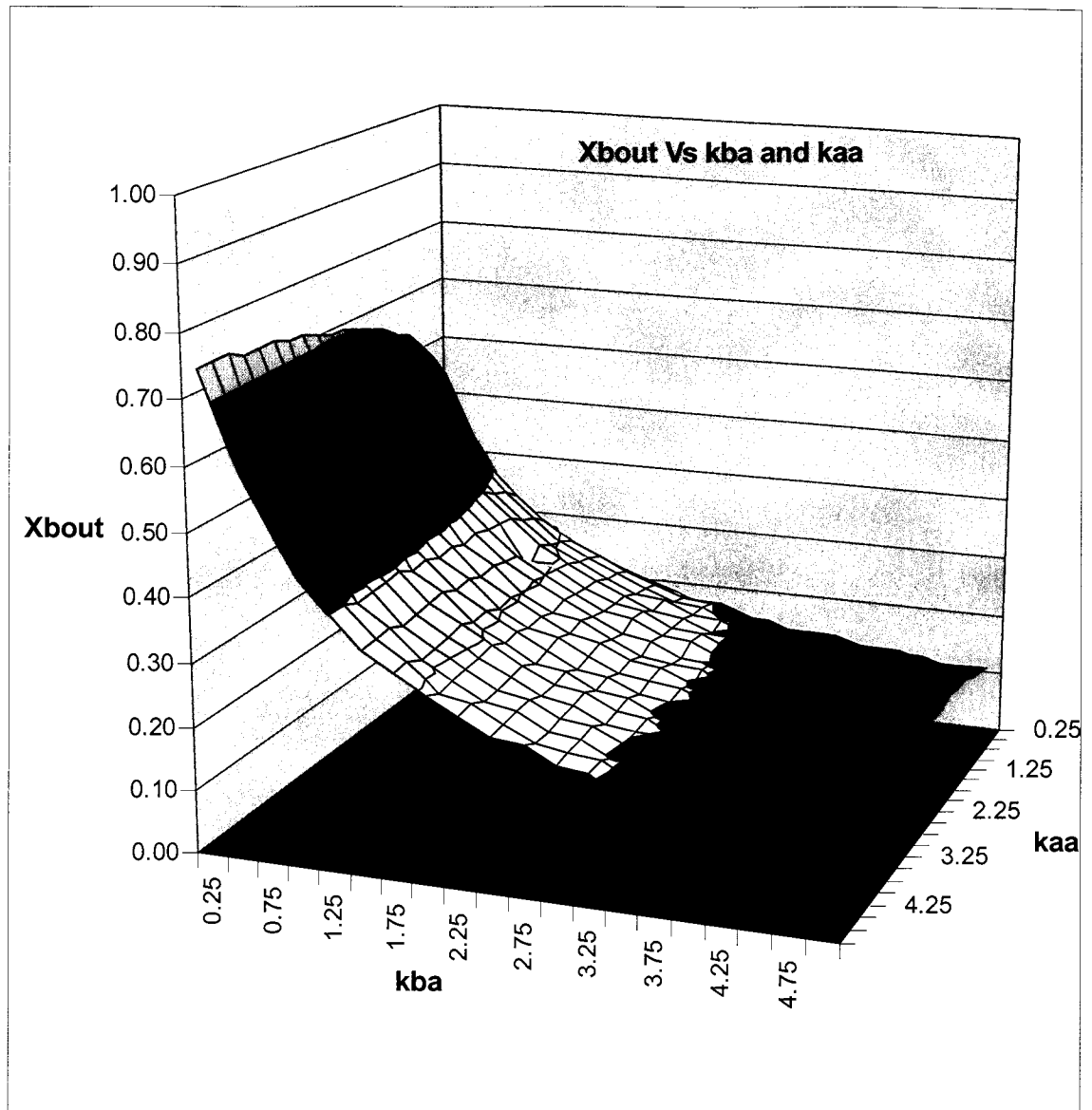


Figure 4.1.10 X_{bout} with Adsorption rate k_{Aa} and k_{Ba} ($\text{m}^3 \text{kgmole}^{-1} \text{sec}^{-1}$),
Reaction rate $k_r = 2500 \text{ kg kg-mole}^{-1} \text{sec}^{-1}$

Figures 4.1.11 through 4.1.14 show the surface concentrations of A and B (y_A and y_B) for both values of k_r , where the product is maximized. It is interesting to note that the surface of the catalyst is far from saturation, where the sum of y_A and y_B would approach unity. Even though many available sites are for adsorption, there still is competition between the two reactants. The surface concentration of components A and B ranged from 0.020 to 0.164 for the slow reaction, and 0.015 to 0.132 for the fast reaction.

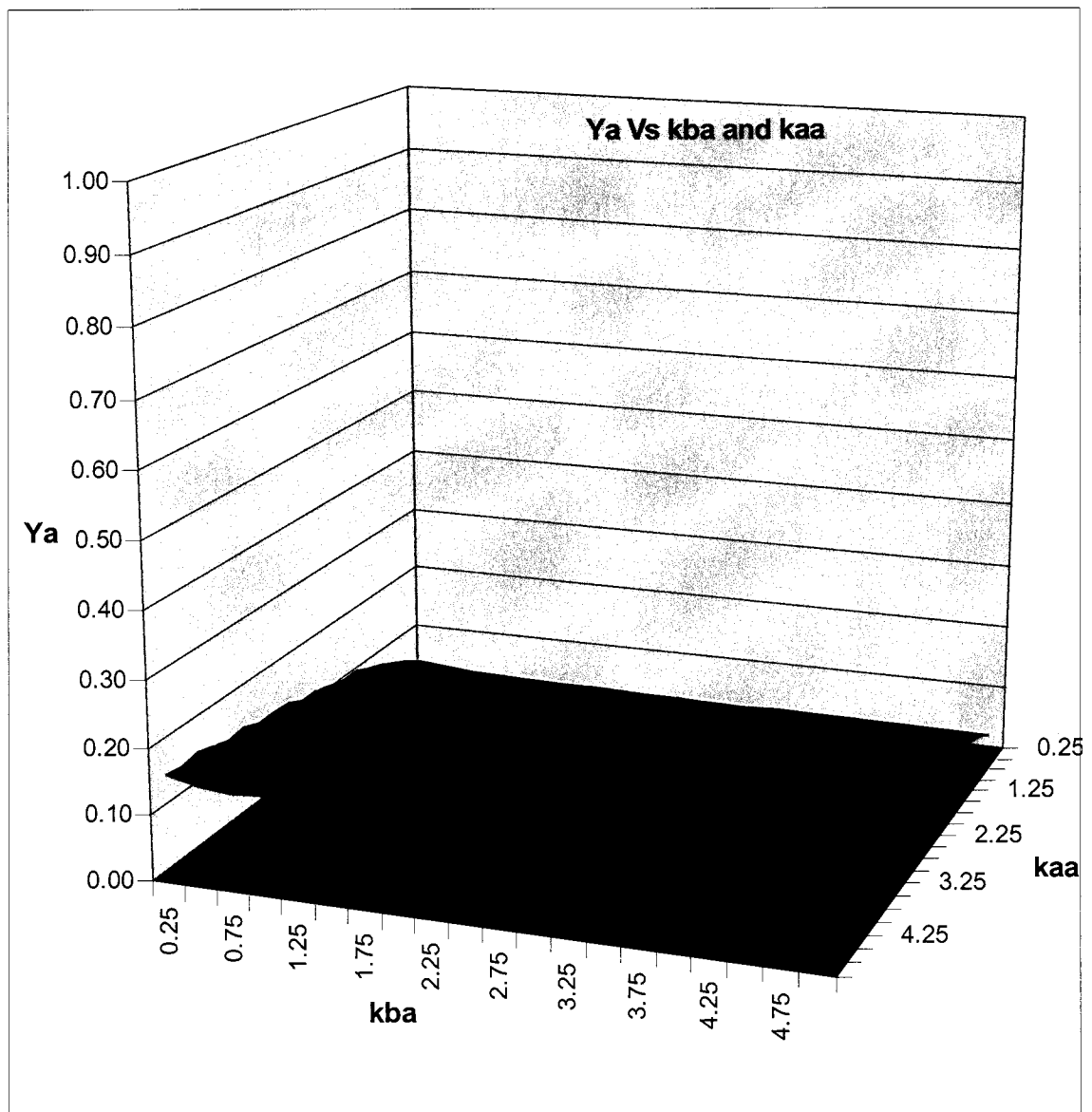


Figure 4.1.11 Y_a with Adsorption rate k_{Aa} and k_{Ba} ($\text{m}^3 \text{kgmole}^{-1} \text{sec}^{-1}$),
Reaction rate $k_r = 1250 \text{ kg kg-mole}^{-1} \text{sec}^{-1}$

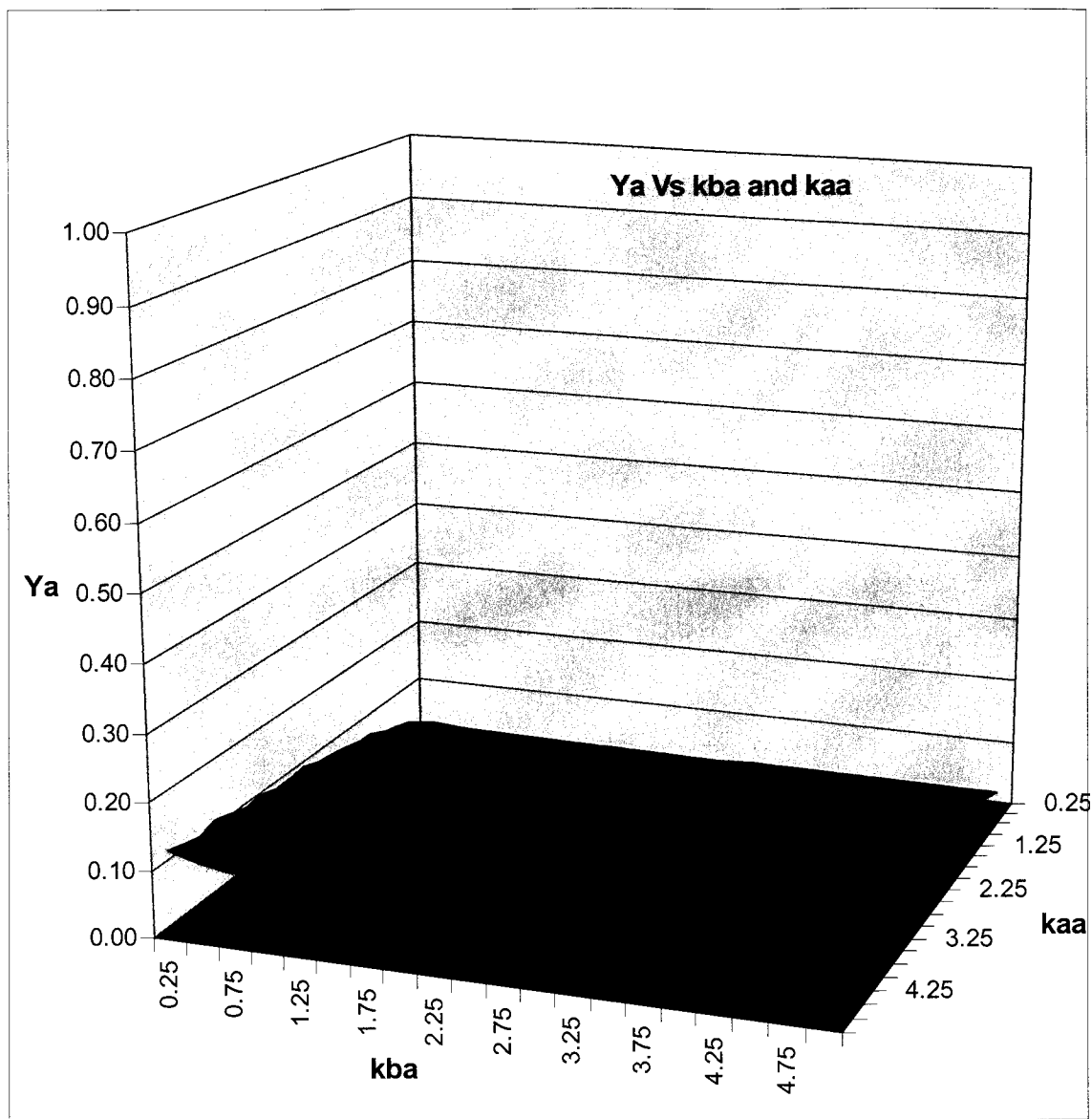


Figure 4.1.12 Y_a with Adsorption rate k_{Aa} and k_{Ba} ($\text{m}^3 \text{kgmole}^{-1} \text{sec}^{-1}$),
 Reaction rate $k_r = 2500 \text{ kg kg-mole}^{-1} \text{sec}^{-1}$

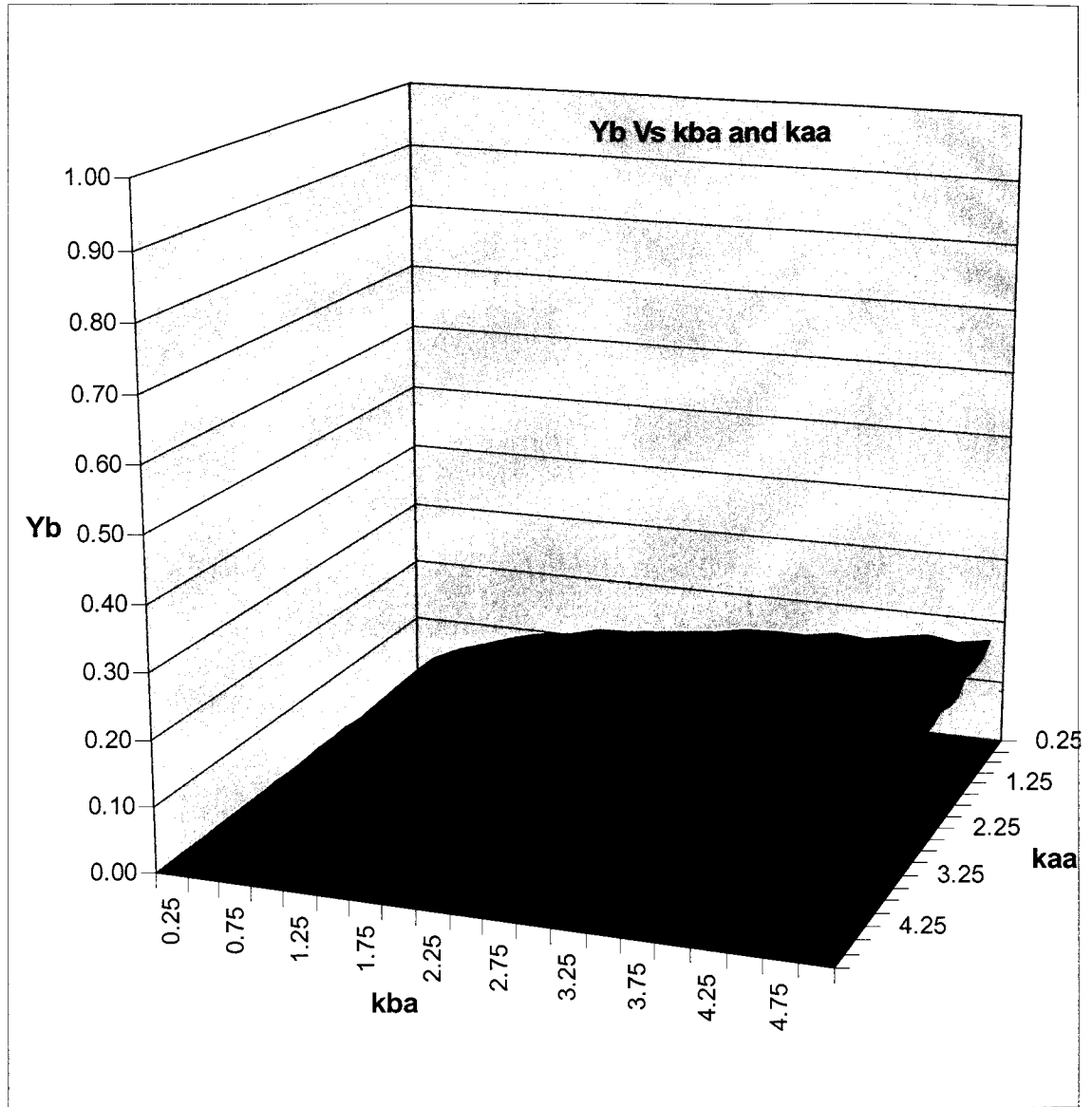


Figure 4.1.13 Y_b with Adsorption rate k_{Aa} and k_{Ba} ($\text{m}^3 \text{kgmole}^{-1} \text{sec}^{-1}$),
 Reaction rate $k_r = 1250 \text{ kg kg-mole}^{-1} \text{sec}^{-1}$

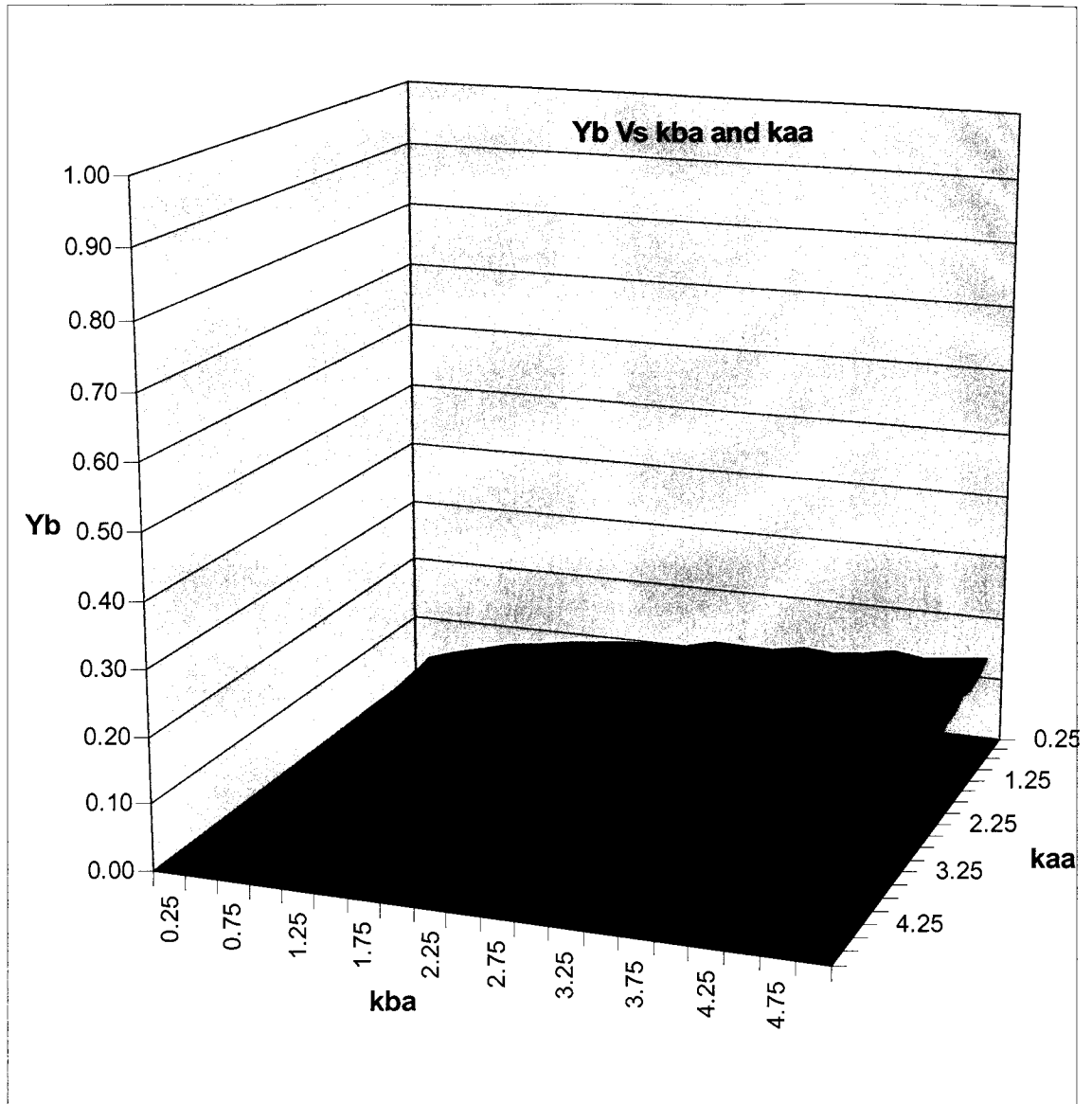


Figure 4.1.14 Y_b with Adsorption rate k_{Aa} and k_{Ba} ($m^3 \text{ kgmole}^{-1} \text{ sec}^{-1}$),
Reaction rate $k_r = 2500 \text{ kg kg-mole}^{-1} \text{ sec}^{-1}$

Figures 4.1.15 and 4.1.16 show the volumetric flow rate, Q (liter sec^{-1}), leaving the reactor for the conditions presented above. Here it can be seen that as the production of product increases, the volumetric flow rate decreases.

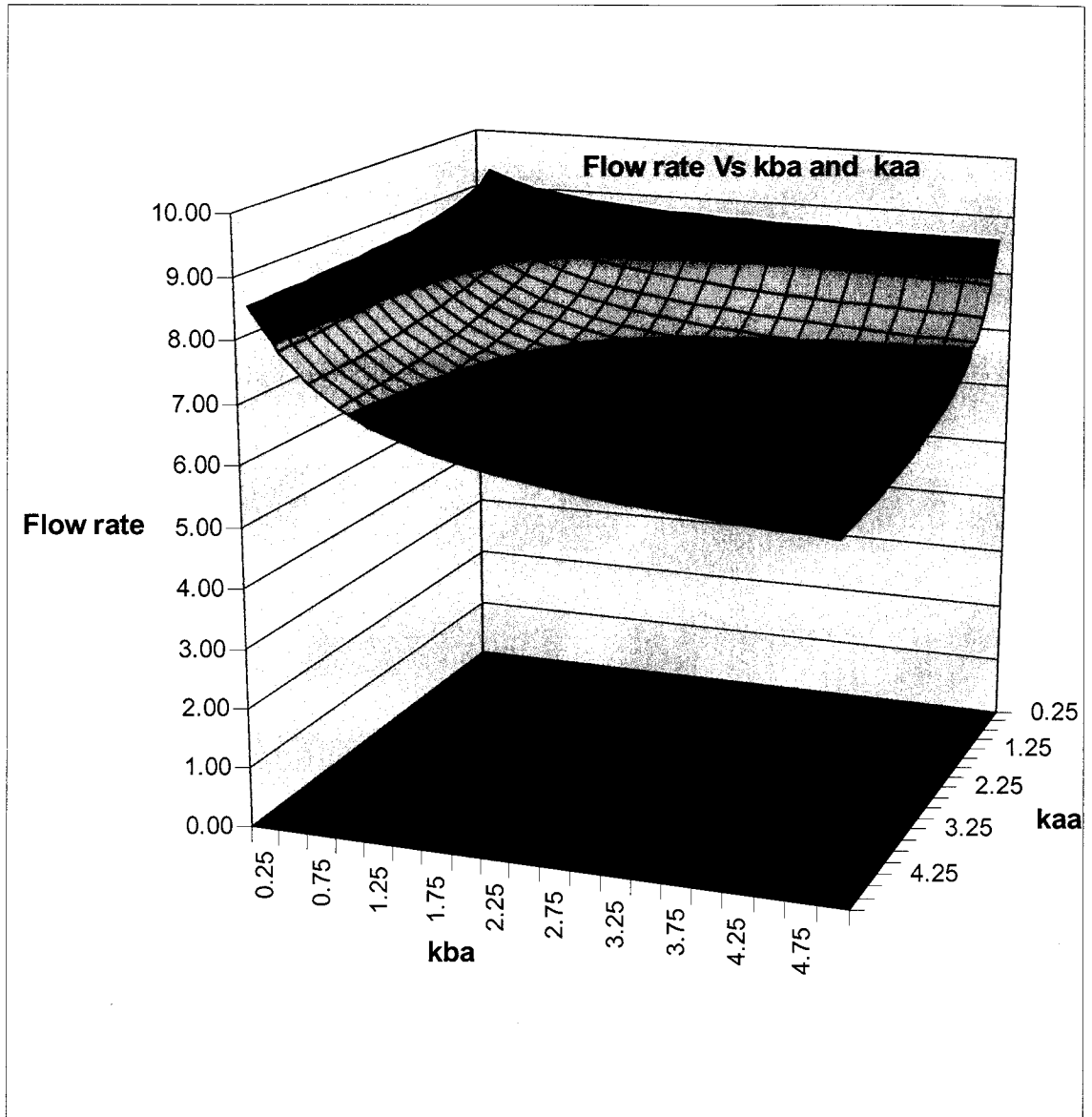


Figure 4.1.15 Flow rate Q (liter sec^{-1}) with Adsorption rate k_{Aa} and k_{Ba} ($\text{m}^3 \text{kgmole}^{-1} \text{sec}^{-1}$), Reaction rate $k_r = 1250 \text{ kg kg-mole}^{-1} \text{sec}^{-1}$

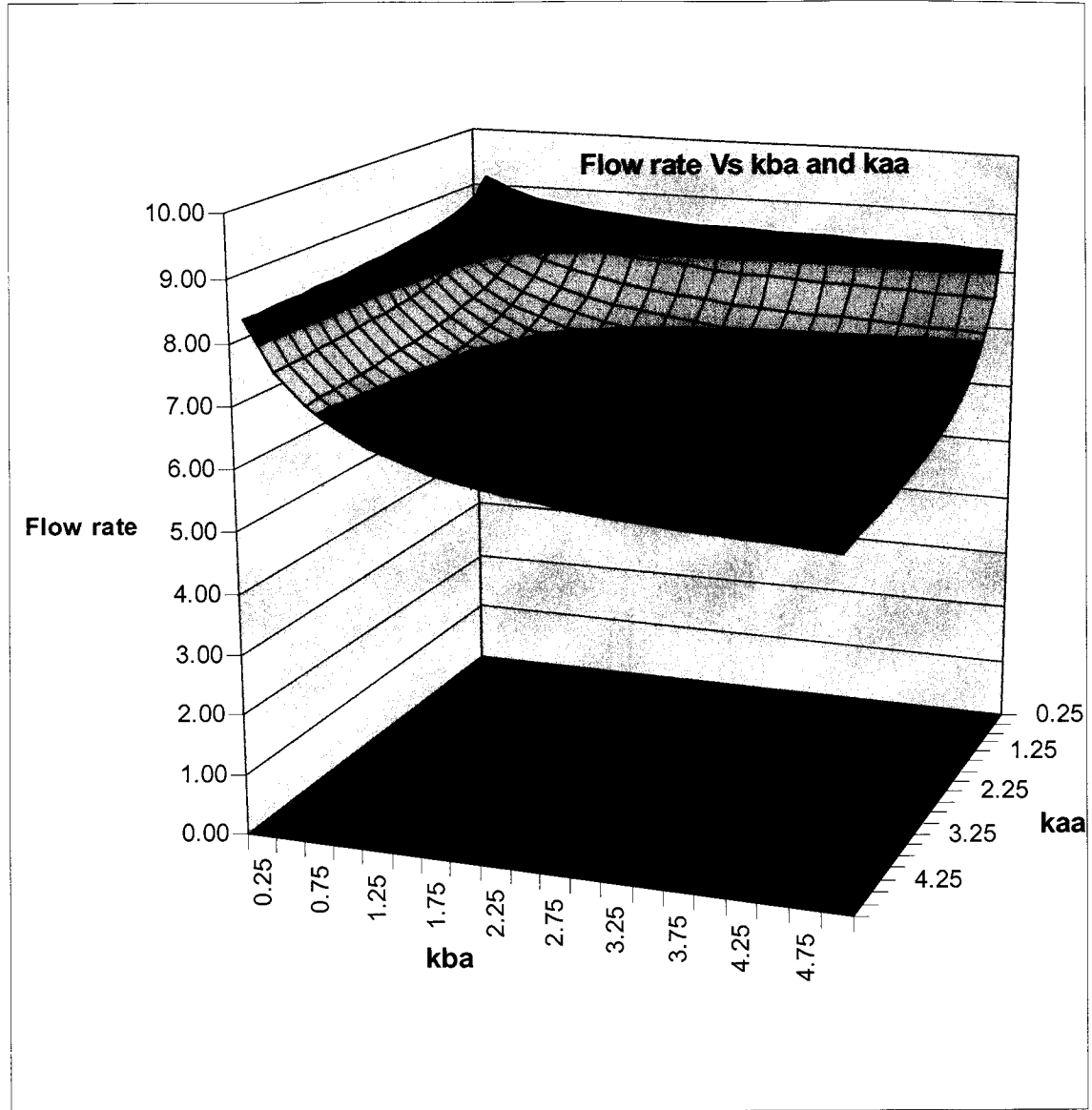


Figure 4.1.16 Flow rate Q (liter sec^{-1}) with Adsorption rate k_{Aa} and k_{Ba} ($\text{m}^3 \text{kgmole}^{-1} \text{sec}^{-1}$), Reaction rate $k_r = 2500 \text{ kg kg-mole}^{-1} \text{sec}^{-1}$

4.2 STEADY STATE MODEL AND TRANSIENT CONDITION

The steady state data from Section 4.1 showed that when the adsorption rate constants, k_{Aa} and k_{Ba} , are equal, the product C is maximized when the feed contains equal amounts of both reactants. In this section, an equimolar concentration of reactants is fed to the fluidized bed reactor in a sinusoidal fashion so that the average total flow would be the

same as that used in the steady-state model, namely $9.8 \text{ liters sec}^{-1}$. The total flow rate had an amplitude of $0.8 \text{ liter sec}^{-1}$ and a frequency of 0.6283 sec^{-1} (Equation 3.2). Figure 4.2.1 shows the results where k_{Aa} and k_{Ba} are varied from 0.25 to $6.0 \text{ m}^3 \text{ kgmole}^{-1} \text{ sec}^{-1}$. The outlet mole fraction of C was averaged over time for the sinusoidal input and compared to the results where the feed flow to the reactor was held constant at $9.8 \text{ liter sec}^{-1}$. The sinusoidal feed increased the overall output of the product by up to 4% at the higher values of the adsorption rate constants.

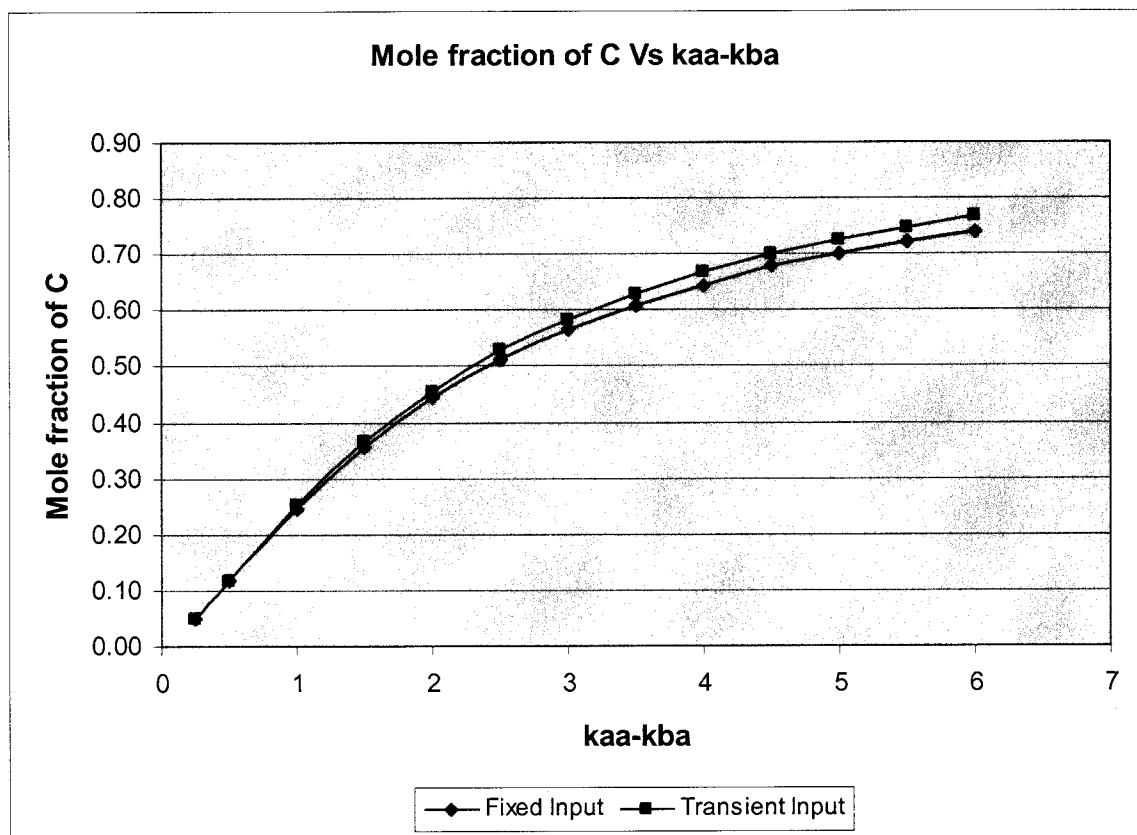


Figure 4.2.1 Mole fraction of C (X_c) with respect to Adsorption rate of components ($\text{m}^3 \text{ kgmole}^{-1} \text{ sec}^{-1}$) for fixed and transient input condition

4.3 EFFECT OF INERT GAS IN FEED

Often, the feed to a chemical reactor contains an inert component that does not participate in the chemical reaction. For steady-state operation, the effect of the inert component reduces the overall reaction rate due to its diluting effect on the reactants. The effect of an inert component on the overall reaction conversion when the feed has a sinusoidal component is not readily apparent and is the focus of study here.

The feed will be broken into the three components, that is A, B, and I. The total flow of the feed was held constant at $9.6 \text{ liters sec}^{-1}$. The feed rate of component A was assumed, and the balance of feed was split between component B and the inert gas. For example, when the flow rate of component A was set at $5.0 \times 10^{-3} \text{ m}^3 \text{ sec}^{-1}$, the balance of the feed was split between component B and the inert gas at $2.8 \times 10^{-3} \text{ m}^3 \text{ sec}^{-1}$, when the inert gas and B are fed at 50%. The physical parameters of the reactor and catalyst charge were maintained as in the previous studies. The reaction rate constant tested was $2500 \text{ kg kg-mole}^{-1} \text{ sec}^{-1}$. In this study, it was assumed that component A was available in pure form, but component B was diluted with the inert gas. Three inert concentrations were tested: 1) 33% I, 67% B, 2) 50% I, 50% B, 3) 67% I, 33% B.

Figure 4.3.1 shows the result obtained from the dynamic model run, when the adsorption rate of component A was equal to $1.0 \text{ m}^3 \text{ kgmole}^{-1} \text{ sec}^{-1}$ and adsorption rate of component B was equal to $3.0 \text{ m}^3 \text{ kgmole}^{-1} \text{ sec}^{-1}$. The flow rate of component B was equal to flow rate of inert gas. The flow rate of component A was considered in range from 1.0×10^{-3} to $6.0 \times 10^{-3} \text{ m}^3 \text{ sec}^{-1}$. The maximum mole fraction of C leaving the reactor was 0.2190

when the flow rate of component A was set to $4.25 \times 10^{-3} \text{ m}^3 \text{ sec}^{-1}$. For every combination of flow rate, there exists one optimized value of product output.

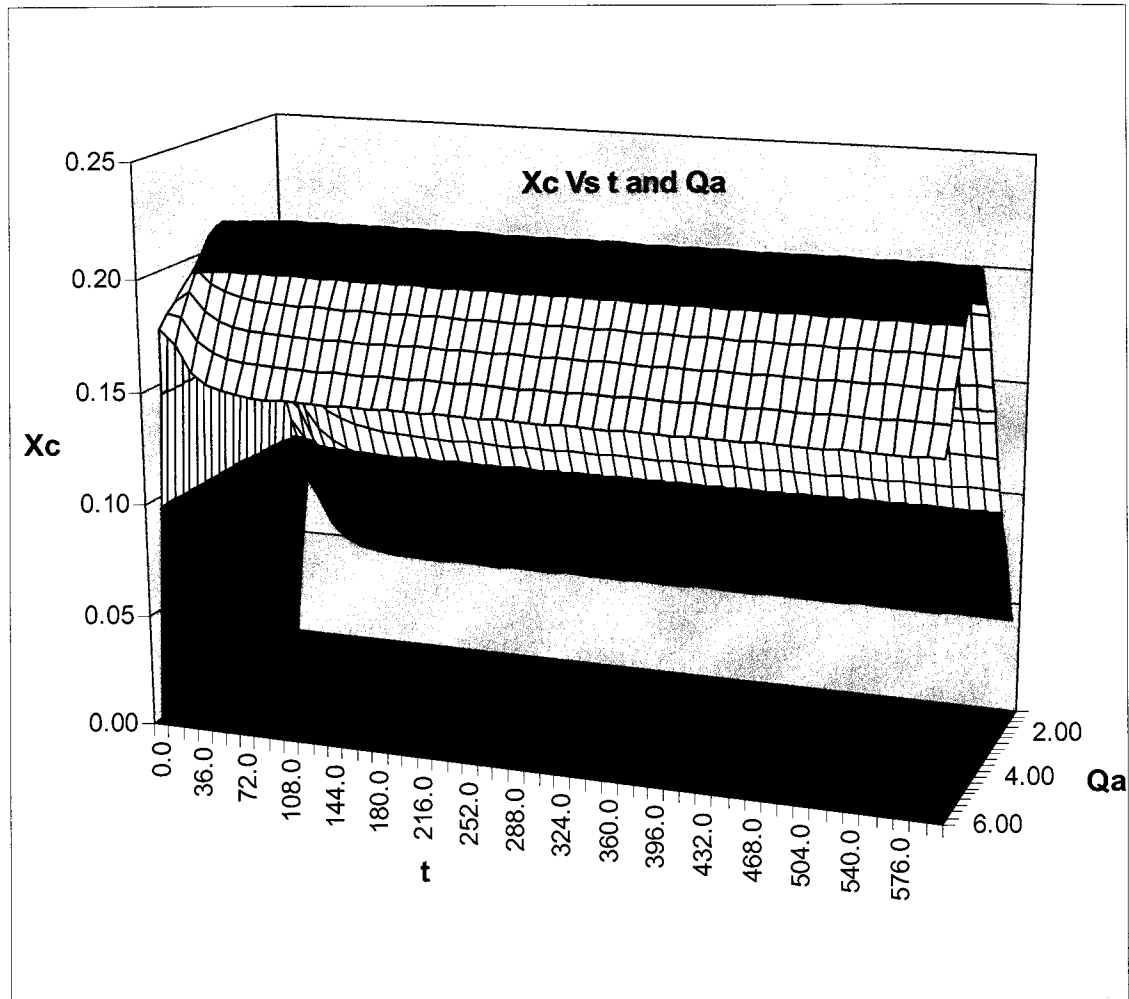


Figure 4.3.1 Mole fraction of C (X_c) with t (seconds) and Q_a (liter sec^{-1}), $k_{Aa} = 1.0 \text{ m}^3 \text{ kgmole}^{-1} \text{ sec}^{-1}$, $k_{Ba} = 3.0 \text{ m}^3 \text{ kgmole}^{-1} \text{ sec}^{-1}$, $Q_b = 50\%$, $Q_i = 50\%$

Figures 4.3.2 through 4.3.5 show similar results for various combinations of the adsorption rate constants for both reactants.

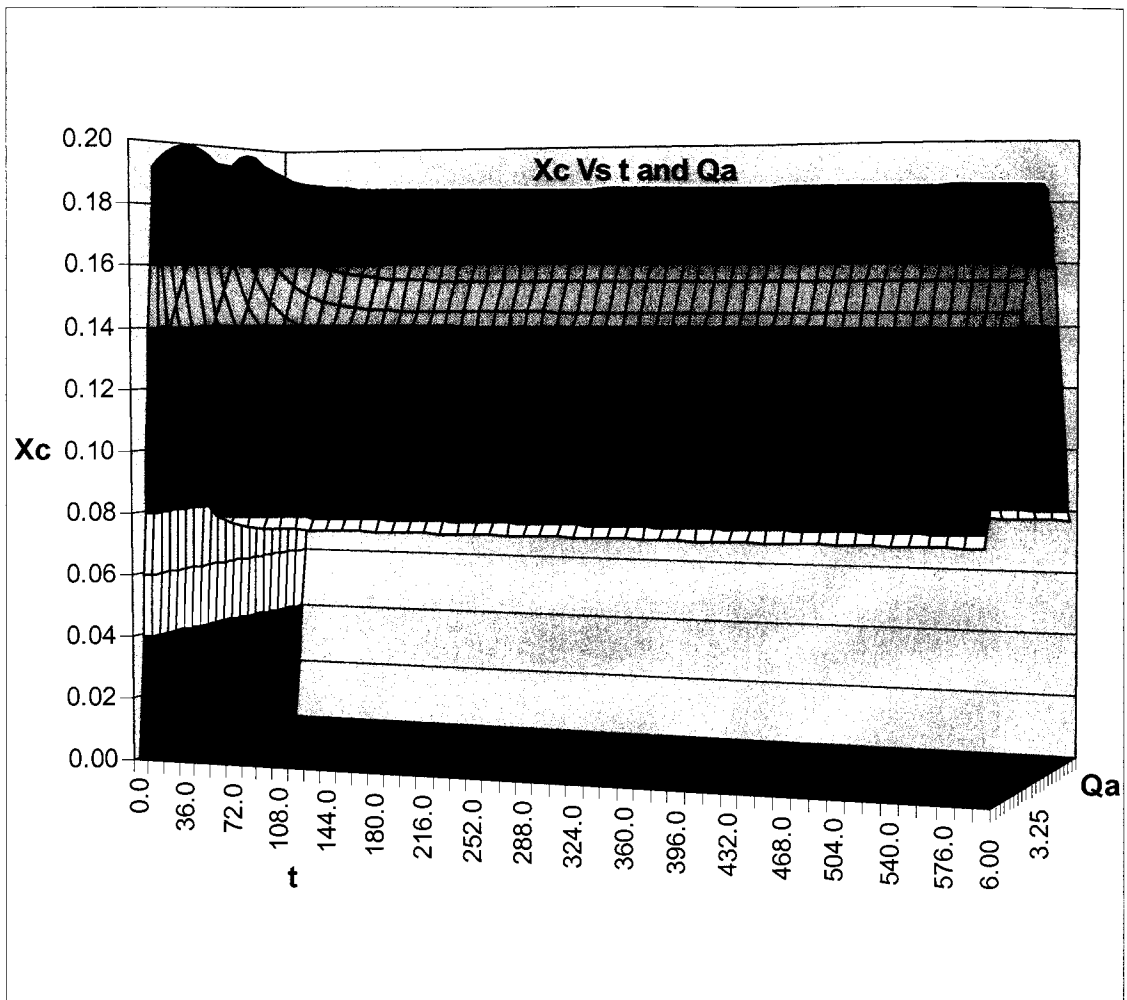


Figure 4.3.2 Mole fraction of C (X_c) with t (seconds) and Q_a (liter sec^{-1}),
 $k_{Aa} = 3.0 \text{ m}^3 \text{ kgmole}^{-1} \text{ sec}^{-1}$, $k_{Ba} = 1.0 \text{ m}^3 \text{ kgmole}^{-1} \text{ sec}^{-1}$, $Q_b = 50\%$, $Q_i = 50\%$

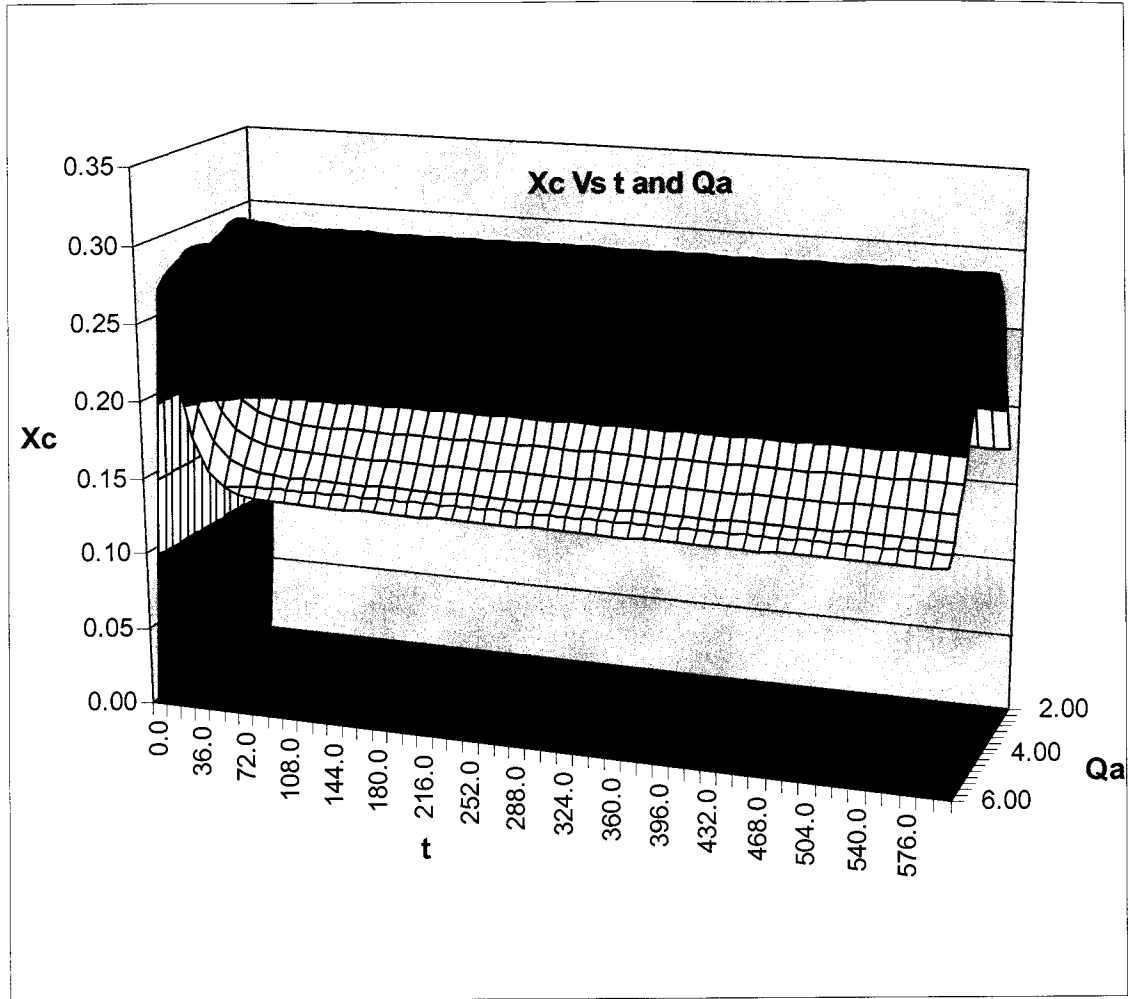


Figure 4.3.3 Mole fraction of C (X_c) with t (seconds) and Q_a (liter sec^{-1}),
 $k_{Aa} = 3.0 \text{ m}^3 \text{ kgmole}^{-1} \text{ sec}^{-1}$, $k_{Ba} = 3.0 \text{ m}^3 \text{ kgmole}^{-1} \text{ sec}^{-1}$, $Q_b = 50\%$, $Q_i = 50\%$

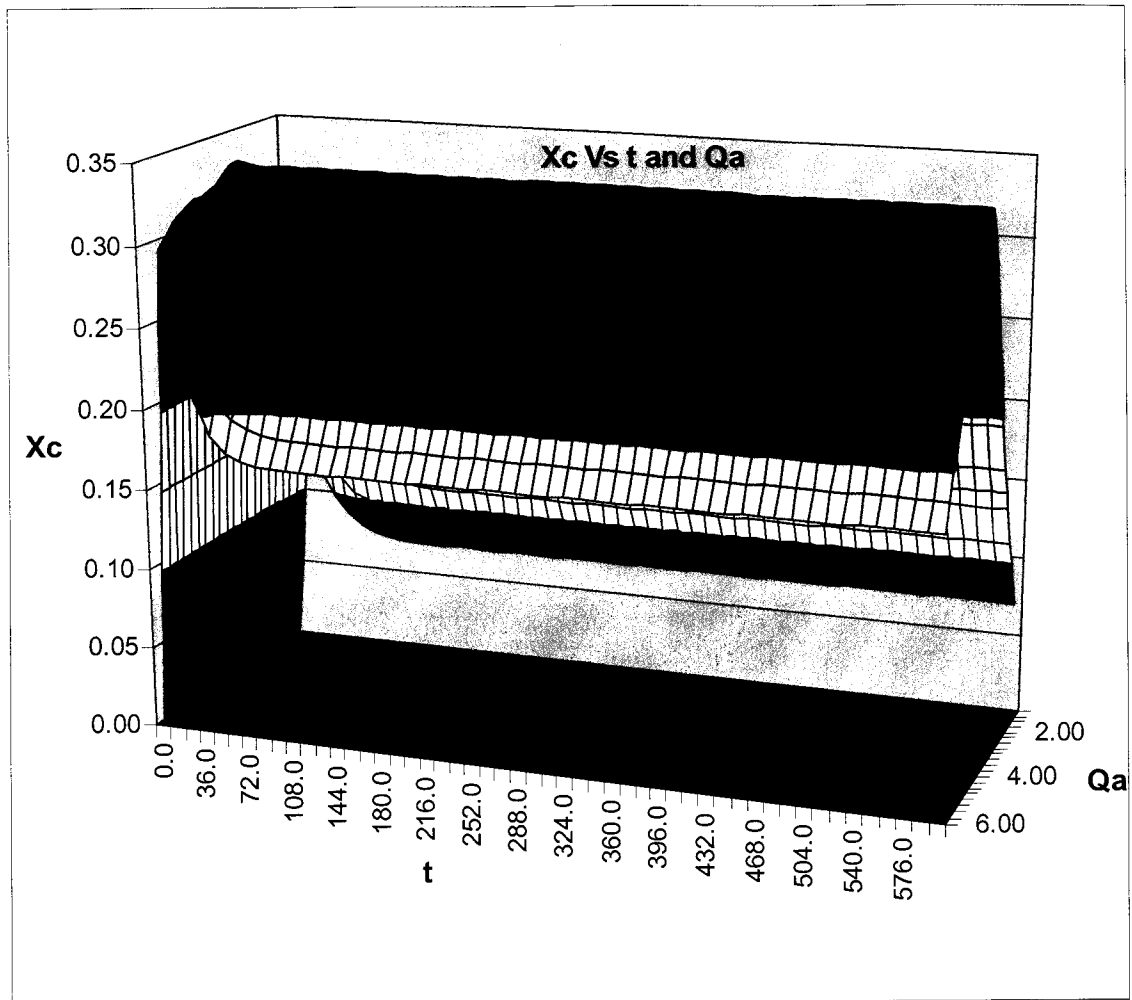


Figure 4.3.4 Mole fraction of C (X_c) with t (seconds) and Q_a (liter sec^{-1})
 $k_{Aa} = 3.0 \text{ m}^3 \text{ kgmole}^{-1} \text{ sec}^{-1}$, $k_{Ba} = 5.0 \text{ m}^3 \text{ kgmole}^{-1} \text{ sec}^{-1}$, $Q_b = 50\%$, $Q_i = 50\%$

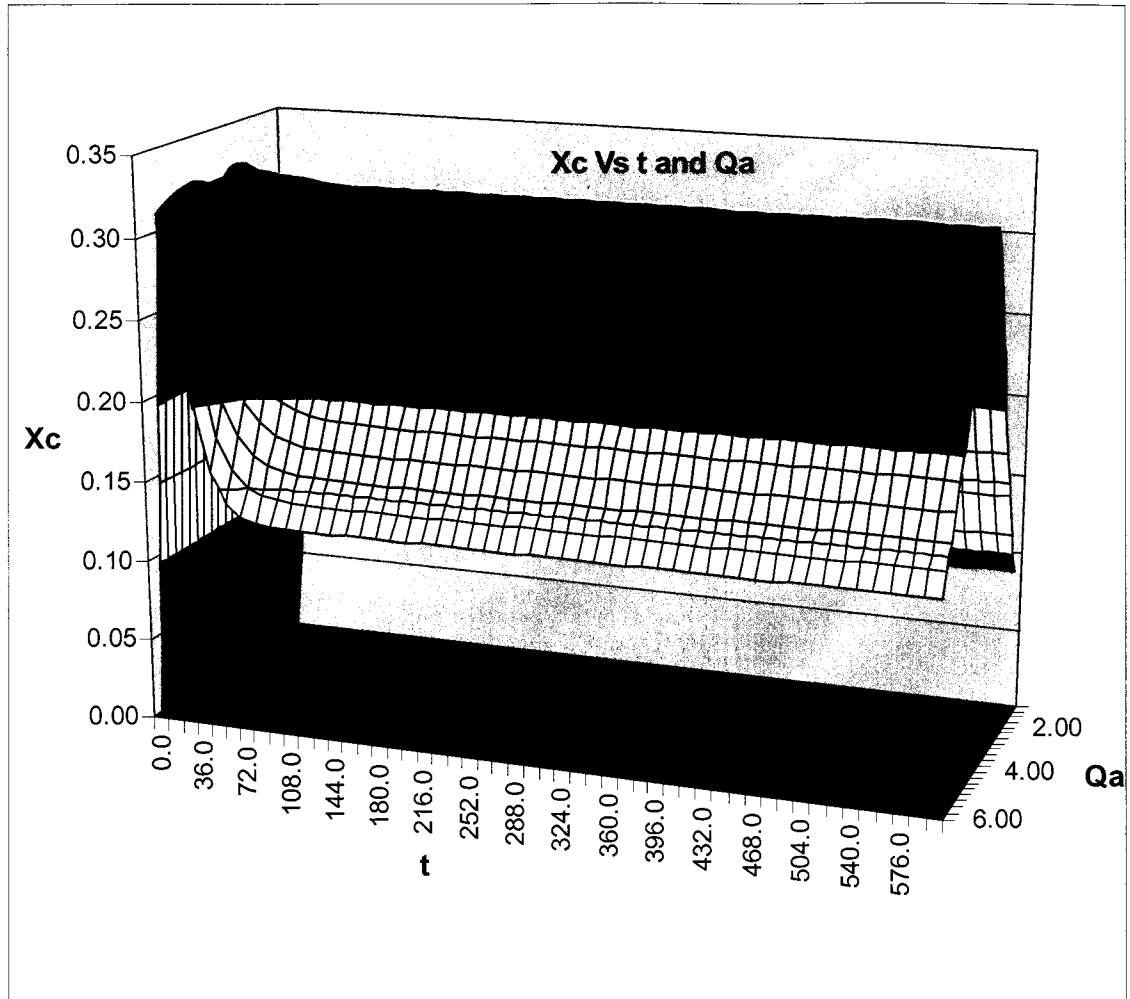


Figure 4.3.5 Mole fraction of C (X_c) with t (seconds) and Q_a (liter sec^{-1}),
 $k_{Aa} = 5.0 \text{ m}^3 \text{ kgmole}^{-1} \text{ sec}^{-1}$, $k_{Ba} = 3.0 \text{ m}^3 \text{ kgmole}^{-1} \text{ sec}^{-1}$, $Q_b = 50\%$, $Q_i = 50\%$

In Figures 4.3.6 to 4.3.10, the flow rate of component B was considered two times the flow rate of inert gas, thus the feed mole fraction of the stream containing B and I was 67% B and 33% I.

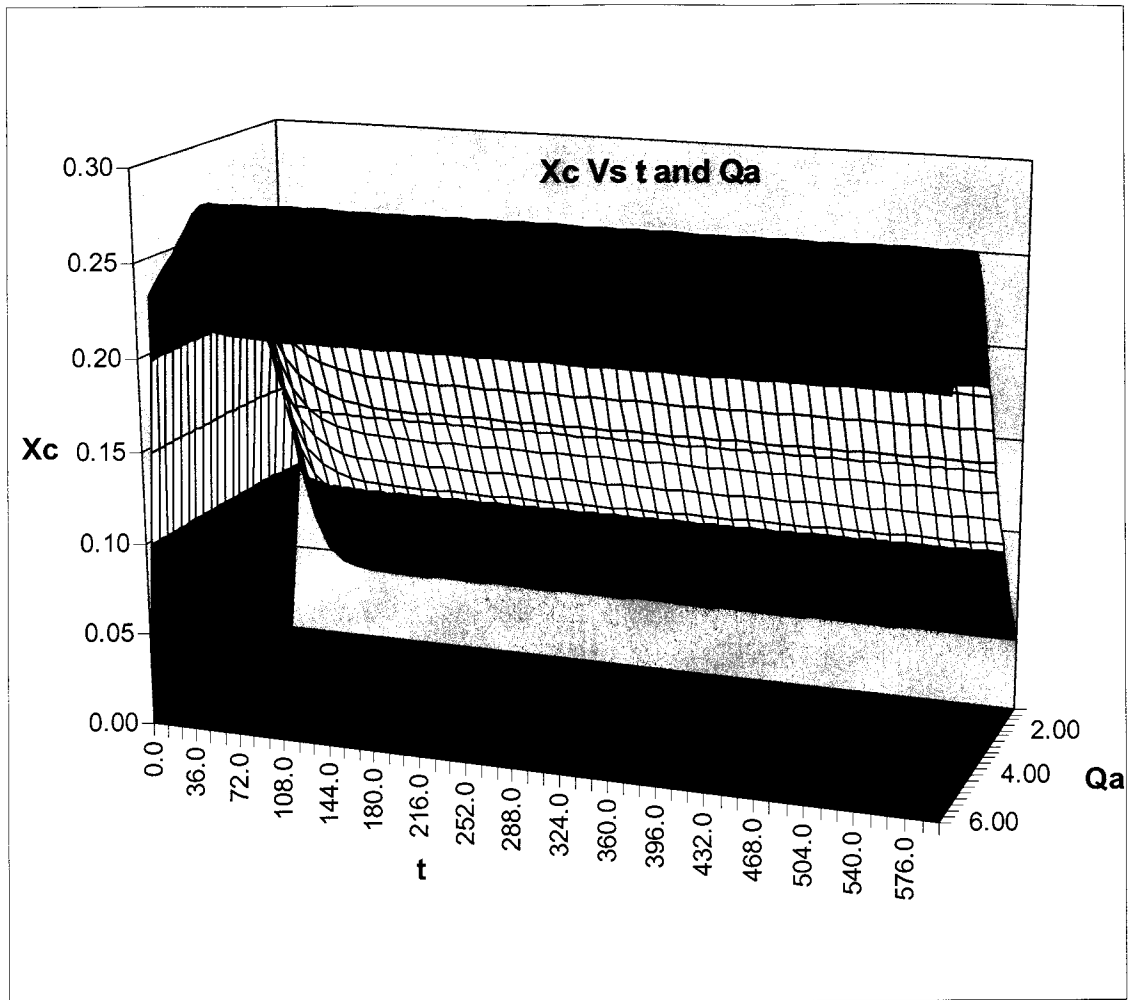


Figure 4.3.6 Mole fraction of C (X_c) with t (seconds) and Q_a (liter sec^{-1}),
 $k_{Aa} = 1.0 \text{ m}^3 \text{ kgmole}^{-1} \text{ sec}^{-1}$, $k_{Ba} = 3.0 \text{ m}^3 \text{ kgmole}^{-1} \text{ sec}^{-1}$, $Q_b = 67\%$, $Q_i = 33\%$

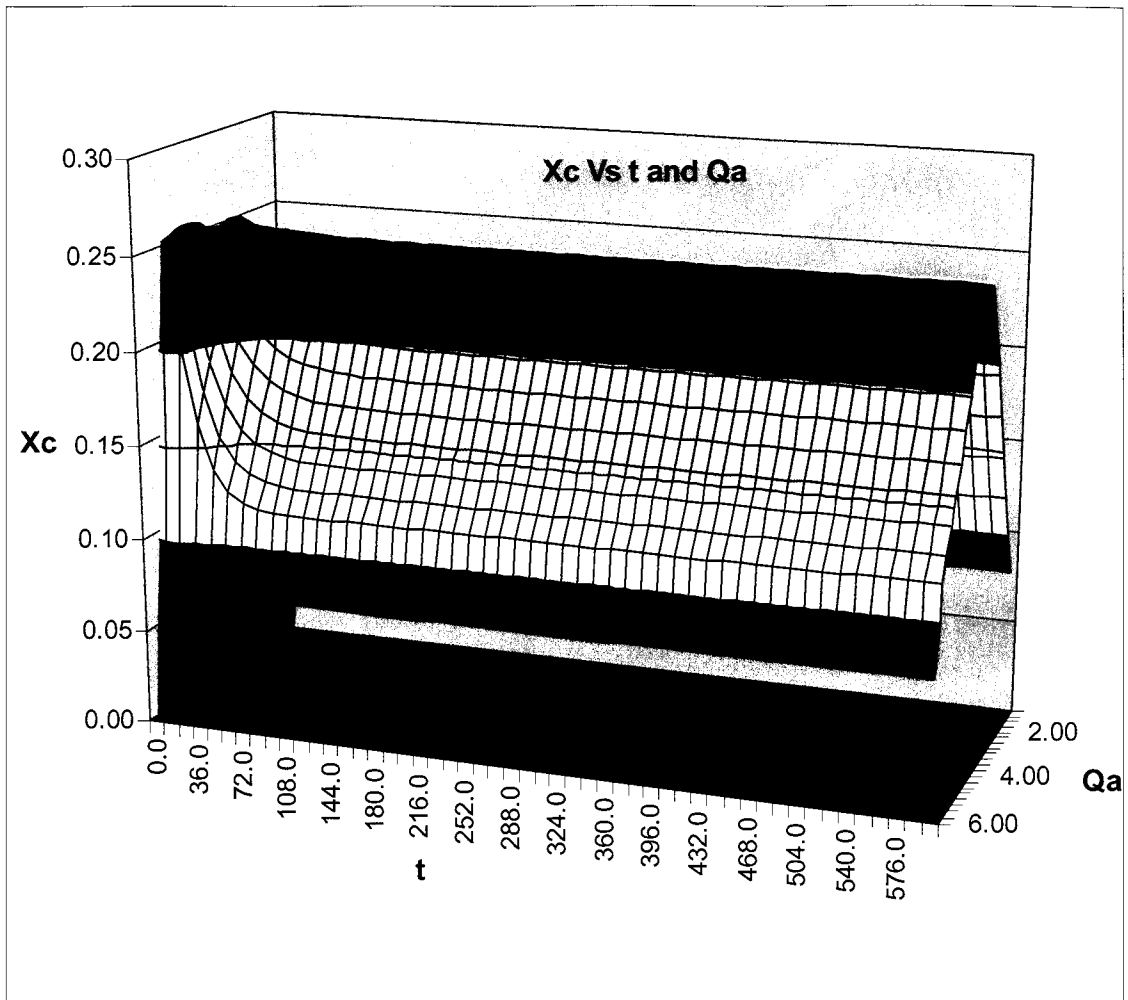


Figure 4.3.7 Mole fraction of C (X_c) with t (seconds) and Q_a (liter sec^{-1}),
 $k_{Aa} = 3.0 \text{ m}^3 \text{ kgmole}^{-1} \text{ sec}^{-1}$, $k_{Ba} = 1.0 \text{ m}^3 \text{ kgmole}^{-1} \text{ sec}^{-1}$, $Q_b = 67\%$, $Q_i = 33\%$

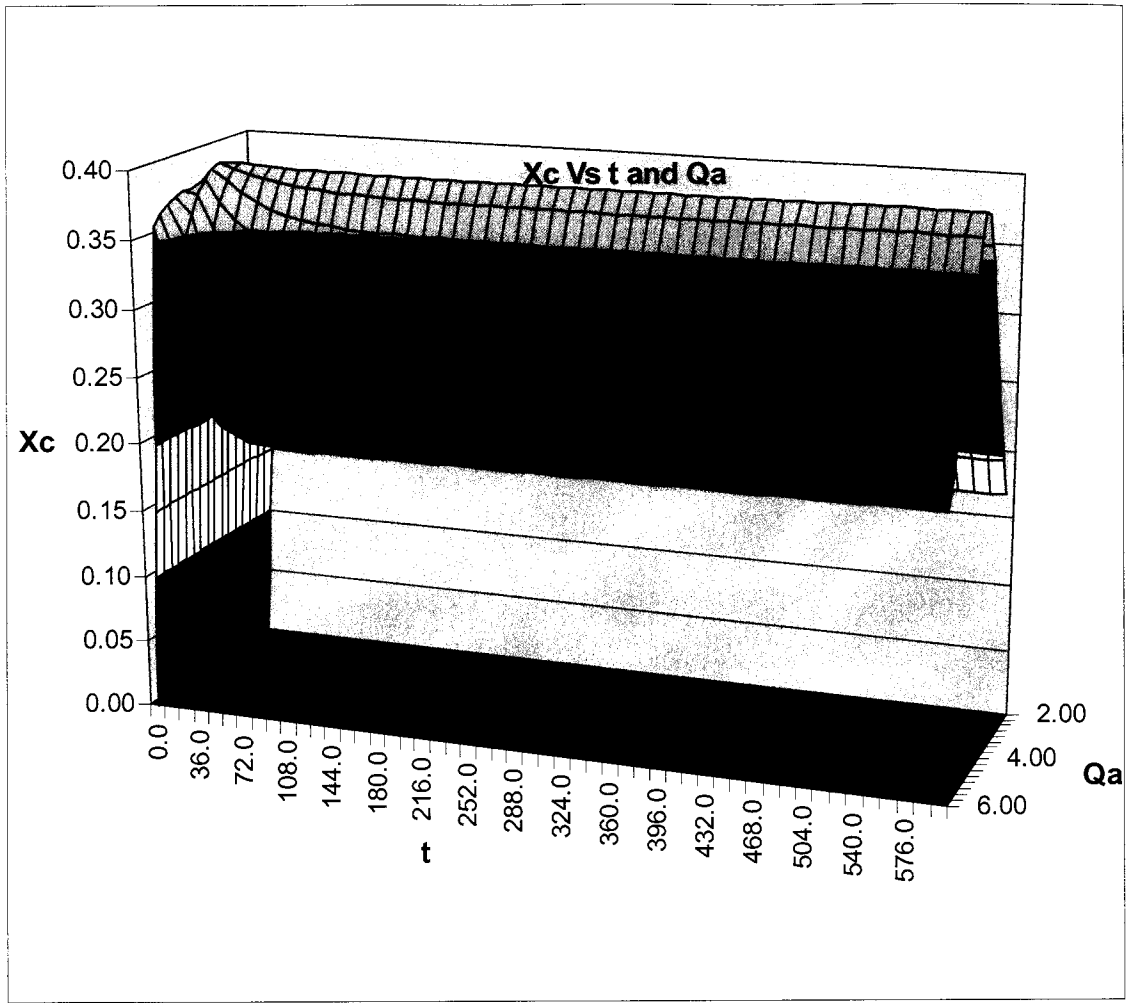


Figure 4.3.8 Mole fraction of C (X_c) with t (seconds) and Q_a (liter sec^{-1}), $k_{Aa} = 3.0 \text{ m}^3 \text{ kgmole}^{-1} \text{ sec}^{-1}$, $k_{Ba} = 3.0 \text{ m}^3 \text{ kgmole}^{-1} \text{ sec}^{-1}$, $Q_b = 67\%$, $Q_i = 33\%$

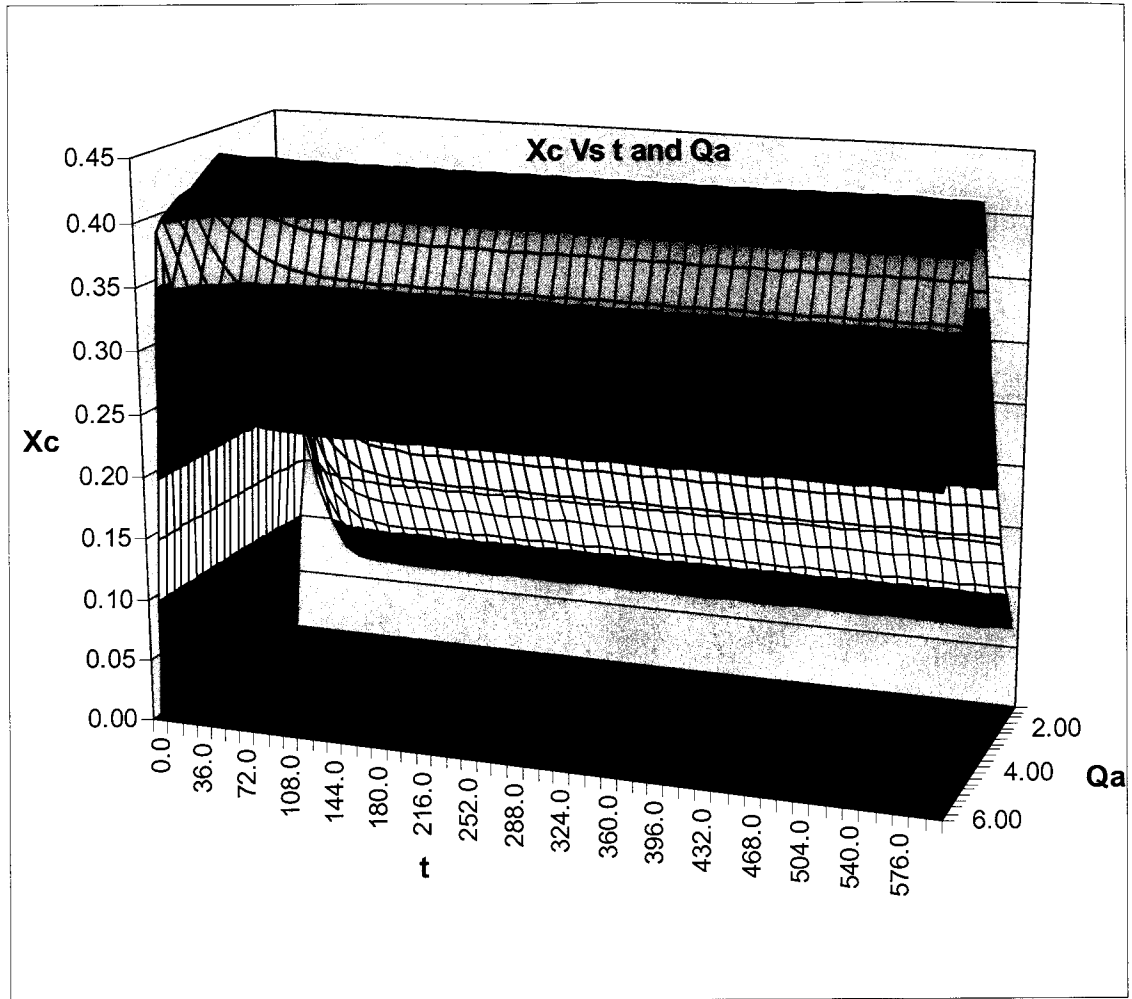


Figure 4.3.9 Mole fraction of C (X_c) with t (seconds) and Q_a liter sec^{-1} ,
 $k_{Aa} = 3.0 \text{ m}^3 \text{ kgmole}^{-1} \text{ sec}^{-1}$, $k_{Ba} = 5.0 \text{ m}^3 \text{ kgmole}^{-1} \text{ sec}^{-1}$, $Q_b = 67\%$, $Q_i = 33\%$

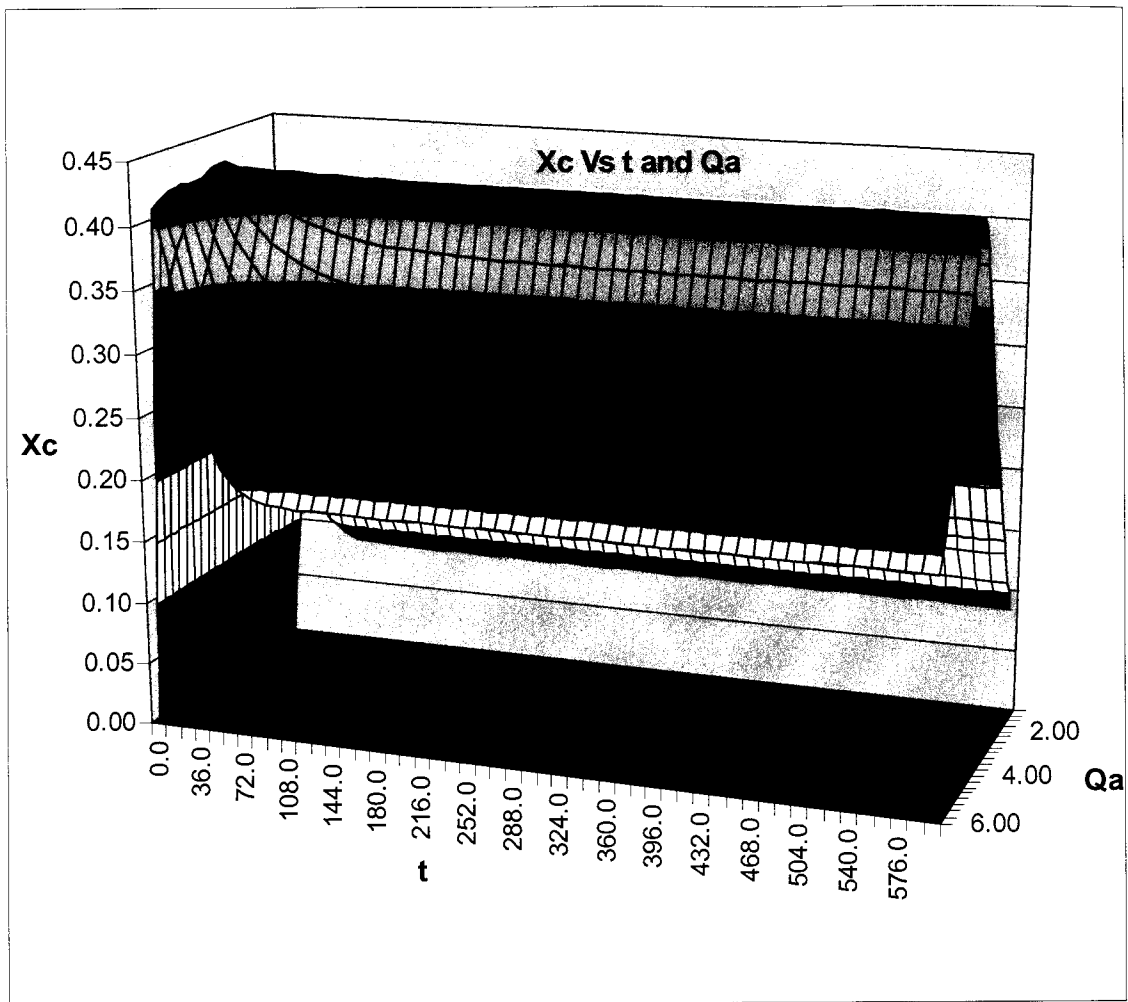


Figure 4.3.10 Mole fraction of C (X_c) with t (seconds) and Q_a (liter sec^{-1}), $k_{Aa} = 5.0 \text{ m}^3 \text{ kgmole}^{-1} \text{ sec}^{-1}$, $k_{Ba} = 3.0 \text{ m}^3 \text{ kgmole}^{-1} \text{ sec}^{-1}$, $Q_b = 67\%$, $Q_i = 33\%$

In Figures 4.3.11 to 4.3.15, the flow rate of the inert gas was considered two times the flow rate of component B, thus the feed mole fraction of the stream containing B and I was 33% B and 67% I.

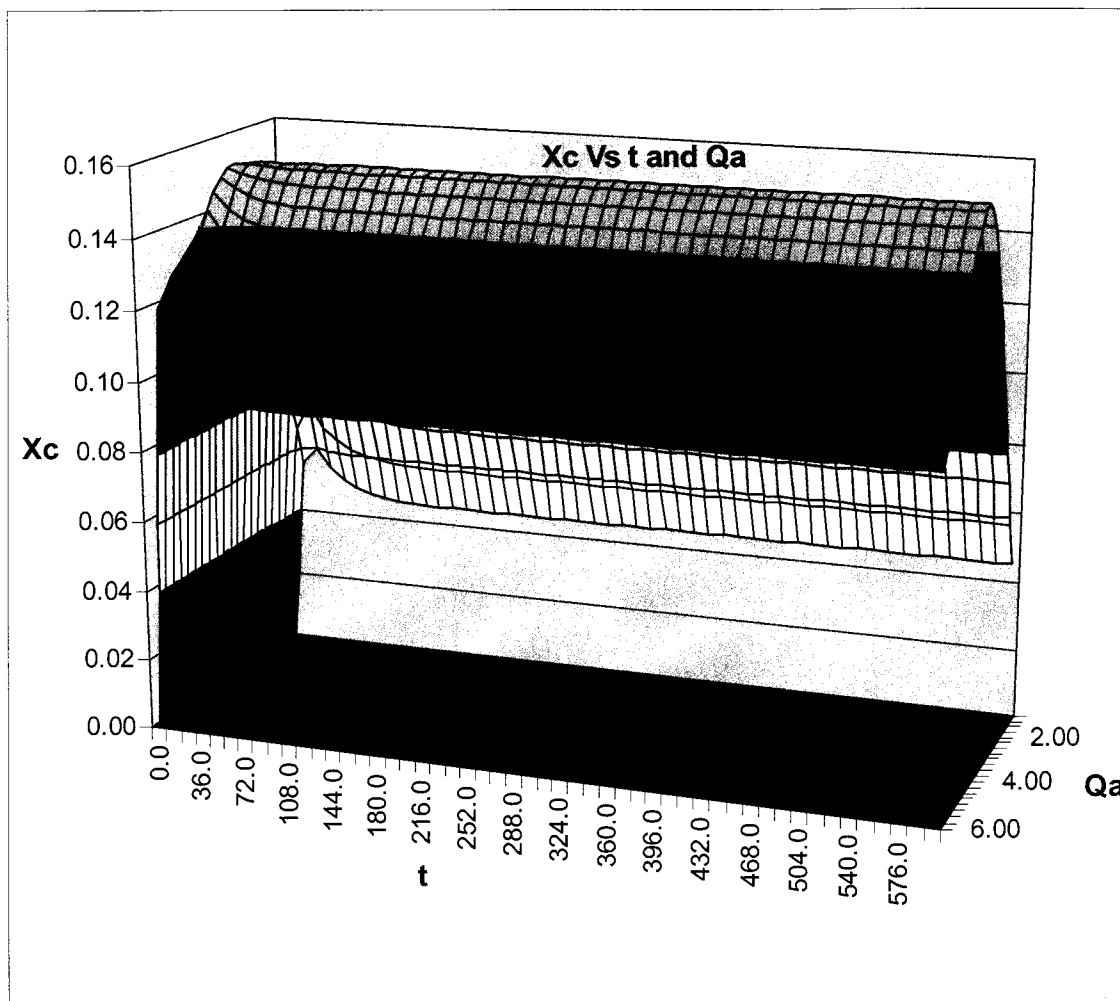


Figure 4.3.11 Mole fraction of C (X_c) with t (seconds) and Q_a (liter sec^{-1}), $k_{Aa} = 1.0 \text{ m}^3 \text{ kgmole}^{-1} \text{ sec}^{-1}$, $k_{Ba} = 3.0 \text{ m}^3 \text{ kgmole}^{-1} \text{ sec}^{-1}$, $Q_b = 33\%$, $Q_i = 67\%$

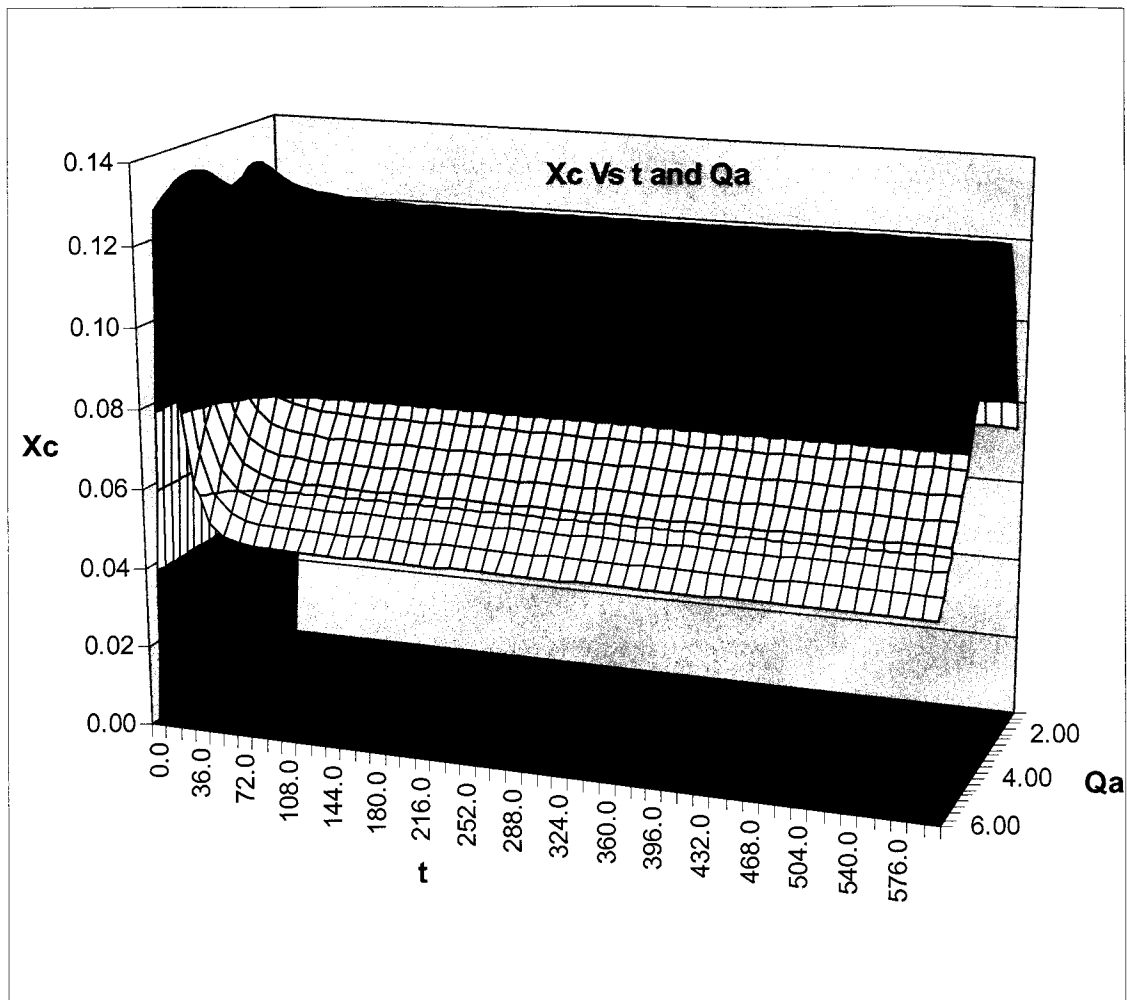


Figure 4.3.12 Mole fraction of C (X_c) with t (seconds) and Q_a (liter sec^{-1}), $k_{Aa} = 3.0 \text{ m}^3 \text{ kgmole}^{-1} \text{ sec}^{-1}$, $k_{Ba} = 1.0 \text{ m}^3 \text{ kgmole}^{-1} \text{ sec}^{-1}$, $Q_b = 33\%$, $Q_i = 67\%$

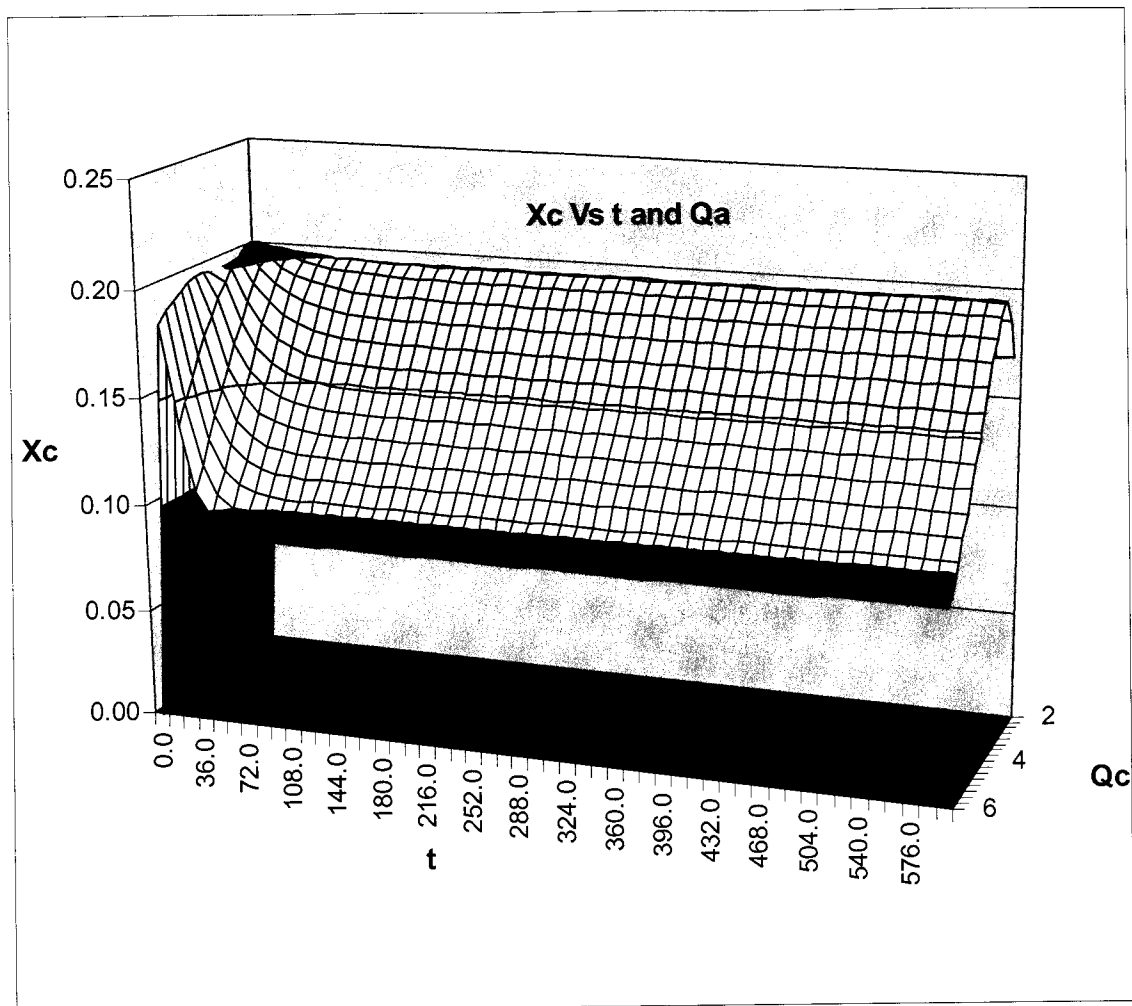


Figure 4.3.13 Mole fraction of C (X_c) with t (seconds) and Q_a (liter sec^{-1}), $k_{Aa} = 3.0 \text{ m}^3 \text{ kgmole}^{-1} \text{ sec}^{-1}$, $k_{Ba} = 3.0 \text{ m}^3 \text{ kgmole}^{-1} \text{ sec}^{-1}$, $Q_b = 33\%$, $Q_i = 67\%$

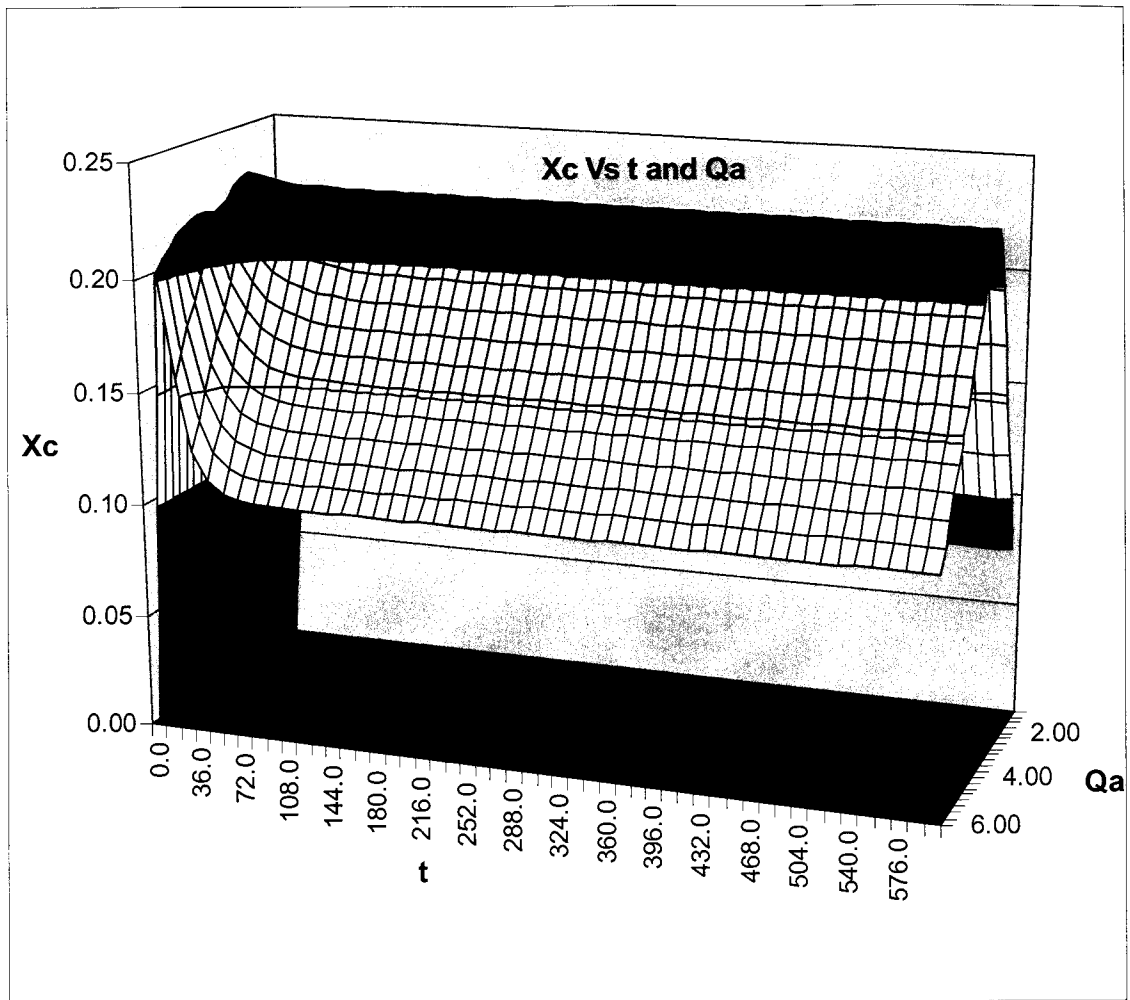


Figure 4.3.14 Mole fraction of C (X_c) with t (seconds) and Q_a (liter sec^{-1}), $k_{Aa} = 3.0 \text{ m}^3 \text{ kgmole}^{-1} \text{ sec}^{-1}$, $k_{Ba} = 5.0 \text{ m}^3 \text{ kgmole}^{-1} \text{ sec}^{-1}$, $Q_b = 33\%$, $Q_i = 67\%$

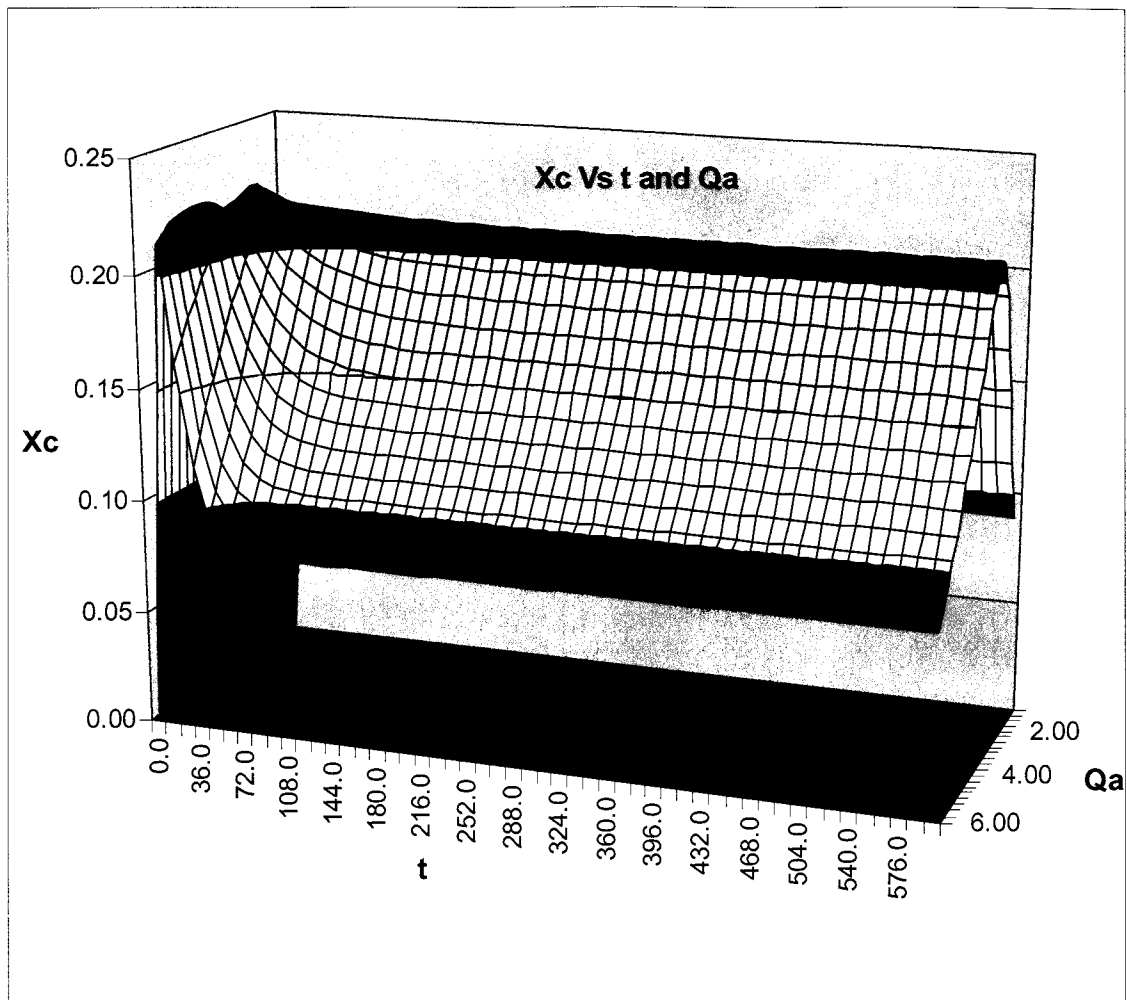


Figure 4.3.15 Mole fraction of C (X_c) with t (seconds) and Q_a (liter sec^{-1}), $k_{Aa} = 5.0 \text{ m}^3 \text{ kgmole}^{-1} \text{ sec}^{-1}$, $k_{Ba} = 3.0 \text{ m}^3 \text{ kgmole}^{-1} \text{ sec}^{-1}$, $Q_b = 33\%$, $Q_i = 67\%$

Higher value of adsorption rate of A increases surface concentration of A on the catalyst surface. System geometry from Equation 1.1 tells equimole of component A and B requires for production of component C. Increase in the adsorption of A will tend to increase the flow rate of component B as we can see from figure and obtained results. Same way increase in the adsorption rate of component B will enhance adsorption of reactant B on the catalyst surface. There will be more molecules of B than A on the catalyst surface. Model tried to balance the molar ratio of both reactants A and B for optimization of product C. That would be resulted into higher rate of component A in the

feed. Inert gas has its effect on the conversion ratio of product. Inert gas will get in the way of the reaction and disturb the whole system geometry. The unwanted molecules of inert gas on the catalyst surface will decrease the adsorption of reactants. Decrease in the adsorption of reactant molecules would give fewer products molecules in the outflow. Increasing in inert gas as compare to component B will always give low product output as we can see from results and figures. Designer can increase adsorption rate of components to overcome adverse effect of inert gas, but that would not be always helpful because of system design and process cost. It is advisable to use product as inert gas. Adsorption rate of one component is higher than other component, then increment in flow rate of other component will counter affect its lesser adsorption rate and gives desired optimized product. From the studies, we can tell that flow rate of components in feed can be inversely varied with respect to their adsorption rates to get maximum output product. Product in terms of inert gas might be helpful in the feed, otherwise it is undesirable. Inert gas can be proved useful for reactivity of catalyst after certain period of operation. That would need more study depending on catalyst structure and reactivity.

4.4 DYNAMIC MODEL AND TRANSIENT CONDITION

The influence due to transient condition on the reaction kinetics has been observed in this section. It has been proved in the previous Section 4.2 that reaction efficiency can be improved by applying continuously simulating dynamic condition. This study was done in order to strengthen that conclusion. Studies were conducted with use of the dynamic model. The feed for reactant B and inert gas were set constant and reactant A was oscillated by Equation 3.1. The amplitude and frequency was assumed to be constant at 0.8 and 0.10 throughout the studies. Another model parameters were assumed to be same as in dynamic state model as discussed in previous Section 4.2. Total flow in the feed will remain same as in the previous studies at $9.6 \times 10^{-3} \text{ m}^3 \text{ sec}^{-1}$. Volume was assumed constant at $13.3 \times 10^{-3} \text{ m}^3$. Rate of reaction was considered constant as $2500 \text{ kg kg-mole}^{-1} \text{ sec}^{-1}$. The time interval considered was 600 seconds and the time step was set at 0.01 for Runge – Kutta algorithm. Figure 4.4.1 shows the result in the chart form obtained from dynamic model run with transient condition, when the adsorption rate of component A was equal to $1.0 \text{ m}^3 \text{ kgmole}^{-1} \text{ sec}^{-1}$ and adsorption rate of component was equal to $3.0 \text{ m}^3 \text{ kgmole}^{-1} \text{ sec}^{-1}$. The flow rate of component B was equal to flow rate of inert gas. The flow rate of component A was varied from 6.0×10^{-3} to $1.0 \times 10^{-3} \text{ m}^3 \text{ sec}^{-1}$. The average value of X_c from the transient run was 0.2150 at Q_a equal to $4.25 \times 10^{-3} \text{ m}^3 \text{ sec}^{-1}$, which is higher than the average value of X_c at 0.2141 obtained from the steady state run of dynamic model for respective flow rate of A.

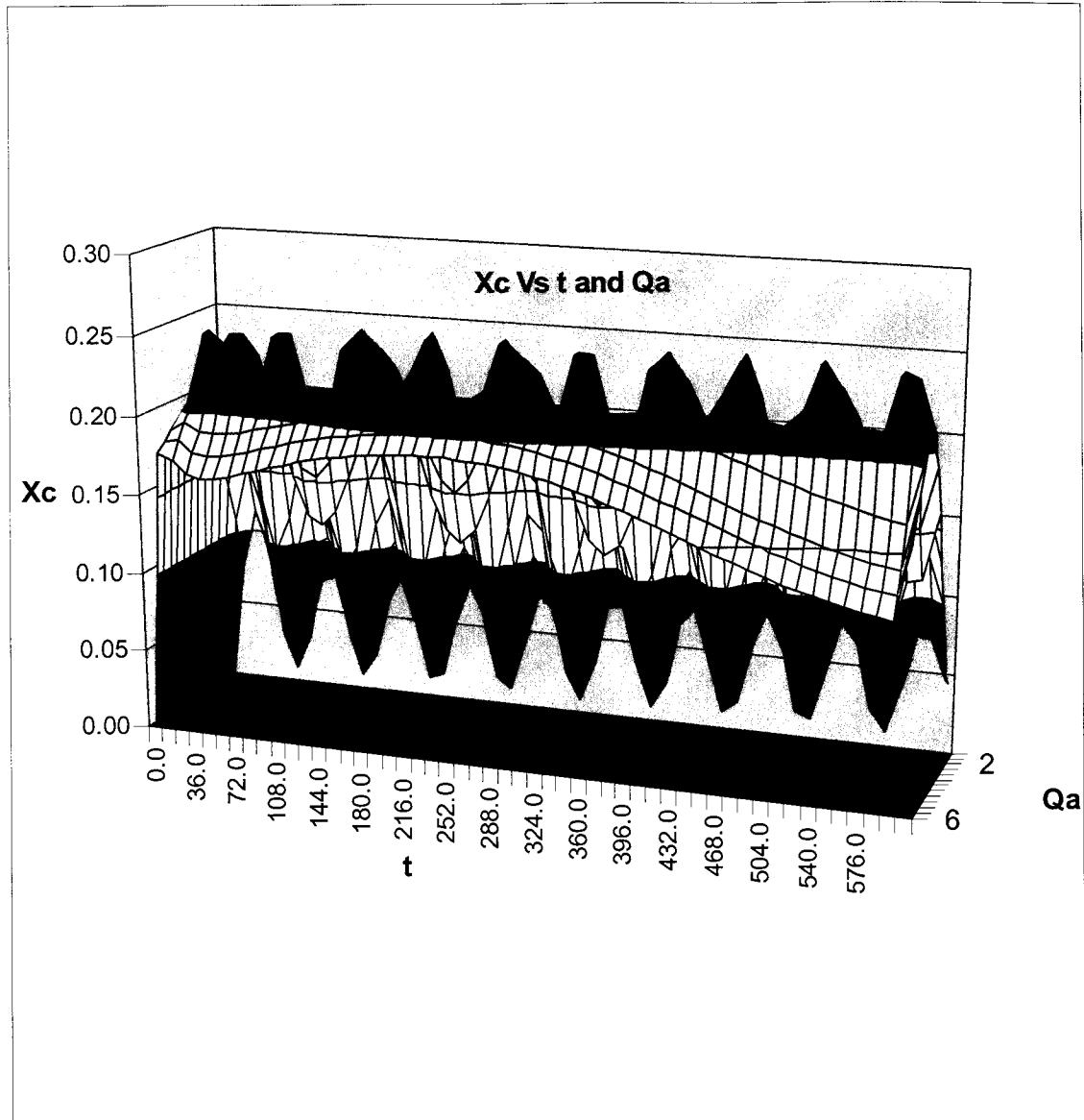


Figure 4.4.1 Mole fraction of C (X_c) with t (seconds) and Q_a (liter sec^{-1}),
 $k_{Aa} = 1.0 \text{ m}^3 \text{ kgmole}^{-1} \text{ sec}^{-1}$, $k_{Ba} = 3.0 \text{ m}^3 \text{ kgmole}^{-1} \text{ sec}^{-1}$, $Q_a = Q_b + Q_i$

The adsorption rate of components A and B was equal to $3.0 \text{ m}^3 \text{ kgmole}^{-1} \text{ sec}^{-1}$ during following study of Figure 4.4.2. The flow rate of component B was assumed equal to the flow rate of inert gas. Flow rate of A was varied by sinusoidal function. The average mole fraction of component C in form of 0.2903 was obtained. The mole fraction of C

with respect to time and flow rate of component A can be seen in Figure 4.4.2. The average value of X_c obtained from steady state run was 0.2876.

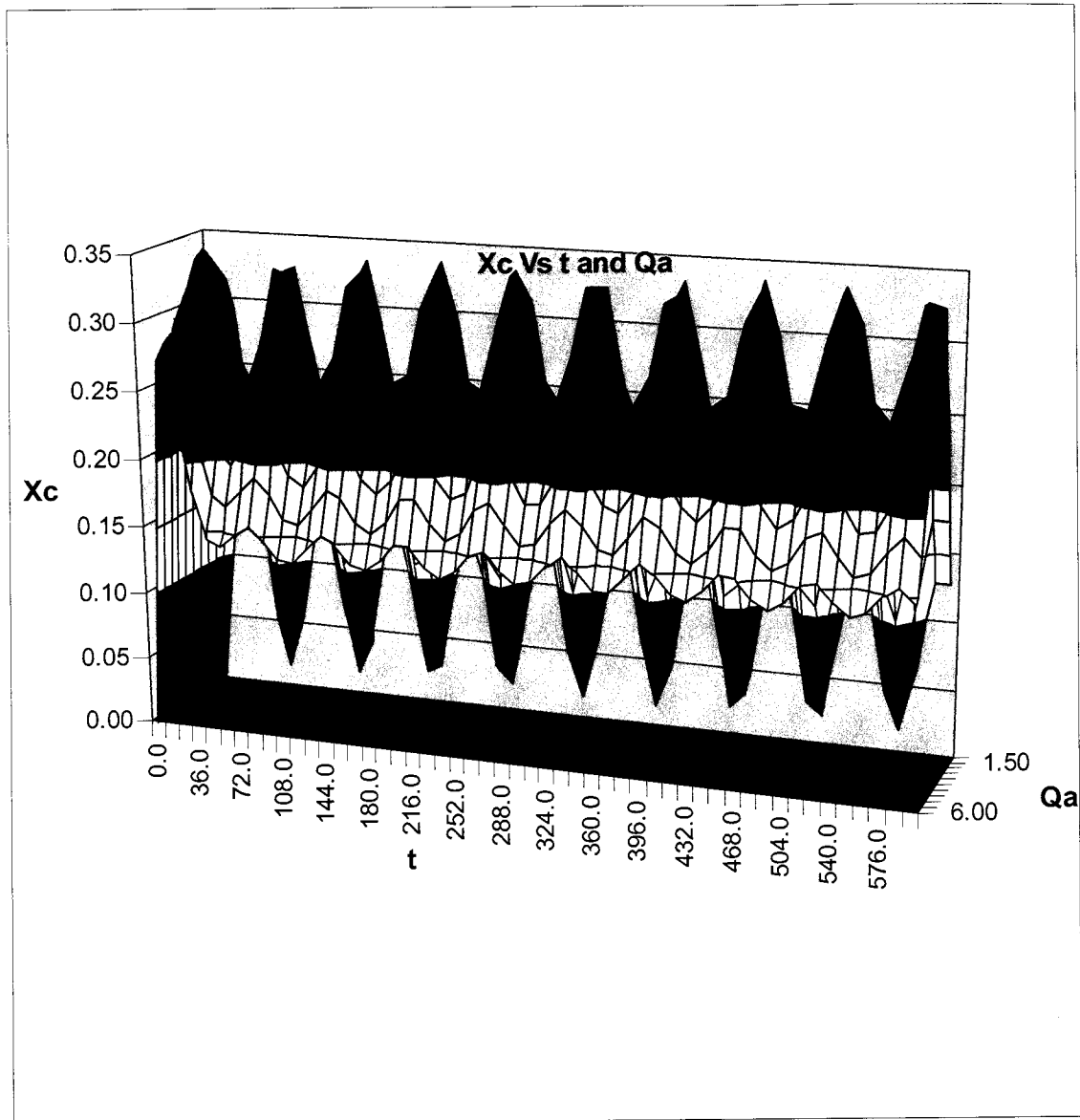


Figure 4.4.2 Mole fraction of C (X_c) with t (seconds) and Q_a (liter sec^{-1}),
 $k_{Aa} = 3.0 \text{ m}^3 \text{ kgmole}^{-1} \text{ sec}^{-1}$, $k_{Ba} = 3.0 \text{ m}^3 \text{ kgmole}^{-1} \text{ sec}^{-1}$, $Q_a = Q_b + Q_i$

The effect of the feed flow rate on the conversion to product using sinusoidal feed can be seen in Figure 4.4.3. The adsorption rate of component A was considered $5.0 \text{ m}^3 \text{ kgmole}^{-1} \text{ sec}^{-1}$ and the adsorption rate of component B was equal to $3.0 \text{ m}^3 \text{ kgmole}^{-1} \text{ sec}^{-1}$. The

average value of X_c was observed to be 0.3130 for the sinusoidal fed. The average value of X_c from the steady state run was lesser at 0.3103 with same applied conditions.

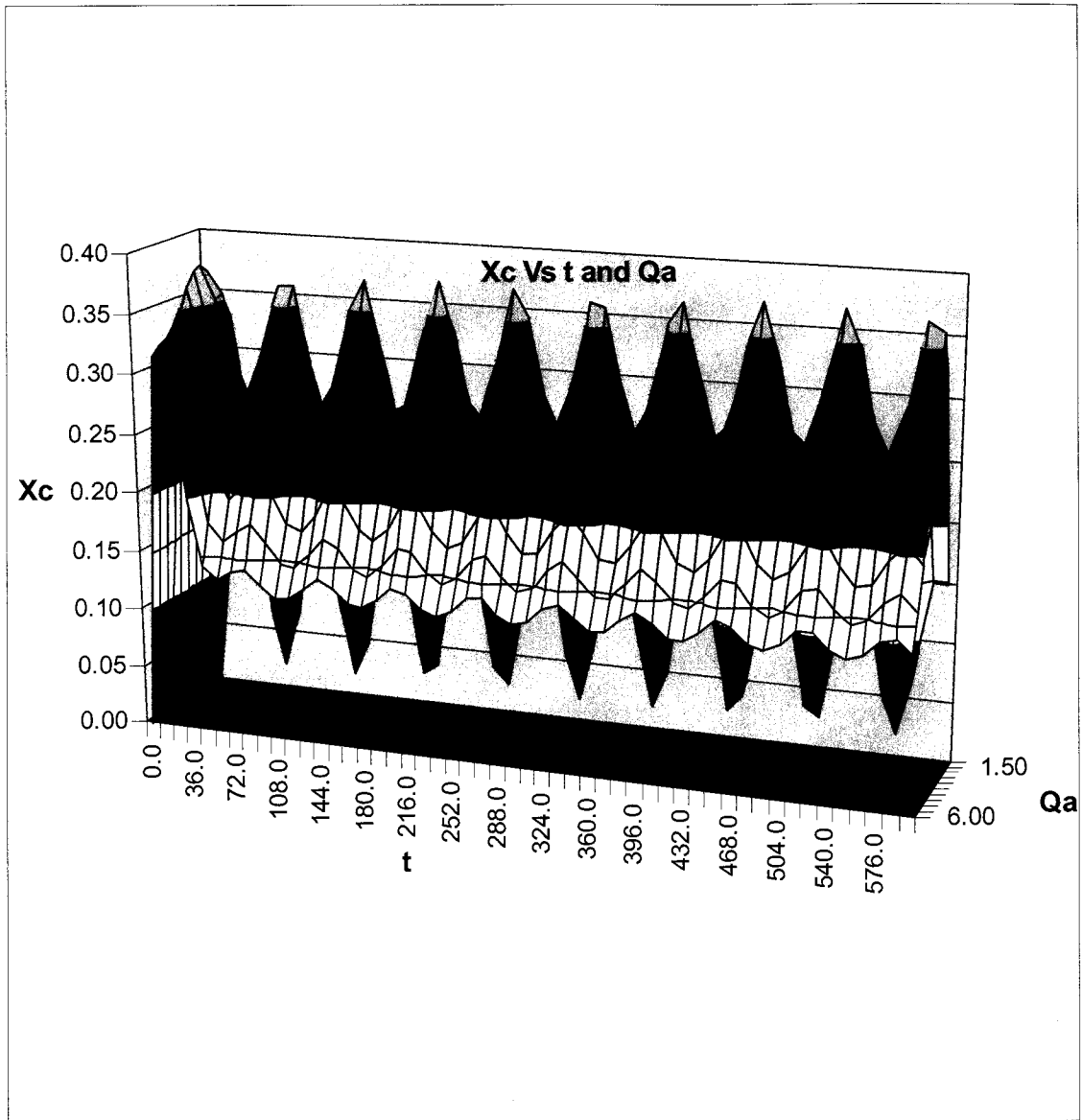


Figure 4.4.3 Mole fraction of C (X_c) with t (seconds) and Q_a (liter sec^{-1}),
 $k_{Aa} = 5.0 \text{ m}^3 \text{ kgmole}^{-1} \text{ sec}^{-1}$, $k_{Ba} = 3.0 \text{ m}^3 \text{ kgmole}^{-1} \text{ sec}^{-1}$, $Q_a = Q_b + Q_i$

The same behavior has been observed in below case of Figure 4.4.4, where the adsorption rate of components A and B was equal to 1.0 and 3.0 $\text{m}^3 \text{ kgmole}^{-1} \text{ sec}^{-1}$, respectively. The flow rate of component B was three times the flow rate of inert gas. Figure 4.4.4 shows

the change in the mole fraction of component C in the outflow with respect to time and flow rate of component A after the application of transient condition. The average mole fraction of C from the transient run of dynamic model was 0.2970, which is surpassed the obtained average X_c of 0.2960 from the steady state run of dynamic model.

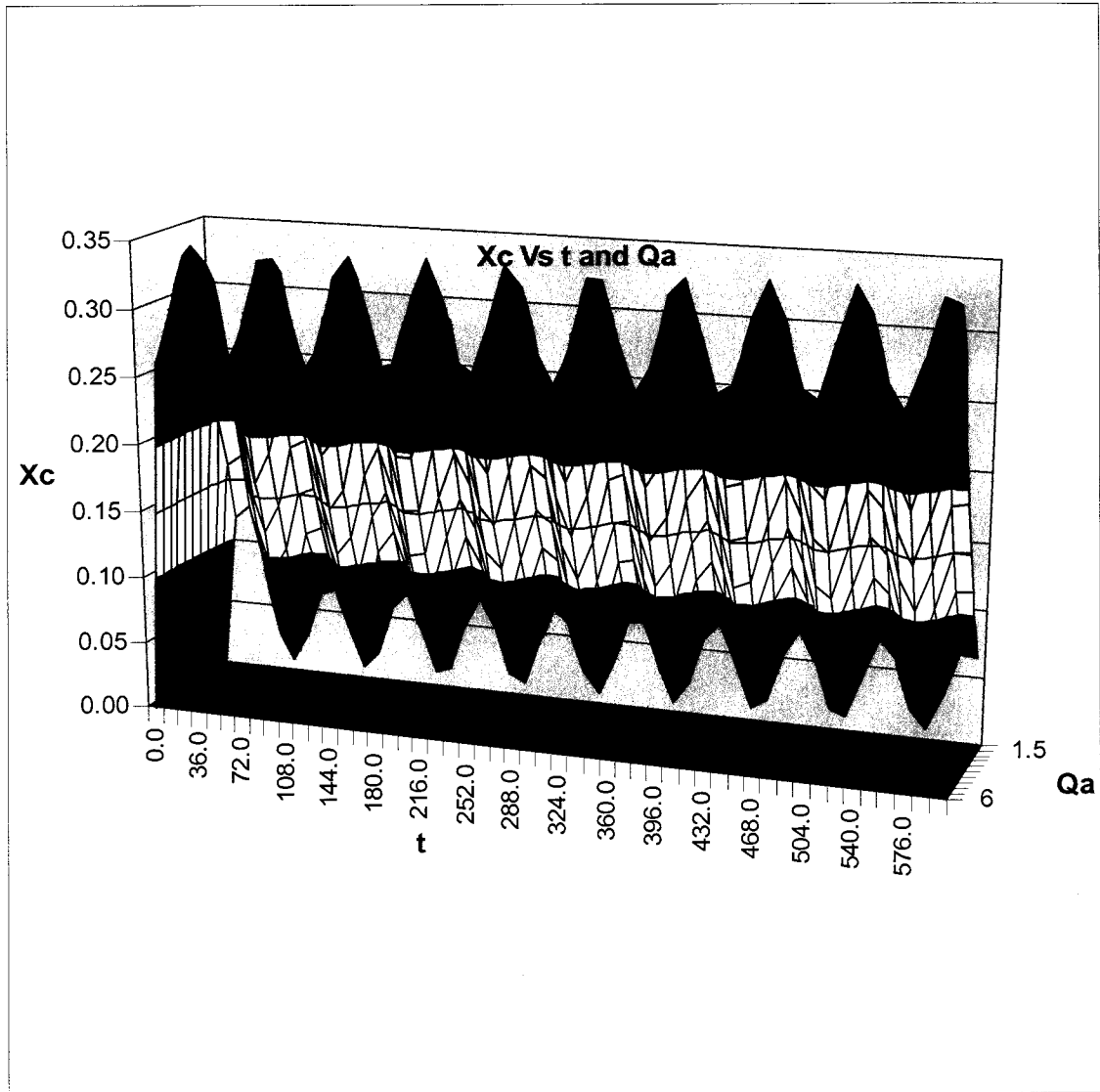


Figure 4.4.4 Mole fraction of C (X_c) with t (seconds) and Q_a (liter sec^{-1}),
 $k_{Aa} = 1.0 \text{ m}^3 \text{ kgmole}^{-1} \text{ sec}^{-1}$, $k_{Ba} = 3.0 \text{ m}^3 \text{ kgmole}^{-1} \text{ sec}^{-1}$, $Q_b = 3 \times Q_i$

The adsorption rate of components A and B was equal to $3.0 \text{ m}^3 \text{ kgmole}^{-1} \text{ sec}^{-1}$ during the case study depicted in Figure 4.4.5. The average X_c was 0.431 from transient run of dynamic model, which is more than the obtained average X_c (0.4276) from steady state run of dynamic model. The transient effect on the mole fraction of C with respect to time and flow rate of component A can be seen in Figure 4.4.5. The flow rate of component B was three times the flow rate of inert gas.

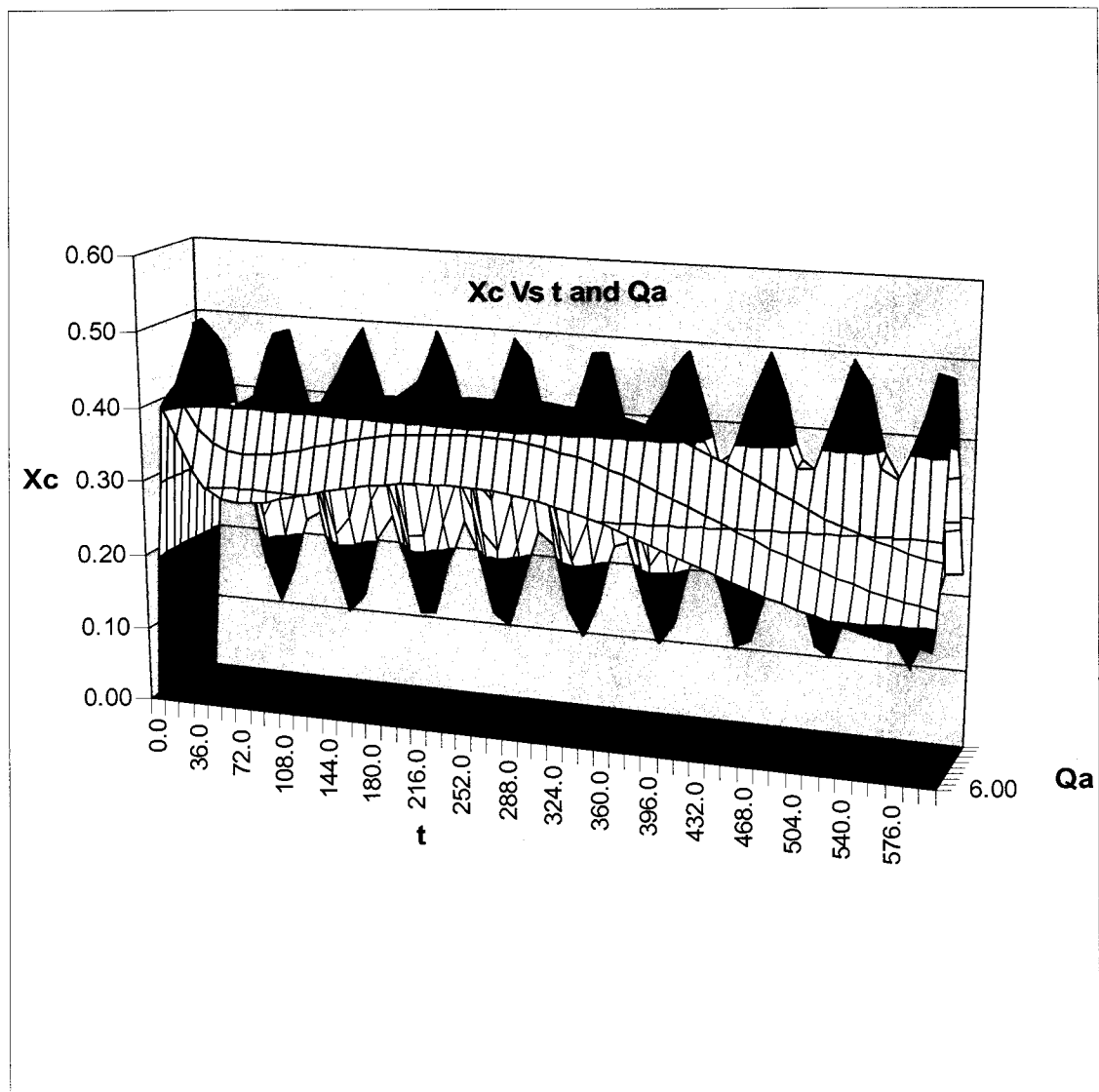


Figure 4.4.5 Mole fraction of C (X_c) with t (seconds) and Q_a (liter sec^{-1}),
 $k_{Aa} = 3.0 \text{ m}^3 \text{ kgmole}^{-1} \text{ sec}^{-1}$, $k_{Ba} = 3.0 \text{ m}^3 \text{ kgmole}^{-1} \text{ sec}^{-1}$, $Q_b = 3 \times Q_i$

The adsorption rate of A was equal to $5.0 \text{ m}^3 \text{ kgmole}^{-1} \text{ sec}^{-1}$ and for B it was equal to $3.0 \text{ m}^3 \text{ kgmole}^{-1} \text{ sec}^{-1}$ during the model run. The flow rate of component B was three times the flow rate of inert gas. The average mole fraction of component C (0.4748) was higher than the average X_c obtained as 0.4699 from steady state run of dynamic model. The impact of transient condition on the mole fraction of C (X_c) with respect to time and flow rate of component A can be seen in Figure 4.4.6.

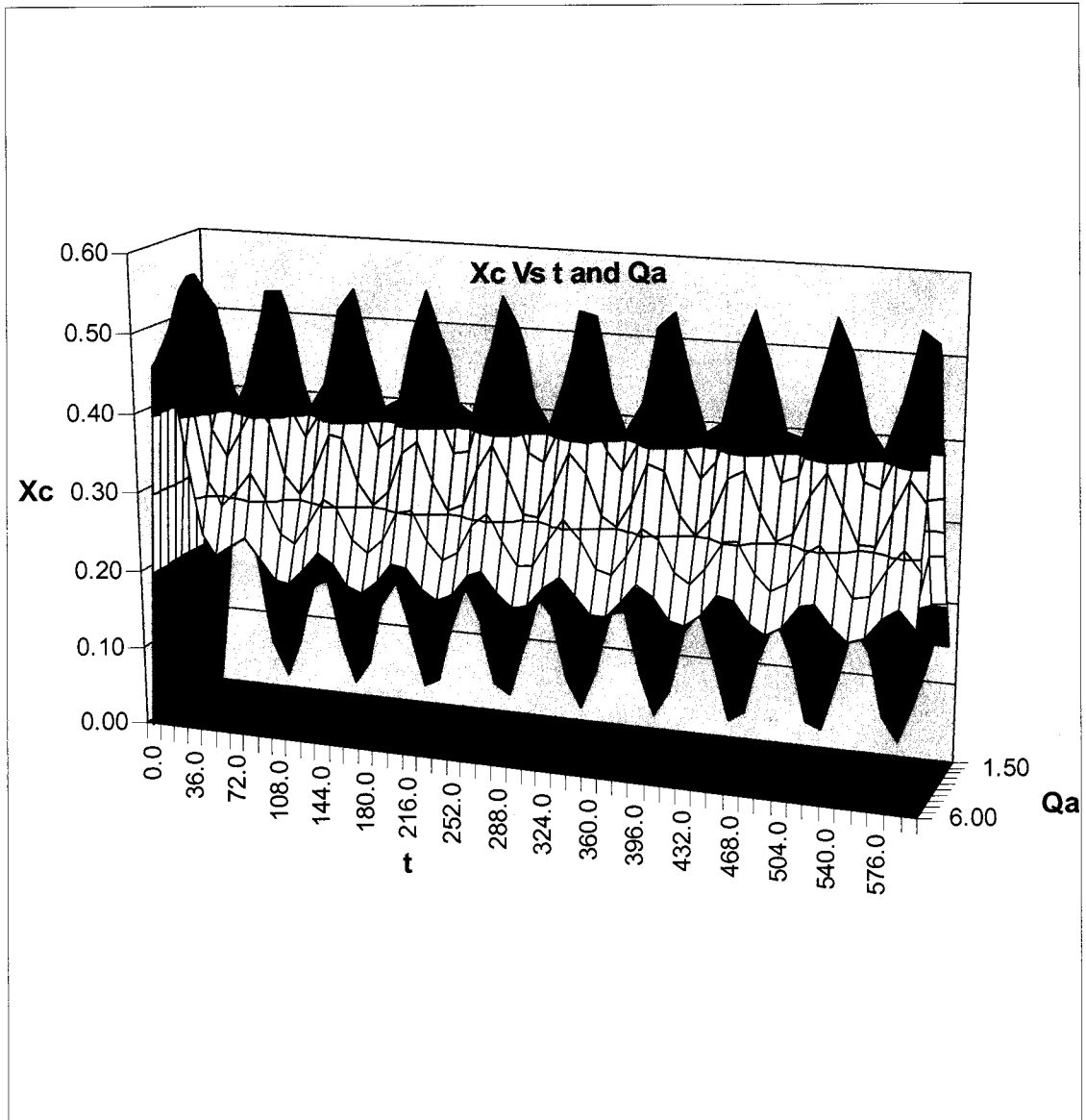


Figure 4.4.6 Mole fraction of C (X_c) with t (seconds) and Q_a (liter sec^{-1}),
 $k_{Aa} = 5.0 \text{ m}^3 \text{ kgmole}^{-1} \text{ sec}^{-1}$, $k_{Ba} = 3.0 \text{ m}^3 \text{ kgmole}^{-1} \text{ sec}^{-1}$, $Q_b = 3 \times Q_i$

The effect due to transient condition in the feed rate of A with respect to adsorption rates and flow rate on the conversion of product can be seen in Figure 4.4.7. The adsorption rate of component A was considered $1.0 \text{ m}^3 \text{ kgmole}^{-1} \text{ sec}^{-1}$ and the adsorption rate of component B was equal to $3.0 \text{ m}^3 \text{ kgmole}^{-1} \text{ sec}^{-1}$. The average X_c was 0.1517 for transient run of dynamic model. The average value of X_c was observed 0.1520 during the steady state run of dynamic model. The flow rate of inert gas was equal to two times the flow rate of component B.

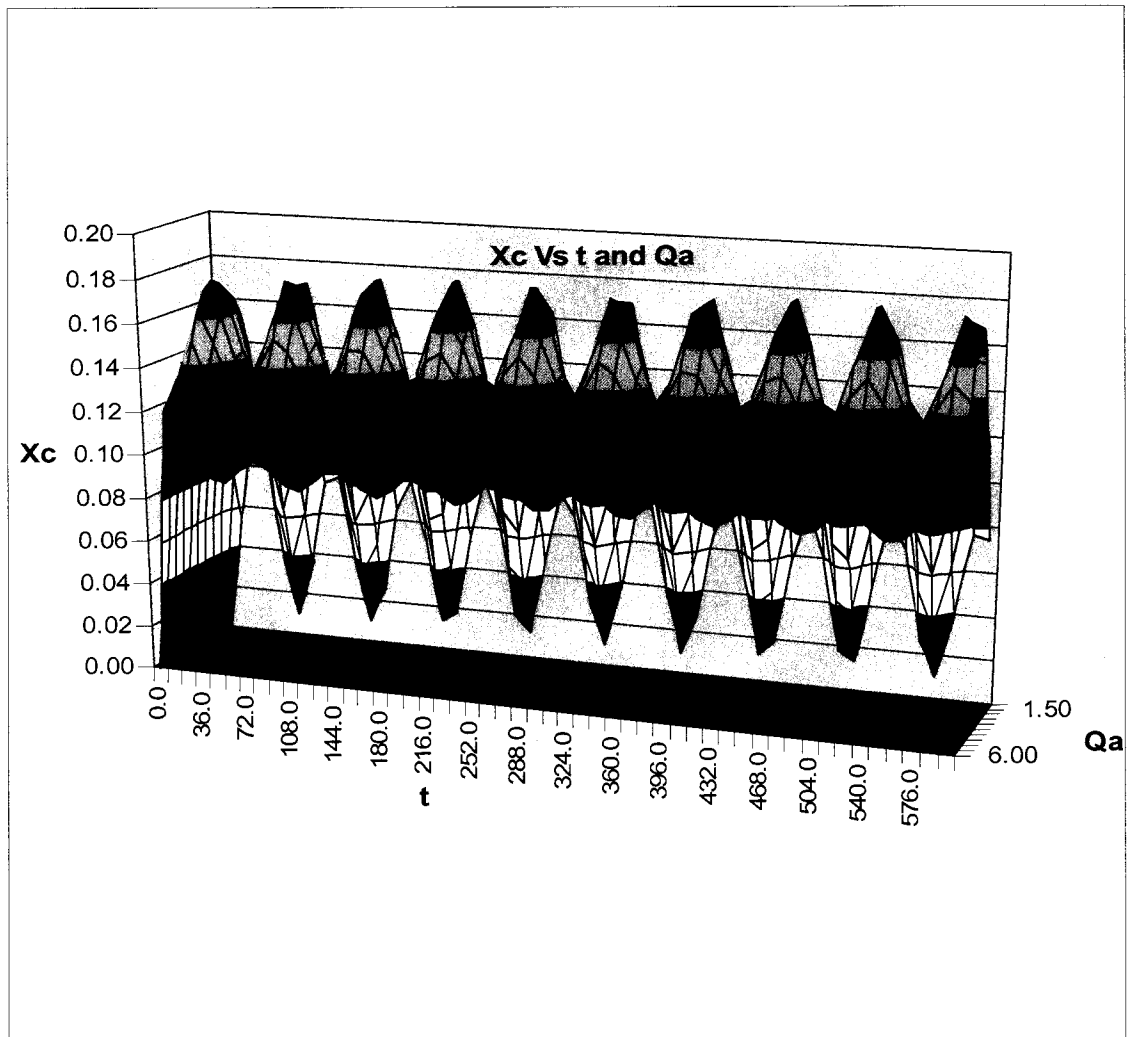


Figure 4.4.7 Mole fraction of C (X_c) with t (seconds) and Q_a (liter sec^{-1}),
 $k_{Aa} = 1.0 \text{ m}^3 \text{ kgmole}^{-1} \text{ sec}^{-1}$, $k_{Ba} = 3.0 \text{ m}^3 \text{ kgmole}^{-1} \text{ sec}^{-1}$, $Q_i = 2 \times Q_b$

The adsorption rate of A and B was taken as $3.0 \text{ m}^3 \text{ kgmole}^{-1} \text{ sec}^{-1}$. The flow rate of inert gas was twice the flow rate of B. The feed rate of A was varied by the sinusoidal input. The average value of X_c 0.1960 from transient run was more than the obtained result of 0.1944 from the steady state run. Figure 4.4.8 shows the mole fraction of component C with respect to time and flow rate of component A for transient run.

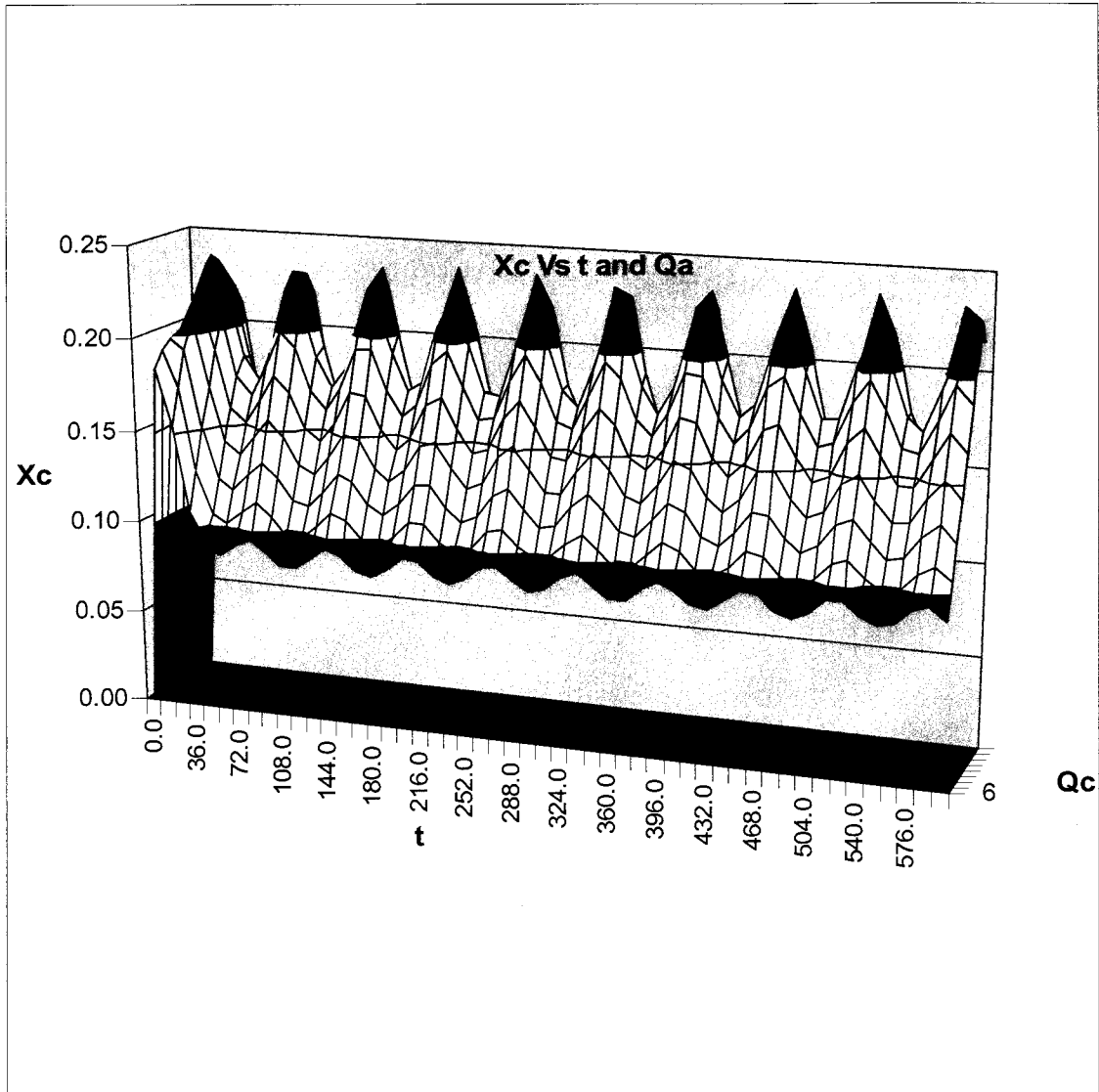


Figure 4.4.8 Mole fraction of C (X_c) with t (seconds) and Q_a (liter sec^{-1}),
 $k_{Aa} = 3.0 \text{ m}^3 \text{ kgmole}^{-1} \text{ sec}^{-1}$, $k_{Ba} = 3.0 \text{ m}^3 \text{ kgmole}^{-1} \text{ sec}^{-1}$, $Q_i = 2 \times Q_b$

The effect of adsorption rate and flow rate on the conversion of product with transient condition can be seen in Figure 4.4.9. The adsorption rate of A and B was considered $5.0 \text{ m}^3 \text{ kgmole}^{-1} \text{ sec}^{-1}$ and $3.0 \text{ m}^3 \text{ kgmole}^{-1} \text{ sec}^{-1}$, respectively during the model run. The mole fraction of component C was observed 0.209 for applied transient condition of the dynamic model. The average value of X_c from the steady state run was at 0.2072 with same applied conditions. The flow rate of component B was twice the flow rate of inert gas.

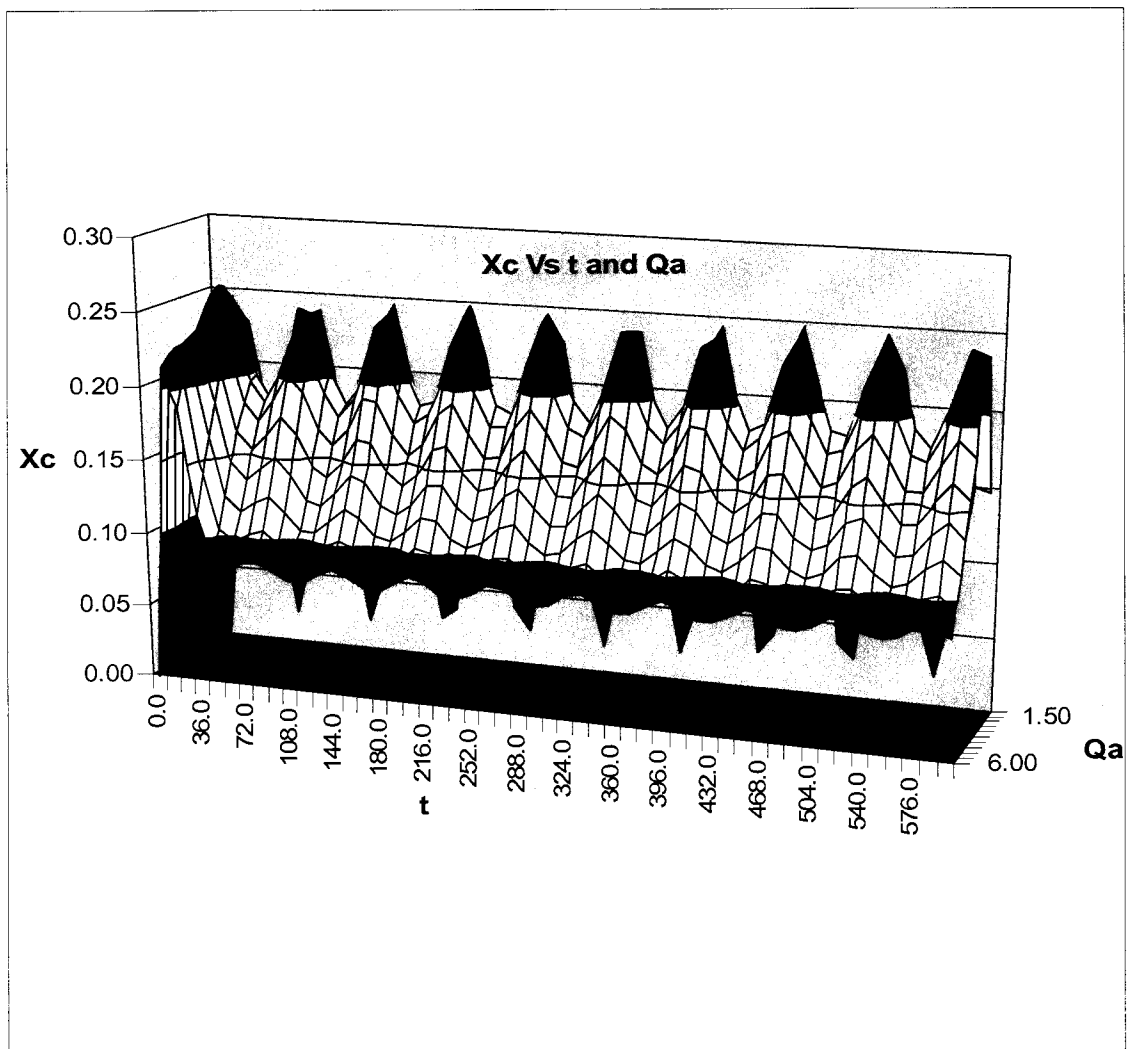


Figure 4.4.9 Mole fraction of C (X_c) with t (seconds) and Q_a (liter sec^{-1}), $k_{Aa} = 5.0 \text{ m}^3 \text{ kgmole}^{-1} \text{ sec}^{-1}$, $k_{Ba} = 3.0 \text{ m}^3 \text{ kgmole}^{-1} \text{ sec}^{-1}$, $Q_i = 2 \times Q_b$

4.5 COMPARISON OF TRANSIENT INPUT AND FIXED INPUT RESPONSE FOR DYNAMIC MODEL STUDY

Table 4.5.1 displays the results obtained of mole fraction of component C from the dynamic model run under the constant and transient input condition. The adsorption rate of A and B was taken as $1.0 \text{ m}^3 \text{ kgmole}^{-1} \text{ sec}^{-1}$ and $3.0 \text{ m}^3 \text{ kgmole}^{-1} \text{ sec}^{-1}$. The flow rate of component B was equal to the flow rate of inert gas. The model run under both this condition has been discussed in the earlier section. The tabulated values are plotted in Figure 4.5.1.

Table 4.5.1 Mole fraction of C (X_c) with transient input and fixed input

| Q_a , liter sec^{-1} | 6 | 5.5 | 5 | 4.5 | 4.25 | 4 |
|---------------------------------|---|--------|--------|--------|--------|--------|
| | Mole fraction of C, (X_c) | | | | | |
| Transient Input | 0.1620 | 0.1844 | 0.2016 | 0.2114 | 0.2150 | 0.2127 |
| Fixed Input | 0.1501 | 0.1739 | 0.1958 | 0.2114 | 0.2141 | 0.2117 |
| Q_a , liter sec^{-1} | 3.5 | 3 | 2.5 | 2 | 1.5 | 1 |
| | Mole fraction of C, (X_c) | | | | | |
| Transient Input | 0.1917 | 0.1612 | 0.1291 | 0.0985 | 0.0706 | 0.0454 |
| Fixed Input | 0.1914 | 0.1601 | 0.1274 | 0.0967 | 0.0688 | 0.0436 |

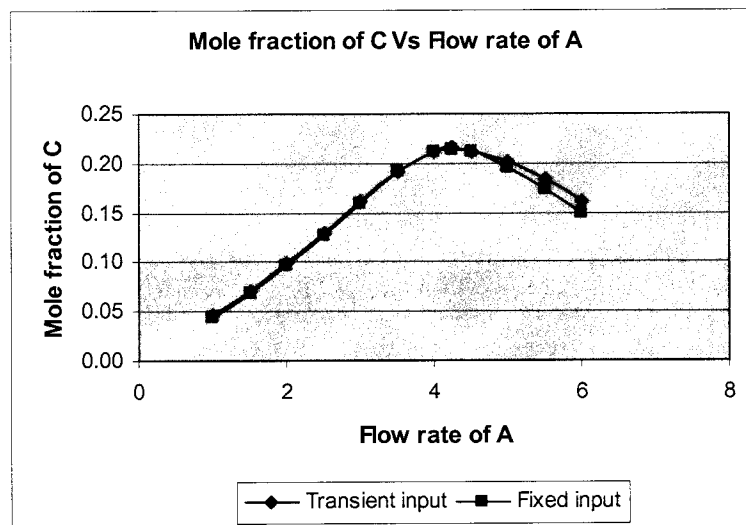


**Figure 4.5.1 Mole fraction of C (X_c) with Flow rate of A (liter sec^{-1}),
 $k_{Aa} = 1.0 \text{ m}^3 \text{ kgmole}^{-1} \text{ sec}^{-1}$, $k_{Ba} = 3.0 \text{ m}^3 \text{ kgmole}^{-1} \text{ sec}^{-1}$, $Q_b = Q_i$**

The tabulated result of Table 4.5.2 shows the mole fraction of the product in the output of the reactor under transient and constant input conditions. The flow rate of inert gas was the same as flow rate of component B. The adsorption rate of A and B was equal to $3.0 \text{ m}^3 \text{ kgmole}^{-1} \text{ sec}^{-1}$. Figure 4.5.2 displays the comparison between these two different characteristic of dynamic model run.

Table 4.5.2 Mole fraction of C (X_c) with transient input and fixed input

| Q_a , liter sec^{-1} | 6 | 5.5 | 5 | 4.5 | 4 |
|---------------------------------|---|--------|--------|--------|--------|
| | Mole fraction of C, (X_c) | | | | |
| Transient Input | 0.1461 | 0.1735 | 0.2032 | 0.2346 | 0.2662 |
| Fixed Input | 0.1454 | 0.1726 | 0.2020 | 0.2332 | 0.2644 |
| Q_a , liter sec^{-1} | 3.5 | 3.25 | 3 | 2.5 | 2 |
| | Mole fraction of C, (X_c) | | | | |
| Transient Input | 0.2897 | 0.2903 | 0.2781 | 0.2292 | 0.1746 |
| Fixed Input | 0.2876 | 0.2876 | 0.2759 | 0.2266 | 0.1716 |

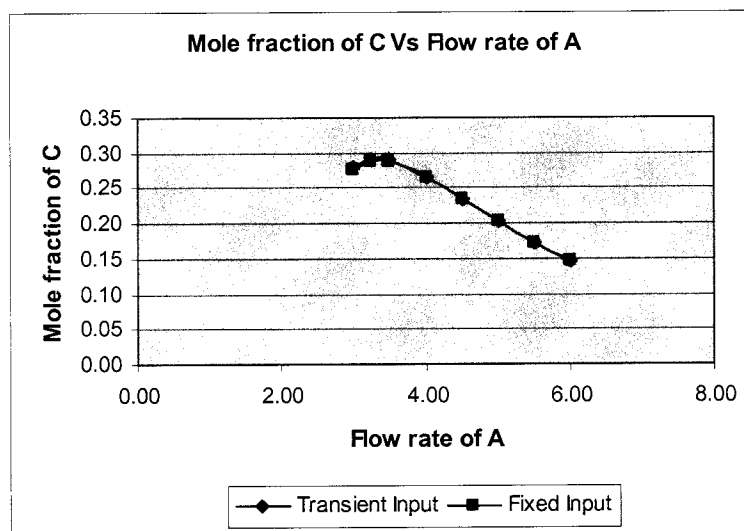


Figure 4.5.2 Mole fraction of C (X_c) with Flow rate of A (liter sec^{-1}), $k_{Aa} = 3.0 \text{ m}^3 \text{ kgmole}^{-1} \text{ sec}^{-1}$, $k_{Ba} = 3.0 \text{ m}^3 \text{ kgmole}^{-1} \text{ sec}^{-1}$, $Q_b = Q_i$

The mole fraction of product in the output under the transient and constant feed conditions can be seen in Table 4.5.3. The flow rate of component B and inert gas was equal to each other. The adsorption rate of components A and B was $5.0 \text{ m}^3 \text{ kgmole}^{-1} \text{ sec}^{-1}$.

¹ and $3.0 \text{ m}^3 \text{ kgmole}^{-1} \text{ sec}^{-1}$, respectively. Figure 4.5.3 is plotted using Table 4.5.3 in order to compare the obtained results from both conditional runs.

Table 4.5.3 Mole fraction of C (X_c) with transient input and fixed input

| | | | | | | |
|---------------------------------|-------------------------------|--------|--------|--------|--------|--------|
| Q_a , liter sec^{-1} | 6 | 5.5 | 5 | 4.5 | 4 | 3.5 |
| | Mole fraction of C, (X_c) | | | | | |
| Transient Input | 0.1367 | 0.1637 | 0.1938 | 0.2274 | 0.2640 | 0.3003 |
| Fixed Input | 0.1358 | 0.1626 | 0.1925 | 0.2257 | 0.2620 | 0.2978 |
| Q_a , liter sec^{-1} | 3.25 | 3.00 | 2.50 | 2.00 | 1.5 | 1 |
| | Mole fraction of C, (X_c) | | | | | |
| Transient Input | 0.3131 | 0.3130 | 0.2661 | 0.2033 | 0.1446 | 0.0921 |
| Fixed Input | 0.3103 | 0.3100 | 0.2631 | 0.2000 | 0.1410 | 0.0884 |

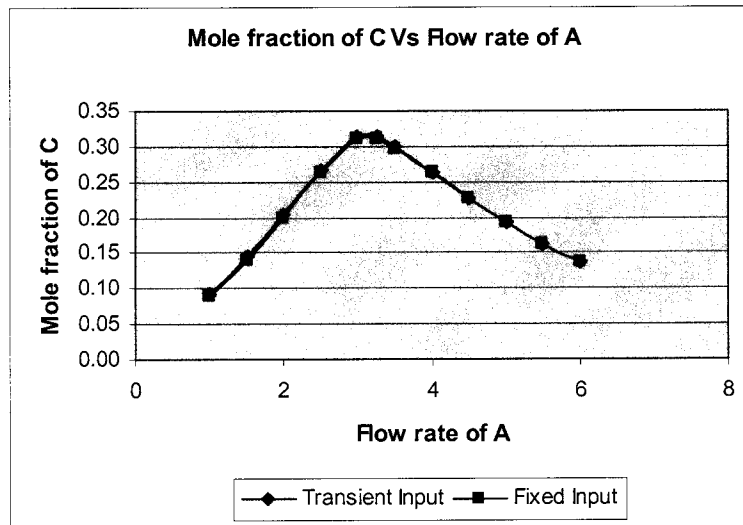


Figure 4.5.3 Mole fraction of C (X_c) with Flow rate of A (liter sec^{-1}), $k_{Aa} = 5.0 \text{ m}^3 \text{ kgmole}^{-1} \text{ sec}^{-1}$, $k_{Ba} = 3.0 \text{ m}^3 \text{ kgmole}^{-1} \text{ sec}^{-1}$, $Q_b = Q_i$

The following Table 4.5.4 is the results of dynamic model run under the constant and transient input. The flow rate of component B was thrice the flow rate of inert gas. In transient condition, the sinusoidal function was applied in the feed rate of A. The adsorption rate of A and B was $1.0 \text{ m}^3 \text{ kgmole}^{-1} \text{ sec}^{-1}$ and $3.0 \text{ m}^3 \text{ kgmole}^{-1} \text{ sec}^{-1}$. The chart displays the mole fraction of component C with respect to the flow rate of component A for two different input conditions.

Table 4.5.4 Mole fraction of C (X_c) with transient input and fixed input

| Q_a , liter sec^{-1} | 6 | 5.5 | 5 | 4.5 | 4 | |
|---------------------------------|---|--------|--------|--------|--------|--------|
| | Mole fraction of C, (X_c) | | | | | |
| Transient Input | 0.2467 | 0.2821 | 0.2973 | 0.2769 | 0.2365 | |
| Fixed Input | 0.2459 | 0.2811 | 0.2960 | 0.2751 | 0.2344 | |
| Q_a , liter sec^{-1} | 3.5 | 3 | 2.5 | 2 | 1.5 | 1 |
| | Mole fraction of C, (X_c) | | | | | |
| Transient Input | 0.1946 | 0.1564 | 0.1227 | 0.0929 | 0.0665 | 0.0428 |
| Fixed Input | 0.1922 | 0.1540 | 0.1202 | 0.0905 | 0.0642 | 0.0406 |

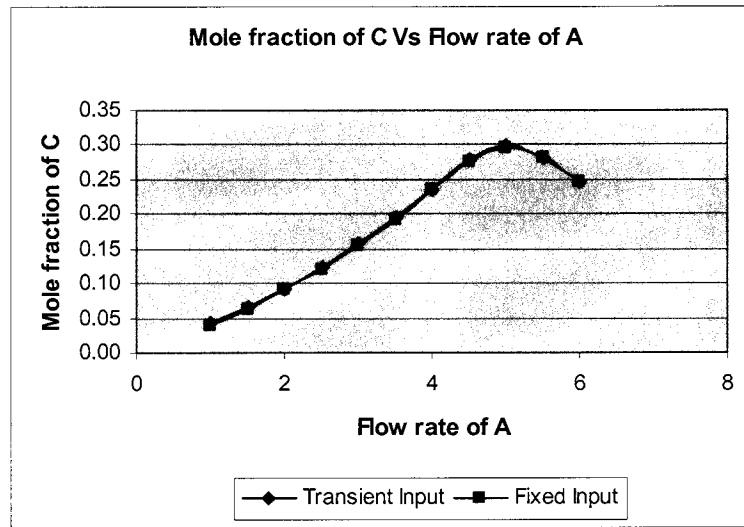


Figure 4.5.4 Mole fraction of C (X_c) with Flow rate of A (liter sec^{-1}), $k_{Aa} = 1.0 \text{ m}^3 \text{ kgmole}^{-1} \text{ sec}^{-1}$, $k_{ba} = 3.0 \text{ m}^3 \text{ kgmole}^{-1} \text{ sec}^{-1}$, $Q_b = 3 \times Q_i$

The adsorption rate of A and B was equal to $3.0 \text{ m}^3 \text{ kgmole}^{-1} \text{ sec}^{-1}$ for the following Table 4.5.5 results. The flow rate of B was three times the flow rate of inert gas. The applied condition of constant feed and transient feed is responsible for the different output of product. Table 4.5.5 shows the obtained results.

Table 4.5.5 Mole fraction of C (X_c) with transient input and fixed input

| Q_a , liter sec^{-1} | 6 | 5.5 | 5 | 4.5 | 4.25 |
|---------------------------------|-------------------------------|--------|--------|--------|--------|
| | Mole fraction of C, (X_c) | | | | |
| Transient Input | 0.2745 | 0.3305 | 0.3847 | 0.4151 | 0.4310 |
| Fixed Input | 0.2534 | 0.2983 | 0.3562 | 0.4116 | 0.4276 |
| Q_a , liter sec^{-1} | 4 | 3.5 | 3 | 2.5 | 2 |
| | Mole fraction of C, (X_c) | | | | |
| Transient Input | 0.4267 | 0.3672 | 0.2946 | 0.2288 | 0.1713 |
| Fixed Input | 0.4231 | 0.3633 | 0.2904 | 0.2242 | 0.1667 |

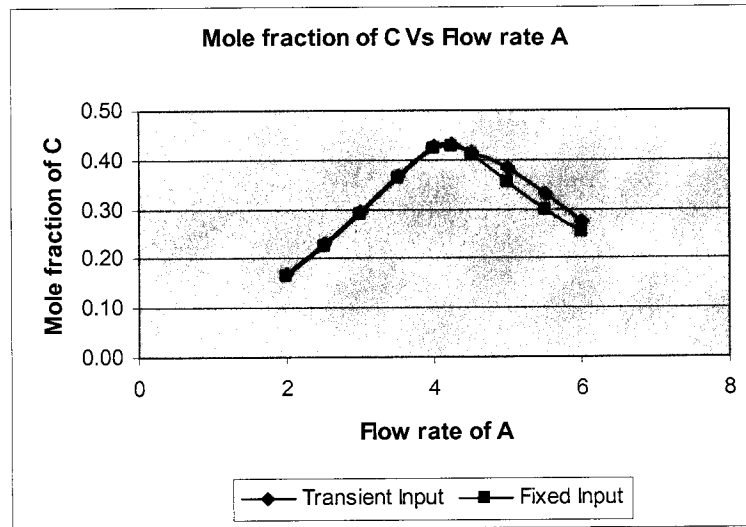


Figure 4.5.5 Mole fraction of C (X_c) with Flow rate of A (liter sec^{-1}), $k_{Aa} = 3.0 \text{ m}^3 \text{ kgmole}^{-1} \text{ sec}^{-1}$, $k_{Ba} = 3.0 \text{ m}^3 \text{ kgmole}^{-1} \text{ sec}^{-1}$, $Q_b = 3 \times Q_i$

The comparison between the output of product mole fraction under constant feed and transient feed condition can be seen in Table 4.5.6 for dynamic model. Figure 4.5.6 displays the tabulated results. The adsorption rate of A and B was $5.0 \text{ m}^3 \text{ kgmole}^{-1} \text{ sec}^{-1}$ and $3.0 \text{ m}^3 \text{ kgmole}^{-1} \text{ sec}^{-1}$, respectively. The flow rate of inert gas was one third of the flow rate of component B.

Table 4.5.6 Mole fraction of C (X_c) with transient input and fixed input

| | | | | | | |
|---------------------------------|-------------------------------|--------|--------|--------|--------|--------|
| Q_a , liter sec^{-1} | 6 | 5.5 | 5 | 4.5 | 4 | |
| | Mole fraction of C, (X_c) | | | | | |
| Transient Input | 0.2319 | 0.2857 | 0.3489 | 0.4204 | 0.4748 | |
| Fixed Input | 0.2301 | 0.2833 | 0.3456 | 0.4162 | 0.4699 | |
| Q_a , liter sec^{-1} | 3.5 | 3 | 2.5 | 2 | 1.5 | 1 |
| | Mole fraction of C, (X_c) | | | | | |
| Transient Input | 0.4300 | 0.3473 | 0.2702 | 0.2025 | 0.1433 | 0.0913 |
| Fixed Input | 0.4254 | 0.3424 | 0.2650 | 0.1972 | 0.1381 | 0.0863 |

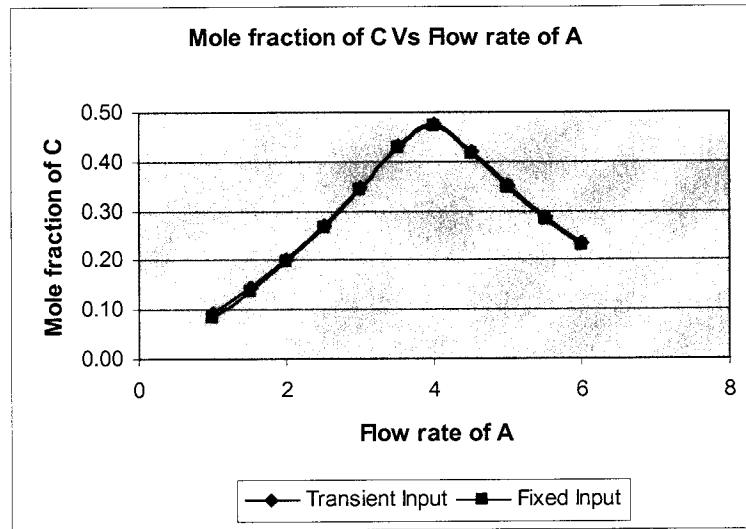


Figure 4.5.6 Mole fraction of C (X_c) with Flow rate of A (liter sec^{-1}), $k_{Aa} = 5.0 \text{ m}^3 \text{ kgmole}^{-1} \text{ sec}^{-1}$, $k_{Ba} = 3.0 \text{ m}^3 \text{ kgmole}^{-1} \text{ sec}^{-1}$, $Q_b = 3 \times Q_i$

The following results were obtained from dynamic model run after the application of fixed and sinusoidal input with adsorption rate of A and B was equal to $3.0 \text{ m}^3 \text{ kgmole}^{-1} \text{ sec}^{-1}$. The flow rate of inert gas was two times the flow rate of B. The dynamic model run gives a different product mole fraction in output for constant and transient input which is displayed in Table 4.5.7. Figure 4.5.7 shows this comparison.

Table 4.5.7 Mole fraction of C (X_c) with transient input and fixed input

| | | | | | | |
|---------------------------------|-------------------------------|--------|--------|--------|--------|--------|
| Q_a , liter sec^{-1} | 6 | 5.5 | 5 | 4.5 | 4 | 3.5 |
| | Mole fraction of C, (X_c) | | | | | |
| Transient Input | 0.0945 | 0.1090 | 0.1230 | 0.1368 | 0.1477 | 0.1523 |
| Fixed Input | 0.0943 | 0.1088 | 0.1231 | 0.1365 | 0.1472 | 0.1517 |
| Q_a , liter sec^{-1} | 3 | 2.5 | 2 | 1.5 | 1 | |
| | Mole fraction of C, (X_c) | | | | | |
| Transient Input | 0.1451 | 0.1251 | 0.0991 | 0.0722 | 0.0468 | |
| Fixed Input | 0.1443 | 0.1241 | 0.0978 | 0.0709 | 0.0453 | |

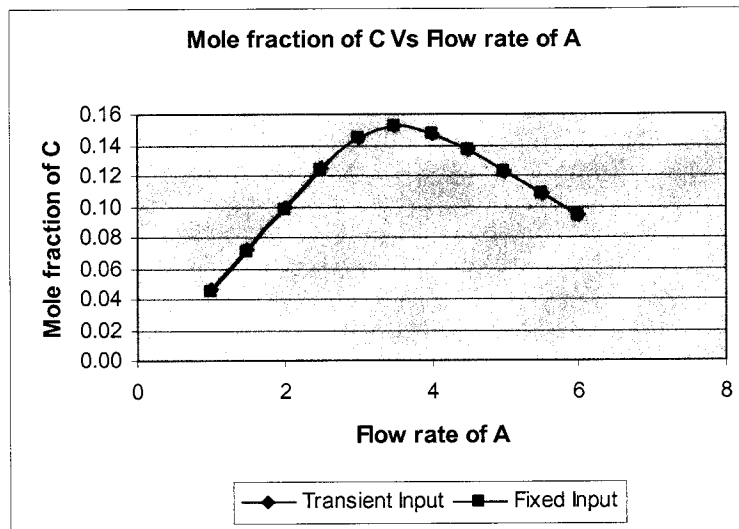


Figure 4.5.7 Mole fraction of C (X_c) with Flow rate of A (liter sec^{-1}), $k_{Aa} = 1.0 \text{ m}^3 \text{ kgmole}^{-1} \text{ sec}^{-1}$, $k_{Ba} = 3.0 \text{ m}^3 \text{ kgmole}^{-1} \text{ sec}^{-1}$, $Q_i = 2 \times Q_b$

Table 4.5.8 displays the results of mole fraction of component C in the outflow for the dynamic model run under the constant and transient input. The flow rate of inert gas was twice the flow rate of component B. In transient condition, the sinusoidal function was applied in the feed rate of A. The adsorption rate of A and B was $1.0 \text{ m}^3 \text{ kgmole}^{-1} \text{ sec}^{-1}$ and $3.0 \text{ m}^3 \text{ kgmole}^{-1} \text{ sec}^{-1}$. The chart displays the mole fraction of C with respect to the flow rate of component A for two different input conditions.

Table 4.5.8 Mole fraction of C (X_c) with transient input and fixed input

| Q_a , liter sec^{-1} | 6 | 5.5 | 5 | 4.5 | 4 |
|---------------------------------|---|--------|--------|--------|--------|
| | Mole fraction of C, (X_c) | | | | |
| Transient Input | 0.0906 | 0.1062 | 0.1228 | 0.1402 | 0.1582 |
| Fixed Input | 0.0903 | 0.1058 | 0.1222 | 0.1395 | 0.1574 |
| Q_a , liter sec^{-1} | 3.5 | 3 | 2.75 | 2.5 | 2 |
| | Mole fraction of C, (X_c) | | | | |
| Transient Input | 0.1762 | 0.1915 | 0.1960 | 0.1943 | 0.1671 |
| Fixed Input | 0.1752 | 0.1903 | 0.1944 | 0.1929 | 0.1654 |

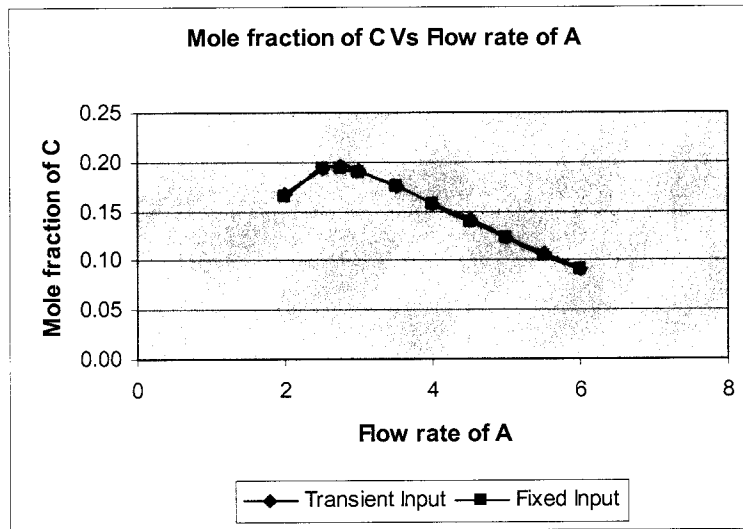


Figure 4.5.8 Mole fraction of C (X_c) with Flow rate of A (liter sec^{-1}), $k_{Aa} = 3.0 \text{ m}^3 \text{ kgmole}^{-1} \text{ sec}^{-1}$, $k_{Ba} = 3.0 \text{ m}^3 \text{ kgmole}^{-1} \text{ sec}^{-1}$, $Q_i = 2 \times Q_b$

The comparison between the output of product mole fraction under constant feed and transient feed conditions can be seen in Table 4.5.9. Figure 4.5.9 displays the tabulated results. The adsorption rate of A and B was $5.0 \text{ m}^3 \text{ kgmole}^{-1} \text{ sec}^{-1}$ and $3.0 \text{ m}^3 \text{ kgmole}^{-1} \text{ sec}^{-1}$, respectively. The flow rate of inert gas was two times the flow rate of component B.

Table 4.5.9 Mole fraction of C (X_c) with transient input and fixed input

| Q_a , liter sec^{-1} | 6 | 5.5 | 5 | 4.5 | 4 | 3.5 |
|---------------------------------|---|--------|--------|--------|--------|--------|
| | Mole fraction of C, (X_c) | | | | | |
| Transient Input | 0.0847 | 0.1000 | 0.1165 | 0.1343 | 0.1536 | 0.1741 |
| Fixed Input | 0.0842 | 0.0994 | 0.1158 | 0.1336 | 0.1527 | 0.1729 |
| Q_a , liter sec^{-1} | 3 | 2.5 | 2 | 1.5 | 1 | |
| | Mole fraction of C, (X_c) | | | | | |
| Transient Input | 0.1946 | 0.2090 | 0.1913 | 0.1425 | 0.0917 | |
| Fixed Input | 0.1932 | 0.2072 | 0.1893 | 0.1402 | 0.0891 | |

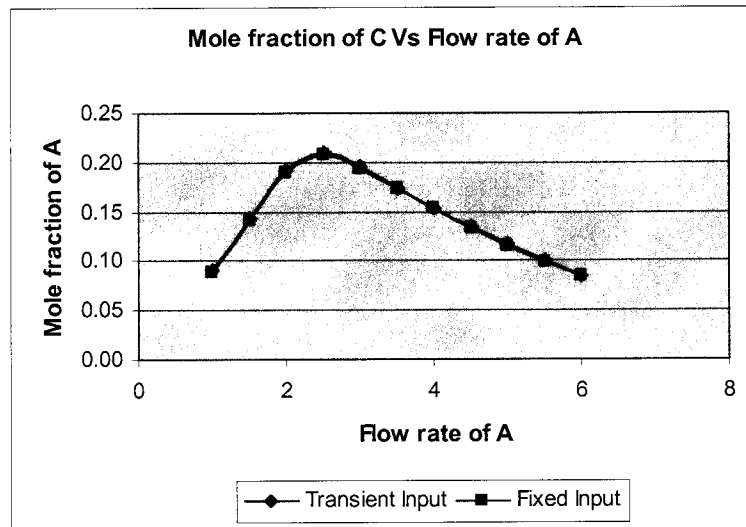


Figure 4.5.9 Mole fraction of C (X_c) with Flow rate of A (liter sec^{-1}), $k_{Aa} = 5.0 \text{ m}^3 \text{ kgmole}^{-1} \text{ sec}^{-1}$, $k_{Ba} = 3.0 \text{ m}^3 \text{ kgmole}^{-1} \text{ sec}^{-1}$, $Q_i = 2 \times Q_b$

Comparison between unsteady and steady state behavior of fluidized bed was done in Section 4.5. Figures 4.5.1 – 4.5.9 show the mole fraction change of component C with respect to the flow rate of component A. It is that after the maximum optimized concentration of product was obtained, the reactor showed better efficiency with unsteady state condition as compared to the steady state condition. So, it is advisable to apply transient condition after the reactor reaches its maximum product concentration in order to improve the overall average product output.

CHAPTER 5

SUMMARY AND RECOMMENDATIONS

5.1 SUMMARY

The optimization of a bimolecular catalytic reaction where adsorption of the reactants onto the catalyst dominates the overall reaction rate in a fluidized bed reactor has been discussed. Two types of computational models, (1) steady state (2) dynamic state, were developed. The application of these models on the fluidized bed reactor showed the extent of competitive adsorption on the fluidized bed reactor performance. From the results, it has been proven that optimal ratio of the reactants fed to the reactor is a function of the adsorption rate constants of the components. If one reactant has a higher adsorption rate constant, it should be fed at lower than stoichiometric amount to maximize the production of product. This is due to the composition of reactants to the available surface sites of the catalyst. Even the catalyst surface is far from the saturation point, the differences in the adsorption rate constants of the reactants influences the optimal feed ratio of the reactants. Introducing an oscillating feed to one or both reactants improved the overall conversion to product when compared to a constant feed rate. This improvement becomes greater at higher values of the adsorption rate constants. The presence of an inert component in the feed reduced the improvement of oscillating the feed with respect to the overall conversion of the reactants.

5.2 RECOMMEDATIONS

Except as background, the designing of adsorption systems and their operations, researchers have a very little interest in the aspects of adsorption on the optimization of catalytic chemical reactions. To the engineer or designer, particularly in the gas phase adsorption, the catalyst adsorbent is a physical part of the system, to be considered in the same way as a fan or blower, a tower or tank, a length of pipe or a fitting that generates pressure energy. The amount of gas adsorbed per gram of the adsorbent at equilibrium is dependent upon the temperature, pressure, and the nature of the adsorbent, the preparation and history of the adsorbent and the adsorbate. The quantity of a gas adsorbed by a given weight of adsorbent varies greatly from one adsorbing solid to another, as well as from different adsorbent of the same apparent chemical composition. Future research with different adsorption rates and their effect in dynamic state has been recommended. It would be interesting to see variance in the result of transient condition and steady state condition away from their optimum value and it would be desire to have established relation between transient conditions with reactor design leading to improve the size of the reactor. Further recommendations can be made with recycling the product flow rate into the reactor and try to see the competitive adsorption effect on the optimization of product. Future master thesis on the experimental development of this computational reactor can be proposed. There are many areas in fluidized bed reactor being untouched by researches over the years and adsorption effect is one of them. This research may be helpful to explore some part of it.

NOMENCLATURE

| | |
|--|--|
| C_A , kg-mole m^{-3} | concentration of component A in the fluid |
| C_B , kg-mole m^{-3} | concentration of component B in the fluid |
| C_C , kg-mole m^{-3} | concentration of component C in the fluid |
| C_f , kg-mole m^{-3} | molar concentration of the gas |
| G, kg | mass of the catalyst in the fluidized bed |
| k_{Aa} , m^3 kg-mole $^{-1}$ s $^{-1}$ | adsorption rate constant of component A |
| k_{Ba} , m^3 kg-mole $^{-1}$ s $^{-1}$ | adsorption rate constant of component B |
| k_{Ad} , s $^{-1}$ | desorption rate constant of component A |
| k_{Bd} , s $^{-1}$ | desorption rate constant of component B |
| k_r , kg kg-mole $^{-1}$ s $^{-1}$ | reaction rate constant |
| n_A , kg-mole kg $^{-1}$ | rate of change of the surface concentration of component A |
| n_B , kg-mole kg $^{-1}$ | rate of change of the surface concentration of component B |
| n_s , kg-mole kg $^{-1}$ | maximum number of surface sites on the catalyst |
| Q_0 , m^3 s $^{-1}$ | inlet gas volumetric flow rate |
| Q , m^3 s $^{-1}$ | outlet gas volumetric flow rate |
| V, m^3 | volume of gas in the fluidized bed |
| t, s | time |
| y_A , | moles of A per number of open surface sites |
| y_B , | moles of B per number of open surface sites |
| x_A , | moles of A per total moles in fluid |
| x_B , | moles of B per total moles in fluid |

| | |
|----------------|---|
| x_C , | moles of C per total moles in fluid |
| $x_{A,feed}$, | moles of A initially fed to the fluidized bed |
| $x_{B,feed}$, | moles of B initially fed to the fluidized bed |

REFERENCES

1. Asif, Mohommad, and Ahmed A.I., *Minimum Fluidization velocity and defluidization behavior of binary-solid liquid-fluidized beds*, Powder Technology **2002**, 126, 241-254
2. Chapra, S.C. and Canale, R. P., *Numerical Methods for Engineers*, McGraw-Hill, New York **2002**
3. C.L Mantell, *Adsorption*, Chemical Engineering Services, Second edition, McGraw-Hill Book Company, Inc. **1951**
4. Daizo Kunii, Octave Levenspiel, *Fluidization Engineering*, Second Edition, Butterworth-Heinemann **1991**
5. Dale L. Keairns, *Fluidization Technology*, Volume I and II, Hemisphere Publishing Corporation **1975**, International Fluidization Conference, California
6. Das, K.A., G.B. Martin, D. Constales, G.S. Yablonsky, *Effect on the kinetics of simultaneous adsorption of SO₂-NO_x over Na- γ -Al₂O₃ sorbent; a coverage-dependent stoichiometry*, Chemical Engineering Science **2002**, 57, 1909-1922
7. Devotta, I.R.A. Mashelkar, Competitive diffusion-adsorption of polymers of differing chain lengths on solid surfaces, Chemical Engineering Science **1996**, Vol. 51, PP.561-569
8. Driscoll, W.D, *Visual Basic for Engineers*, Youngstown State University, Youngstown, OHIO **1999**
9. F. J.R. Van Neer, A.J. Kodde, H.Den Uil, A. Blik, *Can. J. Chem. Eng. Sci.* **1996**, 74, 664
10. *Fluidized bed Fundamentals and Applications*, AIChE Symposium Series **1973**, 128, Volume 69
11. *Fluidization Theories and Applications*, AIChE Symposium Series **1977**, 161 Volume 73
12. H. Scott Fogler , *Chemical Reactors*, ACS Symposium series, American Chemical Society **1981**, 168

13. Hoebink, J.H.B.J., A.J.L., Nievergeld, G.B. Martin, *CO oxidation in a fixed bed reactor with high frequency cycling of the feed*, Chemical Engineering Science **1999**, 54, 4459-4468
14. Ivabov, E.A., S.I. Reshetnikov, M.V. Sidyakin and A.N Startsev, *Benzene hydrogenation on sulfide catalyst under unsteady-state conditions*, React. Kinet, Catal. Lett. **2003**, Vol.78, No.2, 389-395
15. Ivabov, E.A., S.I. Reshetnikov, L. Kiwi-Minsker and A. Renken, *Performance enhancement by unsteady state reactor operation: theoretical analysis for two sites kinetic model*, Borsdkov Institute of Catalyst, Novosibirsk, Russia, Chem. Eng. Tech. **2003**
16. J.F Davidson, R. Clift, D. Harrison, *Fluidization*, second edition, Academic Press **1985**
17. J G Yates, *Fundamentals of Fluidized-bed Chemical Process*, Butterworths **1983**
18. K. Klusacek, R.R. Hudgins, P.L Silverston, *Can. J. Chem. Eng. Sci.* **1989**, 67,516
19. Kim, Dong Hyun, Mee Sook Lim, Kinetics of selective CCO oxidation in hydrogen rich mixtures on Pt/aluminum catalyst, Applied Catalysis A: General **2002**, 224, 27-38
20. King, A. R, R.J. Johnson, D.M. Price, *Kinetic model for the optimization of a Fluidized bed reactor*, Youngstown State University, Youngstown, Ohio **2003**
21. Klusacek, Karel and Vladimir Stuchly, *Increasing of carbon monoxide methanation rate by forced feed composition cycling*, Catalysis Today **1995**, 25, 169-174
22. Klusacek, Karel and Valdimir Stuchly, Unsteady-state carbon monoxide methanation on an Ni/SO₂ catalyst, Journal of Catalysis **1993**, 139, 62-71
23. Koubek, J. Pasek, V. Ruzicka, in New Horizons in Catalysis, Elsevier-Kodansha, Amsterdam-Tokyo **1980**, 853
24. Mawarti, Y. , Yuji Tatemoto and Katsuji Noda, *Prediction of minimum Fluidization velocity for vibrated fluidized bed*, Power Technology **2003**, 131, 66-70
25. Peter Harriott, *Chemical Reactor Design*, Marcel Dekker, Inc. **2003**
26. Price, D.M., *The preparation of platinum/gamma – aluminum – oxide pellets with an internal step – distribution of catalyst: experiment and theory*, PhD dissertation, The University of Notre Dame **1988**

27. Quah, B.H., Joseph F. Mathews, and Chun-Zhu Li, *Interinfluence between reactions on the catalytic surface and reactions in the gas phase during catalytic oxidation of methane with air*, Journal of Catalysis **2001**, 197, 315-323
28. S.I. Reshetnikov, E.A. Ivanov, L.kiwi-Minsker, and A.Renken, *Performance Enhancement by Unsteady-State Reactor Operation: Theoretical Analysis for Two-sites Kinetic Model*, Chem. Eng. Technol. **2003**, 26
29. U. Pannek, L. Mleczko, *Chem. Eng. Technol.* **1998**, 21, 811
30. Vivek V. Ranade, *Computational Flow modeling for Chemical Reaction Engineering*, Process Systems Engineering, Academic Press **2002**, Vol. 5
31. Wen, C.Y., and Yu, Y.H., *A generalized method of predicting the minimum fluidization velocity*, AIChE Journal **1996**, Vol. 12, 610
32. Y.S. Matros, *Catalytic Processes under Unsteady-State Conditions*, Elsevier, Amsterdam **1989**
33. Y.S. Matros, *Can. J. Chem. Eng. Sci.* **1996**, 74, 566
34. Engineering Fundamentals, Properties of Air, <http://www.efunda.com>
35. Process Associates of America, Archimedes Number.
<http://www.processassociates.com>

APPENDIX

A.I.1 Steady State Model Code

Library Code

```
*****
'Gauss
*****
Public Sub Gauss(aa, Bb, neqs, mx, tol, er)
ReDim s(neqs)
er = 0
For i = 1 To neqs
    s(i) = Abs(aa(i, 1))
For j = 2 To neqs
    If Abs(aa(i, j)) > s(i) Then s(i) = Abs(aa(i, j))
Next j
Next i
Call Eliminate(aa, s, neqs, Bb, tol, er)
If er <> -1 Then
    Call Substitute(aa, neqs, Bb, mx)
End If
End Sub

Public Sub Eliminate(aa, s, neqs, Bb, tol, er)
For k = 1 To neqs - 1
    Call Pivot(aa, Bb, s, neqs, k)
If Abs(aa(k, k) / s(k)) < tol Then
    er = -1
Exit For
End If
For i = k + 1 To neqs
    factor = aa(i, k) / aa(k, k)
For j = k + 1 To neqs
    aa(i, j) = aa(i, j) - factor * aa(k, j)
Next j
Bb(i) = Bb(i) - factor * Bb(k)
Next i
Next k
If Abs(aa(k, k) / s(k)) < tol Then er = -1
End Sub

Public Sub Pivot(aa, Bb, s, neqs, k)
Pp = k
big = Abs(aa(k, k) / s(k))
```

```

For ii = k + 1 To neqs
  dummy = Abs(aa(ii, k) / s(ii))
If dummy > big Then
  big = dummy
  Pp = ii
End If
Next ii
If Pp <> k Then
For jj = k To neqs
  dummy = aa(Pp, jj)
  aa(Pp, jj) = aa(k, jj)
  aa(k, jj) = dummy
Next jj
dummy = Bb(Pp)
Bb(Pp) = Bb(k)
Bb(k) = dummy
dummy = s(Pp)
s(Pp) = s(k)
s(k) = dummy
End If
End Sub
Public Sub Substitute(aa, neqs, Bb, mx)
mx(neqs) = Bb(neqs) / aa(neqs, neqs)
For i = neqs - 1 To 1 Step -1
  Sum = 0
  For j = i + 1 To neqs
    Sum = Sum + aa(i, j) * mx(j)
  Next j
  mx(i) = (Bb(i) - Sum) / aa(i, i)
Next i
End Sub
*****
'Newton Raphson
*****
Public Sub Newtraph(xNR, ea, iter, imax, neqs)
ReDim fxNR(neqs), df(neqs, neqs), bNR(neqs)
iter = 0
Do
iter = iter + 1
For i = 1 To neqs
xold(i) = xNR(i)
Next i
Call nrfunc(fxNR, xold, neqs)
Call nrderiv(df, xold, neqs)
For j = 1 To neqs
  bNR(j) = 0

```

```

    For i = 1 To neqs
        bNR(j) = bNR(j) + xold(i) * df(j, i)
    Next i
    bNR(j) = bNR(j) - fxNR(j)
Next j
If neqs = 1 Then
    xnew(neqs) = xold(neqs) - (fxNR(neqs) / (df(neqs, neqs)))
Else
    Call Gauss(df, bNR, neqs, xnew, tol, er)
    For kk = 1 To neqs
        xnew(kk) = xold(kk) + (xnew(kk) - xold(kk)) * stiff
    Next kk
End If
alooop = -1
For i = 1 To neqs
    xNR(i) = xnew(i)
    If xnew(i) = 0 Then
        eact1 = 1.1 * ea
    Else
        eact1 = Abs((xnew(i) - xold(i)) / xnew(i)) * 100
    End If
    If eact1 > ea Then aloop = 1
Next i
If aloop < 0 Then Exit Do
If iter > imax Then Exit Do
Loop
End Sub

```

```

Public Sub nrderiv(df, xold, neqs)
    ReDim df(neqs, neqs), xhigh(neqs), XLow(neqs), fhigh(neqs), flow(neqs)
    ReDim xhigh2(neqs), xlow2(neqs), fhigh2(neqs), flow2(neqs)
    For j = 1 To neqs
        For k = 1 To neqs
            xhigh2(k) = xold(k)
            xhigh(k) = xold(k)
            XLow(k) = xold(k)
            xlow2(k) = xold(k)
        Next k
        For i = 1 To neqs
            xhigh2(i) = xold(i) * 1.02
            xhigh(i) = xold(i) * 1.01
            XLow(i) = xold(i) * 0.99
            xlow2(i) = xold(i) * 0.98
        Next i
        Call nrfunc(fhigh2, xhigh2, neqs)
        Call nrfunc(fhigh, xhigh, neqs)
        Call nrfunc(flow, XLow, neqs)
    Next j
End Sub

```

```

Call nrfunc(flow2, xlow2, neqs)
df(j, i) = (-fhigh2(j) + 8 * fhigh(j) - 8 * flow(j) + flow2(j)) / (12 * 0.01 * xold(i))
df(i, j) = df(i, j)
xhigh2(i) = xold(i)
xhigh(i) = xold(i)
XLow(i) = xold(i)
xlow2(i) = xold(i)
Next i
Next j
End Sub
*****

Rem golden search
*****

'Public Sub golden(XLow, XUp, imax, Err, Xopt, ActErr, Iter2)
'Iter2 = 0
'Xopt = (XLow + XUp) / 2
'Do
'xold1 = Xopt
'  x1 = XLow + 0.618 * (XUp - XLow)
'  x2 = XUp - 0.618 * (XUp - XLow)
'  F1 = gf(x1)
'  F2 = gf(x2)
'If F1 > F2 Then
'  Xopt = x1
'ElseIf F2 > F1 Then
'  Xopt = x2
'End If
'  ActErr = ((1 - 0.618) * Abs((XUp - XLow) / Xopt)) * 100
'If (ActErr < Err) Or (Iter2 > imax) Then
'  Exit Do
'End If
'If F1 > F2 Then
'  XLow = x2
'ElseIf F2 > F1 Then
'  XUp = x1
'End If
'  Iter2 = Iter2 + 1
'Loop
'End Sub

*****

Rem Multipul golden search
*****

Public Sub MultipulGold(MXUp, MXLow, MEa, MXopt, ActMEa, Iterg, imaxg, nvar)
ReDim MXopt(nvar)
For i = 1 To nvar

```

```

    MXopt(i) = (MXUp(i) + MXLow(i)) / 2
Next i
Iterg = 0
Do
    Iterg = Iterg + 1
For i = 1 To nvar
    MX1 = MXLow(i) + 0.618 * (MXUp(i) - MXLow(i))
    MXopt(i) = MX1
    xNR(3) = MX1
    xNR(4) = 0.001
Call GoldFunc(MXopt, Fobj1)
    MX2 = MXUp(i) - 0.618 * (MXUp(i) - MXLow(i))
    MXopt(i) = MX2
    xNR(3) = MX2
    xNR(4) = 0.001
Call GoldFunc(MXopt, Fobj2)
    ActMEa(i) = (1 - 0.618) * (Abs(((MXUp(i) - MXLow(i)) / MXopt(i))) * 100)
If Fobj1 > Fobj2 Then
    MXLow(i) = MX2
    MXopt(i) = MX1
Else
    MXUp(i) = MX1
    MXopt(i) = MX2
End If
Next i
    Emax = ActMEa(1)
'For j = 2 To nvar
'If ActMEa(j) > Emax Then
'Emax = ActMEa(j)
'End If
'Next j
If (Emax < MEa) Or (Iterg > imaxg) Then Exit Do
Loop
End Sub
*****
Rem GoldFunc
*****
Public Sub GoldFunc(mx, Fobj)
For i = 1 To nvar
    xin(i) = mx(i)
Next i
    xain = mx(1)
    xin(1) = xain
Call Newtraph(xNR, ea, iter, imax, neqs)
Fobj = c
End Sub

```

Driver Code

```
Public neqs, tol, xold(100), xnew(100), ddf(100, 100), nout
Public xin(100), npts, x1(100)
Public kaa, kba, kad, kbd, kr, V, Q0, ns, Cf, G, Q, Fa, Fb, ea, imax, iter, xbin, ya, yb, c,
xain, xcin
Public xNR(100), kbastore(100), kaastore(100), stiff
Public MXLow(100), MXUp(100), ActMEa(100)
Public xamax(100, 100), xbmax(100, 100), xcmax(100, 100)
Public xbout(100, 100), ybout(100, 100), xaout(100, 100), yaout(100, 100), xcout(100,
100)
Public Fobj1, Fobj2, Iterg, Optimum(100), imaxg, MEa
Public Function XMultipulGold(XLow1, XUp1, x1, neq, nva, toll, qn1, ea1, imax1,
xain1, xbin1, xcin1, kaa1, kba1, kad1, kbd1, kr1, V1, Q01, ns1, Cf1, G1, imaxg1, MEa1,
npts1, stiff1)
nout = nout1
neqs = neq
nvar = nva
MXUp(1) = XUp1(1)
For i = 1 To neqs
xNR(i) = x1(i)
Next i
xain = xain1
xbin = xbin1
xcin = xcin1
kaa = kaa1
kba = kba1
kad = kad1
kbd = kbd1
kr = kr1
V = V1
Q0 = Q01
ns = ns1
Cf = Cf1
G = G1
ea = ea1
imax = imax1
tol = toll
qn = qn1
imaxg = imaxg1
MEa = MEa1
kamax = kaa
kbmax = kba
npts = npts1
stiff = stiff1
For jj = 1 To npts
```

```

kba = kbmax / npts * jj
kbastore(jj) = kba
For ii = 1 To npts
  kaa = kamax / npts * ii
  kaastore(ii) = kaa
  xcmax(ii, jj) = 0
  xamax(ii, jj) = 0
  xbmax(ii, jj) = 0
  c = 0
  For i = 1# To 99#
    xbin = i / 100#
    MXUp(1) = 1# - xbin
    MXLow(1) = 0.001
    ' For ik = 1 To neqs
    ' xNR(ik) = x1(ik)
    ' Next ik
    xNR(1) = xbin
    xNR(2) = 0.001
    Call MultipulGold(MXUp, MXLow, MEa, MXopt, ActMEa, Iterg, imaxg, nvar)
    Optimum(1) = MXopt(1)
    If c >= xcmax(ii, jj) Then
      xamax(ii, jj) = xain
      xbmax(ii, jj) = xbin
      xcmax(ii, jj) = c
      xbout(ii, jj) = xnew(1)
      ybout(ii, jj) = xnew(2)
      xaout(ii, jj) = xnew(3)
      yaout(ii, jj) = xnew(4)
      xcout(ii, jj) = xnew(5)
    Else
      End If
  Next i
Next ii
Next jj
XMultipulGold = "Complete"
End Function
Public Sub nrfunc(f, xx, neqs)
  ReDim f(neqs)
  AST = G * Cf * ns * (kaa * xx(3) * (1 - xx(2) - xx(4)) - kad / Cf * xx(4))
  BST = G * Cf * ns * (kba * xx(1) * (1 - xx(2) - xx(4)) - kbd / Cf * xx(2))
  CST = G * ns ^ 2 * kr * xx(4) * xx(2)
  b = G * (ns ^ 2) * kr / (Q0 * Cf)
  GMA = Q0 * kr * ns / V
  Aaa = kaa * Cf / (kr * ns)
  Aab = kba * Cf / (kr * ns)
  Aad = kad / (kr * ns)

```

```

Abd = kbd / (kr * ns)
f(1) = xbin - (xx(5) / Q0) * xx(1) - b * (Aba * xx(1) * (1 - xx(2) - xx(4)) - Abd * xx(2))
f(2) = Aba * xx(1) * (1 - xx(2) - xx(4)) - Abd * xx(2) - xx(2) * xx(4)
f(3) = xin(1) - (xx(5) / Q0) * xx(3) - b * (Aaa * xx(3) * (1 - xx(4) - xx(2)) - Aad * xx(4))
f(4) = Aaa * xx(3) * (1 - xx(2) - xx(4)) - Aad * xx(4) - xx(2) * xx(4)
f(5) = Q0 + (CST - (AST + BST)) / Cf - xx(5)
c = (Q0 / xx(5)) * (xcin + b * xx(2) * xx(4))
Fa = 1 - xx(5) * xx(3) / (Q0 * xin(1))
Fb = 1 - xx(5) * xx(1) / (Q0 * xbin)
End Sub
Public Sub Results()
Cells(34, 3) = "Iter"
Cells(34, 4) = iter
Cells(35, 3) = "Iterg"
Cells(35, 4) = Iterg
Cells(36, 3) = "Kaa"
Cells(36, 4) = kaa
Cells(37, 3) = "Kba"
Cells(37, 4) = kba
Cells(39, 3) = "Cmax"
Cells(40, 3) = "Xain"
Cells(41, 3) = "Xbin"
Cells(42, 3) = "Xaout"
Cells(43, 3) = "Yaout"
Cells(44, 3) = "Xbout"
Cells(45, 3) = "Ybout"
Cells(46, 3) = "Qout"
Cells(39, 4) = xcmax(1, 1)
Cells(40, 4) = xamax(1, 1)
Cells(41, 4) = xbmax(1, 1)
Cells(42, 4) = xaout(1, 1)
Cells(43, 4) = yaout(1, 1)
Cells(44, 4) = xbout(1, 1)
Cells(45, 4) = ybout(1, 1)
Cells(46, 4) = xcout(1, 1)
End Sub

```


A.II.1 DYNAMIC MODEL

Library Code

```
Public Sub LUDecomp(aa, bb, n, x, tol, er)
ReDim slu(n), olu(n)
er = 0
Call decompose(aa, n, tol, olu, slu, er)
If er <> -1 Then
  Call LUSub(aa, olu, n, bb, x)
End If
End Sub
Public Sub decompose(aa, n, tol, olu, slu, er)
For i = 1 To n
  olu(i) = i
  slu(i) = Abs(aa(i, 1))
  For j = 2 To n
    If Abs(aa(i, j)) > slu(i) Then slu(i) = Abs(aa(i, j))
  Next j
Next i
For k = 1 To n - 1
  Call LUPivot(aa, olu, slu, n, k)
  If Abs(aa(olu(k), k) / slu(olu(k))) < tol Then
    er = -1
    Exit For
  End If
  For i = k + 1 To n
    factor = aa(olu(i), k) / aa(olu(k), k)
    aa(olu(i), k) = factor
    For j = k + 1 To n
      aa(olu(i), j) = aa(olu(i), j) - factor * aa(olu(k), j)
    Next j
  Next i
Next k
If Abs(aa(olu(k), k) / slu(olu(k))) < tol Then
  er = -1
End If
End Sub
Public Sub LUPivot(aa, olu, slu, n, k)
P = k
big = Abs(aa(olu(k), k) / slu(olu(k)))
For ii = k + 1 To n
  dummy = Abs(aa(olu(ii), k) / slu(olu(ii)))
  If dummy > big Then
    big = dummy
    P = ii
  End If
End For
```

```

End If
Next ii
dummy = olu(P)
olu(P) = olu(k)
olu(k) = dummy
End Sub
Public Sub LUSub(aa, olu, n, bb, x)
For i = 2 To n
Sum = bb(olu(i))
For j = 1 To i - 1
Sum = Sum - aa(olu(i), j) * bb(olu(j))
Next j
bb(olu(i)) = Sum
Next i
x(n) = bb(olu(n)) / aa(olu(n), n)
For i = n - 1 To 1 Step -1
Sum = 0
For j = i + 1 To n
Sum = Sum + aa(olu(i), j) * x(j)
Next j
x(i) = (bb(olu(i)) - Sum) / aa(olu(i), i)
Next i
End Sub
Public Sub Gauss(aa, bb, n, x, tol, er)
ReDim s(n)
er = 0
For i = 1 To n
s(i) = Abs(aa(i, 1))
For j = 2 To n
If Abs(aa(i, j)) > s(i) Then s(i) = Abs(aa(i, j))
Next j
Next i
Call Eliminate(aa, s, n, bb, tol, er)
If er <> -1 Then
Call Substitute(aa, n, bb, x)
End If
End Sub
Public Sub Eliminate(aa, s, n, bb, tol, er)
For k = 1 To n - 1
Call Pivot(aa, bb, s, n, k)
If Abs(aa(k, k) / s(k)) < tol Then
er = -1
Exit For
End If
For i = k + 1 To n
factor = aa(i, k) / aa(k, k)

```

```

For j = k + 1 To n
  aa(i, j) = aa(i, j) - factor * aa(k, j)
Next j
bb(i) = bb(i) - factor * bb(k)
Next i
Next k
If Abs(aa(k, k) / s(k)) < tol Then er = -1
End Sub
Public Sub Pivot(aa, bb, s, n, k)
P = k
big = Abs(aa(k, k) / s(k))
For ii = k + 1 To n
  dummy = Abs(aa(ii, k) / s(ii))
  If dummy > big Then
    big = dummy
    P = ii
  End If
Next ii
If P <> k Then
  For jj = k To n
    dummy = aa(P, jj)
    aa(P, jj) = aa(k, jj)
    aa(k, jj) = dummy
  Next jj
  dummy = bb(P)
  bb(P) = bb(k)
  bb(k) = dummy
  dummy = s(P)
  s(P) = s(k)
  s(k) = dummy
End If
End Sub
Public Sub Substitute(aa, n, bb, x)
x(n) = bb(n) / aa(n, n)
For i = n - 1 To 1 Step -1
  Sum = 0
  For j = i + 1 To n
    Sum = Sum + aa(i, j) * x(j)
  Next j
  x(i) = (bb(i) - Sum) / aa(i, i)
Next i
End Sub
Public Sub Newtraph(x, ea, iter, imax, neqs)
ReDim fx(neqs), df(neqs, neqs), b(neqs), xold(neqs)
iter = 0
Do

```

```

iter = iter + 1
'
'Set the value of xold to the updated x
'
For i = 1 To neqs
  xold(i) = x(i)
Next i
'
'Calculate f(i)
'
'Call nrfunc(fx, xold, neqs)
'
'Calculate df(i)/dx
'
Call nrderiv(df, xold, neqs)
For j = 1 To neqs
  For i = 1 To neqs
    df(j, i) = df(j, i)
  Next i
Next j
'
'Calculate the rhs of the NR equation
'
For j = 1 To neqs
  b(j) = 0
  For i = 1 To neqs
    b(j) = b(j) + xold(i) * df(j, i) * 0.5
  Next i
  b(j) = b(j) - fx(j)
Next j
'
'Solve for the new values of x(i) using Gauss Elimination
'
Call LUDecomp(df, b, neqs, xnew, tolss, er)
'Call Gauss(df, b, neqs, xnew, tolss, er)
'
'Calculate relative error of each x(i)
'
aloop = 1
For i = 1 To neqs
  x(i) = xnew(i)
  If x(i) = 0 Then
    eact = 1.1 * ea
  Else
    eact = Abs((xnew(i) - xold(i)) / xnew(i)) * 100
  End If

```

```

    If (eact > ea) Then
        aloop = 1
    Else
        aloop = -1
    End If
Next i
If (aloop < 0) Or (iter > imax) Then Exit Do
Loop
End Sub
Public Sub nrderiv(df, xold, neqs)
ReDim df(neqs, neqs), xhigh(neqs), xlow(neqs), fhigh(neqs), flow(neqs)
ReDim xhigh2(neqs), xlow2(neqs), fhigh2(neqs), flow2(neqs)
For j = 1 To neqs
    For k = 1 To neqs
        xhigh2(k) = xold(k)
        xhigh(k) = xold(k)
        xlow(k) = xold(k)
        xlow2(k) = xold(k)
    Next k
    For i = 1 To neqs
        xhigh2(i) = xold(i) * 1.02
        xhigh(i) = xold(i) * 1.01
        xlow(i) = xold(i) * 0.99
        xlow2(i) = xold(i) * 0.98
        'Call nrfunc(fhigh2, xhigh2, neqs)
        'Call nrfunc(fhigh, xhigh, neqs)
        'Call nrfunc(flow, xlow, neqs)
        'Call nrfunc(flow2, xlow2, neqs)
        'df(j, i) = (fhigh(j) - flow(j)) / (xhigh(i) - xlow(i))
        df(j, i) = (-fhigh2(j) + 8 * fhigh(j) - 8 * flow(j) + flow2(j)) / (12 * 0.01 * xold(i))
        xhigh2(i) = xold(i)
        xhigh(i) = xold(i)
        xlow(i) = xold(i)
        xlow2(i) = xold(i)
    Next i
Next j
End Sub
Public Sub Integrator(t, y, n, h, tend)
h2 = h
Do
    If (tend - t < h) Then h2 = tend - t
    Call RK4(t, y, n, h2)
    If (t >= tend) Then Exit Do
Loop
End Sub
Public Sub RK4(t, y, n, h)

```

```

ReDim K1(n), k2(n), k3(n), k4(n), ym(n), ye(n)
Call Derivs2(t, y, K1)
For i = 1 To n
ym(i) = y(i) + K1(i) * h / 2
Next i
Call Derivs2(t + h / 2, ym, k2)
For i = 1 To n
ym(i) = y(i) + k2(i) * h / 2
Next i
Call Derivs2(t + h / 2, ym, k3)
For i = 1 To n
ye(i) = y(i) + k3(i) * h
Next i
Call Derivs2(t + h, ye, k4)
For i = 1 To n
Slope = (K1(i) + 2 * (k2(i) + k3(i)) + k4(i)) / 6
y(i) = y(i) + Slope * h
Next i
t = t + h
End Sub
Public Sub RKkc(y, dy, t, h, yout, yerr, n)
ReDim k2(n), k3(n), k4(n), k5(n), k6(n), yout(n), yerr(n), ytemp(n)
a2 = 0.2
a3 = 0.3
a4 = 0.6
a5 = 1#
a6 = 0.875
b21 = 0.2
b31 = 3# / 40#
b32 = 9# / 40#
b41 = 0.3
b42 = -0.9
b43 = 1.2
b51 = -11# / 54#
b52 = 2.5
b53 = -70# / 27#
b54 = 35# / 27#
b61 = 1631# / 55296#
b62 = 175# / 512#
b63 = 575# / 13824#
b64 = 44275# / 110592#
b65 = 253# / 4096#
c1 = 37# / 378#
c3 = 250# / 621#
c4 = 125# / 594#
c6 = 512# / 1771#

```

```

dc1 = c1 - 2825# / 27648#
dc3 = c3 - 18575# / 48384#
dc4 = c4 - 13525# / 55296#
dc5 = -277# / 14336#
dc6 = c6 - 0.25
For i = 1 To n
  ytemp(i) = y(i) + b21 * h * dy(i)
Next i
Call Derivs2(t + a2 * h, ytemp, k2)
For i = 1 To n
  ytemp(i) = y(i) + h * (b31 * dy(i) + b32 * k2(i))
Next i
Call Derivs2(t + a3 * h, ytemp, k3)
For i = 1 To n
  ytemp(i) = y(i) + h * (b41 * dy(i) + b42 * k2(i) + b43 * k3(i))
Next i
Call Derivs2(t + a4 * h, ytemp, k4)
For i = 1 To n
  ytemp(i) = y(i) + h * (b51 * dy(i) + b52 * k2(i) + b53 * k3(i) + b54 * k4(i))
Next i
Call Derivs2(t + a5 * h, ytemp, k5)
For i = 1 To n
  ytemp(i) = y(i) + h * (b61 * dy(i) + b62 * k2(i) + b63 * k3(i) + b64 * k4(i) + b65 * k5(i))
Next i
Call Derivs2(t + a6 * h, ytemp, k6)
For i = 1 To n
  yout(i) = y(i) + h * (c1 * dy(i) + c3 * k3(i) + c4 * k4(i) + c6 * k6(i))
  yerr(i) = h * (dc1 * dy(i) + dc3 * k3(i) + dc4 * k4(i) + dc5 * k5(i) + dc6 * k6(i))
Next i
End Sub
Public Sub Adapt(t, y, dy, htry, yscal, eps, hnxt, n)
  ReDim ytemp(n)
  safety = 0.9
  econ = 0.000189
  h = htry
  Do
    Call RKkc(y, dy, t, h, ytemp, yerr, n)
    emax = 0
    For i = 1 To n
      emax1 = Abs(yerr(i) / yscal(i) / eps)
    If emax1 > emax Then emax = emax1
    Next i
  If emax <= 1 Then Exit Do
  htemp = safety * h * emax ^ (-0.25)
  If Abs(htemp) > (0.25 * Abs(h)) Then
    h = Abs(htemp)

```

```

Else
  h = 0.25 * Abs(h)
End If
  tnew = t + h
If tnew = t Then Exit Do
Loop
If emax > econ Then
  hnxt = safety * (emax ^ (-0.2)) * h
Else
  hnxt = 4# * h
End If
  t = t + h
For i = 1 To n
  y(i) = ytemp(i)
Next i
End Sub

```

Driver Code

```

Public G, V, Q0, Q, ns, Cf, kaa, kad, kba, kbd, kr, xain, xbin, xcin
Public Gss, Vss, Q0ss, Qss, nsss, Cfss, kaass, kadss, kbass, kbdss, krss, xainss, xbinss,
xcinss
Public tolss, xnew(100), ddf(100, 100), fxx(100), iter, Fa, Fb
Public hipt, lopt, ythree, ntotal, xain1
'Driver for Cash-Carp Runge-Kutta Fehlberg
'Calls Derivs2 for system of ODE's
'x1 = Initial Value of the Independent Variable
'y1 = Array of Initial Values of the Dependent Variables
'xend = Final Value of Independent Variable Which will be used for output
'n = Number of Dependent Variables
'h1 = Initial Step Size Estimate
'nout = Dependent Variable Array Subscript for Output
'

Public Sub Rungekutta()
n = Cells(2, 3)
ReDim y(n), dy(n), yscal(n)
For i = 1 To n
  y(i) = Cells(20, i + 2)
Next i
G = Cells(4, 3)
V = Cells(5, 3)
Q0 = Cells(6, 3)
Q = Q0
Q3 = Q1
ns = Cells(12, 3)
Cf = Cells(13, 3)

```



```

kaa = Cells(7, 3)
kad = Cells(9, 3)
kba = Cells(8, 3)
kbd = Cells(10, 3)
kr = Cells(11, 3)
tinitial = Cells(14, 3)
tfinal = Cells(15, 3)
npts = Cells(16, 3)
maxstep = 1000
tiny = 1E-30
eps = 0.0001
h = Cells(3, 3)
ntotal = 0
t = tinitial
For i1 = 1 To npts
Cells(20 + i1, 2) = 0
Cells(20 + i1, 3) = 0
Cells(20 + i1, 4) = 0
Cells(20 + i1, 5) = 0
Cells(20 + i1, 6) = 0
Cells(20 + i1, 7) = 0
Cells(20 + i1, 8) = 0
Cells(20 + i1, 9) = 0
Cells(20 + i1, 10) = 0
Cells(20 + i1, 11) = 0
Next i1
For i2 = 1 To npts
tend = tfinal / npts * i2
xain = Cells(3, 9)
xbin = Cells(3, 10)
xcin = Cells(3, 11)
Cells(14, 3) = tend
istep = 0
Call Integrator(t, y, n, h, tend)
ntotal = (Q * Cf * y(5) * (tend - t1)) + ntotal
t = tend
Cells(20 + i2, 2) = t
Cells(20 + i2, 3) = y(1)
Cells(20 + i2, 4) = y(2)
Cells(20 + i2, 5) = y(3)
Cells(20 + i2, 6) = y(4)
Cells(20 + i2, 7) = y(5)
Cells(20 + i2, 8) = Q
Cells(20 + i2, 9) = xain
Cells(20 + i2, 10) = xbin
Cells(20 + i2, 11) = xcin

```

```

Next i2
Cells(14, 3) = tinitial
End Sub
Public Sub Derivs2(t, y, dydt)
  Adr = G * Cf * ns * (kaa * y(3) * (1 - y(1) - y(2)) - kad / Cf * y(1))
  Bdr = G * Cf * ns * (kba * y(4) * (1 - y(1) - y(2)) - kbd / Cf * y(2))
  Cdr = G * ns ^ 2 * kr * y(1) * y(2)
  Q = Q0 + (Cdr - (Adr + Bdr)) / Cf
  dydt(1) = Cf * kaa * y(3) * (1 - y(1) - y(2)) - kad * y(1) - kr * ns * y(1) * y(2)
  dydt(2) = Cf * kba * y(4) * (1 - y(1) - y(2)) - kbd * y(2) - kr * ns * y(1) * y(2)
  dydt(3) = (Q0 * xain - Q * y(3)) / V - G * ns / V * (kaa * y(3) * (1 - y(1) - y(2)) - kad / Cf * y(1))
  dydt(4) = (Q0 * xbin - Q * y(4)) / V - G * ns / V * (kba * y(4) * (1 - y(1) - y(2)) - kbd / Cf * y(2))
  dydt(5) = (Q0 * xcin - Q * y(5)) / V + G * ns ^ 2 / (V * Cf) * kr * y(1) * y(2)
End Sub

```